ADENO-ASSOCIATED VIRUS TYPE-2 MEDIATED EXPRESSION OF PIGMENTED EPITHELIUM DERIVED FACTOR OR KRINGLES 1-3 OF ANGIOSTATIN REDUCED NEOVASCULAR RETINOPATHIES

By

BRIAN RAISLER

A DISSERTATION PRESENTED TO THE GRADUATE SCHOOL
OF THE UNIVERSITY OF FLORIDA IN PARTIAL FULFILLMENT
OF THE REQUIREMENTS FOR THE DEGREE OF
DOCTOR OF PHILOSOPHY

UNIVERSITY OF FLORIDA

2003

This dissertation is dedicated to my grandfather Robert “Pat” Raisler who lost his sight to age-related macular degeneration. Pat is a kind and good-hearted man who brings much happiness to all of those around him. He is unerringly honest in all of his dealings. He has a life-long passion for fixing things and for working in wood. Sadly, the untimely loss of his vision curtailed his ability to enjoy his favorite past-times. Even with his disability, Pat remains upbeat and joyous in his life attending church functions, outdoor symphony concerts, and visiting family and friends with his wife Leora. He is an inspiration whenever things might seem grim. I hope that I can learn from his example and lead my life taking in as much enjoyment and pleasure as he does. My only regret as I reflect back on the research in this dissertation was that it did not come in time to help preserve the vision of this wonderful man.

ACKNOWLEDGMENTS

For their extensive assistance in the completion of my graduate work I would like to thank the members of my committee. I thank Dr. Adrian Timmers who aided my understanding and technical proficiency in intraocular injections. Dr. Timmers is an excellent instructor and has a broad and deep knowledge of vision science which he is generous in sharing with his students. I thank Dr. Maria Grant who was instrumental in my education about the role of vascularization in the eye and the retinopathy of prematurity model in particular. Dr. Grant always provided me meaningful encouragement and advice about my ongoing research. Dr. Nickolas Muzyczka is a continuing inspiration to any young scientist hoping to make his mark in academic life. Dr. Muzyczka has garnered the kind of recognition and acclaim for his work that I hope to reach in my own endeavours. Dr. Alfred Lewin frequently prompted me to remain current on my chosen field and to keep abreast of parallel developments in the literature without losing sight of my larger goals. Dr. Lewin evinces the kind of intellectual prowess that inspires, rather than intimidates, his colleagues into searching to increase their own knowledge. I owe a particular debt of gratitude to my mentor, Dr. William Hauswirth. Dr. Hauswirth brought me into his group and guided my interests in vascular development and focused them toward an immensely interesting and rewarding project within his research team. He provided the tools and guidance necessary to reach my academic goals. Special thanks are offered to John Alexander and Clive Wasserfal for their help in designing ELISA systems, to Denis Beliaev for cloning and plasmid

construct design, and to Vince Chiodo for viral packaging. I thank my wife, Audra Strahl, for her patience and support throughout this arduous journey. Without her by my side, I would have never made it as far as I have. She is my inspiration, my sounding board, and my best friend.

TABLE OF CONTENTS

Page

LIST OF TABLES

LIST OF FIGURES

Abstract of Dissertation Presented to the Graduate School
of the University of Florida in Partial Fulfillment of the
Requirements for the Degree of Doctor of Philosophy

ADENO-ASSOCIATED VIRUS TYPE-2 MEDIATED EXPRESSION OF PIGMENTED EPITHELIUM DERIVED FACTOR OR KRINGLES 1-3 OF ANGIOSTATIN REDUCE NEOVASCULAR RETINOPATHIES

By

Brian Raisler

December 2003

Chair: William W. Hauswirth
Major Department: Molecular Genetics and Microbiology

Diabetic retinopathy causes blindness because of an abnormal proliferation of retinal blood vessels. Pigment epithelium-derived factor (PEDF) is the primary developmental and environmental regulator of angiogenesis in the eye. Kringle domains 1-3 of angiostatin (K1K3) have also been demonstrated to have potent anti-angiogenic properties. In the hypoxic diabetic retina, PEDF down-regulation and/or vascular endothelial growth factor (VEGF) up-regulation leads to retinal microvascular proliferation. This proliferation of new blood vessels causes a gradual but progressive and debilitating loss of vision in over half of diabetic patients. A similar patho-physiology is shared by premature infants at risk for developing retinopathy of prematurity (ROP). This thesis will test the hypothesis that increased local expression of PEDF or K1K3 will inhibit retinal neovascularization (NV) in an animal model of vascular retinopathy. To this end, we have developed an in vivo retinal gene

delivery/expression system involving recombinant adeno-associated virus (rAAV) and secreted PEDF or K1K3 that is efficient and persists for years. Recombinant AAV vectors expressing PEDF or K1K3 from five different promoters, each restricting gene expression to distinct classes of retinal cells, were tested and the ocular PEDF levels were optimized by inoculating each vector into one of two locations, the subretinal space or the intravitreal space. Secreted PEDF or K1K3 from each local cell type could communicate with the retinal vascular bed. Vectored production of either PEDF or K1K3 was found to be most robust using the chicken beta-actin (CBA) hybrid promoter. Using a mouse model of ROP (oxygen induced retinopathy) as a surrogate for diabetic retinopathy, I investigated the therapeutic potential of AAV driving these anti-NV genes. In this animal model, retinal NV occurs following an acute retinal ischemia and can be quantitatively and reproducibly followed. Both CBA optimal promoter-PEDF or K1K3 vectors effectively inhibited retinal NV in this animal model. This represents a significant advance toward the use of gene therapy delivering anti-angiogenic factors for the treatment of vascular retinopathies.

CHAPTER 1
INTRODUCTION

Retinal Neovascular Diseases

Pathologic neovascularization of the retina is central to several debilitating ocular diseases including proliferative diabetic retinopathy (PDR), age-related macular degeneration (AMD), and retinopathy of prematurity (ROP). Diabetic retinopathy and AMD are the leading causes of blindness in developed countries. Regulation of vascularization in the mature retina involves a balance between endogenous positive growth factors, such as vascular endothelial growth factor (VEGF) (1;2), and inhibitors of angiogenesis, such as pigment epithelium derived factor (PEDF) (3). When this balance is upset, pathologic angiogenesis can occur, ultimately leading to a loss of vision.

Retinopathy of Prematurity

Retinopathy of prematurity (ROP) is characterized by the abnormal growth of blood vessels in the retina of premature infants. Early reports of ROP indicated that there existed a link between the higher levels of oxygen used to cope with the underdeveloped lungs of premature infants and the subsequent neovascularization and damage to the retina (4;5). Infants in whom ROP is diagnosed during the perinatal period are at risk for ocular abnormalities and for deficits in visual function. Subsequent improvements in the modulation of oxygen therapy, the supplementation of Vitamin E, and the use of steroids for bronchopulmonary dysplasia in premature infants has helped to reduce the number and severity of ROP cases (6-8).

The following data are from The Multicenter Cryotherapy for Retinopathy of Prematurity (CRYO-ROP) study reported according to international classification based on the severity of ROP (9-11). The data were collected from 4,099 infants born between January 1986 and November 1987 with birth weights of less than 1251 grams. The birth weight measurement is a more accurate predictor of post-natal complications than the gestational age at delivery.

Of 4,099 infants in the CRYO-ROP study:

- 2,699 (65.8%) developed some degree of ROP, with no effect on visual acuity.
- 730 (17.8%) were classified as prethreshold, with little effect on visual acuity.
- 246 (6%) were classified as threshold in one or both eyes. Within this group of 246 infants, 123 (50%) were blind and 123 (50%) had visual acuity that was significantly below normal. For the group of 123 infants with visual acuity significantly below normal, cryotherapy improved 49 (40%) of the cases.
- For each 100-gram decrease in birth weight, there was a 27% higher risk that an infant would develop threshold ROP. (12)

More recent work has suggested that transpupillary diode laser photocoagulation may be more effective than transscleral cryotherapy for treating some types of ROP (13).

Diabetic Retinopathy

Diabetic retinopathy is characterized by a retinal neovascularization due to damage of the normal retinal blood vessels of the retina caused by high blood glucose levels. The blood vessel damage is characterized by a loss of pericytes and deterioration of the vessel walls. The effects of high blood glucose are cumulative, and the longer a person has had diabetes and the higher the blood glucose levels, the more likely is that person to develop diabetic retinopathy. In people who have had diabetes for 10 years or longer, nearly half have some degree of diabetic retinopathy. An estimated 100 to 120 million people worldwide have diabetes. In the United States, it is estimated that approximately 15.7

million Americans, nearly 6 percent of the population, have diabetes. Additionally, 800,000 new cases are diagnosed each year (14;15).

Diabetic retinopathy is classified in progressive stages, non-proliferative to proliferative, but the first stage does not inevitably lead to the next, particularly if optimum blood glucose control is practiced. In the non-proliferative stage, blood vessels may leak a clear fluid which causes macular edema. Macular edema is responsible for blurred vision, which may come and go as the fluid fluctuates. In many cases, non-proliferative diabetic retinopathy presents no symptoms. As the condition progresses, new abnormal blood vessels proliferate in the retina, bleed into the vitreous, and result in cloudy vision. The vessels are accompanied by the growth of fibrous tissue. This fibrosis can cause the retina to contract, pulling it from the back wall of the eye and causing retinal detachment. The new blood vessels can also grow on the iris and into the trabecular meshwork, increasing pressure in the eye and causing glaucoma.

The current method of treatment involves intensive management of blood glucose levels to prevent progression from non-proliferative to proliferative diabetic retinopathy. For more advanced cases of PDR, laser photocoagulation slows the loss of vision caused by the invasion of new blood vessels. Unfortunately no current treatment is successful in very many patients for a significant length of time. The need therefore clearly exists to develop alternative therapies that deal more directly with the biochemical basis of retinal neovascularization.

Age-related Macular Degeneration

Age-related macular degeneration (AMD) is the leading cause of acquired blindness in the elderly in industrialized countries. Choriodal neovascularization (CNV) is the main cause of severe vision loss in AMD patients (16). The neovascular component

of AMD is less well understood than in other ocular neovascular diseases. Some background information on AMD was summarized in the excellent review by P. Campochiaro et al. (17) and is worth repeating here. Early AMD, also known as “dry” or non-exudative AMD, is characterized by the accumulation of drusen in the retinal pigment epithelium (RPE) tissue beneath the macula. Drusen are deposits of waste products most likely produced by photoreceptor outer segments. For reasons that are not completely clear, the RPE loses its ability to process this waste. These drusen deposits are thought to interfere with the normal functioning of photoreceptors in and around the macula eventually leading to their degeneration (18-20). Accumulation, size, and composition of drusen have been speculated to be predictive of the eventual loss of vision from dry AMD or progression from dry AMD to the wet or proliferative stage of the disease. The accumulation of drusen is accompanied by a thickening in Bruch's membrane, a change in its membrane composition, and increases in lipid deposition and protein crosslinking. There is also a change in Bruch's membrane permeability to nutrients such that water soluble plasma constituents are unable to cross Bruch's membrane (21).

In late stage AMD abberant vessels derived from the choriodal vasculature breach Bruch’s membrane and grow into the sub-retinal space (22;23). These vessels often leak causing an accumulation of blood or serum anterior to the retinal pigmented epithelium (RPE), where it is not efficiently cleared, ultimately causing retinal detachment. Subretinal hemorrhage also causes scarring and fibrosis which, in turn, leads to the death of the photoreceptors (24).

Laser photocoagulation can be used to treat patients presenting with CNV if it can be localized by fluorescein angiography and if the CNV does not involve the fovea. This treatment can be effective in temporarily preventing severe vision loss, but most patients suffer recurrent CNV, negating this initial benefit of laser photocoagulation (25). If laser photocoagulation is used in those cases where CNV involves the center of the fovea, it destroys the fovea, and reading vision is immediately and permanently lost (26). Experimental approaches that destroy subfoveal CNV while sparing the fovea are being tested, including surgical removal of CNV (27), macular translocation (28), and photodynamic therapy (PDT) (29;30).

Photodynamic therapy is the most commonly used alternative to laser photocoagulation. This therapy (PDT) has been used in the field of oncology to treat vascularized tumors (31;32). More recently PDT has entered the arena of ophthalmology as a treatment for CNV in AMD or secondary to DR (33;34). Briefly, PDT consists of systemically injecting a photoreactive dye; verteporfin (Visudyne, Novartis AG, Basel, Switzerland) is the most commonly used. The injection is followed by the use of low energy, non-damaging laser aimed at the vessels of the retina to excite this photoreactive dye and initiate a photochemical process that generates free-radicals and reactive oxygen species and ultimately leads to the apoptotic death of leaky, newly formed vessels (34).

These approaches may prove to be effective in controlling central vision loss due to AMD. However these treatments do not deal with the underlying angiogenic stimuli for neovascularization. Furthermore, for each of the above mentioned treatments recurrences are a problem in the clinic. Drug or gene therapy based treatments that block or counterbalance stimuli for CNV growth would be a major clinical improvement, but

development of such treatment is hindered by our poor understanding of the pathogenesis of CNV.

Comparing Neovascularization in the Retina and Choriod

The cause and progression of retinal NV are known in greater detail than the facts surrounding choriodal NV. While the microenvironment of the choroidal vascular is similar to the retinal vasculature, there are important differences. Early clinical and experimental observations have indicated the importance of ischemia to the development of retinal NV(35-38). Each of the diseases in which retinal NV occurs shares the development of retinal ischemia due to the occlusion of retinal vessels. However, it is unclear whether this hypoxic response is central to the development of CNV. Some studies have demonstrated changes in the blood flow in choriodal vessels of patients with AMD (39;40), but these changes in blood flow may not be sufficient to cause ischemia. It is possible that other complications of AMD, such as the thickening of Bruch's membrane or deposition of fatty materials, might contribute to the relative hypoxia responsible for a neovascular response. Another disease state that shares the pathology of CNV is ocular histoplasmosis. This disease occurs in younger patients, 20 to 40 years of age, and there is no evidence for hypoxia in these patients' eyes. Taken together, there is no conclusive evidence that CNV in AMD patients is regulated by hypoxia or ischemia.

Stimulatory Factors in AMD

Angiogenic stimulatory factors such as vascular endothelial growth factor (VEGF), insulin-like growth factor (IGF-1), and fibroblast growth factor 2 (FGF-2), are major stimulatory factors for retinal neovascularization (41-43). It is not as clear whether these factors also have a role in choriodal NV. There is good evidence that VEGF plays a central role in stimulating angiogenesis elsewhere in the eye. Increased expression of

VEGF in retinal photoreceptors of rhodopsin/VEGF transgenic mice stimulates neovascularization within the retina (44;45) and VEGF antagonists partially inhibit retinal or iris NV in animal models (46-48). Clinical trials of an RNA aptamer that binds VEGF (Macugen) are underway. Macugen binds VEGF and prevents it from binding to its receptor. This anti-VEGF aptamer inhibits neovascularization by 80% in the ROP model (49). VEGF is upregulated by hypoxia (2) and its levels are increased in the retina and vitreous of patients (50-52) or laboratory animals with ischemic retinopathies (53;54).

Is VEGF a Stimulatory Factor for CNV?

There is some evidence that suggests VEGF may be involved in CNV. VEGF is present in fibroblastic cells and transdifferentiated RPE cells of surgically removed choroidal neovascular membranes (55-58). Also, in both rat and monkey models of laser-induced choroidal neovascularization, increases in VEGF mRNA are seen in RPE-like cells, choroidal vascular endothelial cells, and fibroblast-like cells in the lesions (59;60). Intravitreal injection of an antibody fragment against VEGF reduced CNV in a primate model (61), indicating some role for VEGF in the development or persistence of CNV. However, increased expression of VEGF in photoreceptors of mice does not result in CNV (62). More recent work, where proliferation of vessels in the deep capillary bed does occur when VEGF is expressed under the control of the rhodopsin promoter, seems to contradict these earlier results (63). Development of CNV may require the prior breakdown of Bruch's membrane. Therefore, additional studies are needed to determine if, and precisely how, VEGF is involved in the development of CNV.

What Can Animal Models Show Us About the Pathogenesis of CNV?

Rupture of Bruch's membrane with laser photocoagulation is a reliable way to produce CNV and has been used to establish models in primates (64), rabbits (65), rats (66;67), and mice (68). Sustained release of VEGF in primates (69) also causes CNV. However, as noted above, increased expression of VEGF in photoreceptors of transgenic mice does not result in CNV (70). Perhaps surgical or laser trauma to Bruch's membrane, resulting in disturbed extracellular matrix of the RPE and/or perturbation of an endogenous inhibitor such as tissue inhibitor of metalloproteinase-3 or PEDF, is a critical component of sustained release models that is absent in overexpression models. Additional studies are needed to determine if Bruch's membrane provides a physical and/or biochemical barrier to CNV. Demonstration of the molecular nature of any biochemical barrier would provide an important target for therapeutic intervention.

Current Clinical Management of Ocular NV

Several clinical treatment options are currently available for patients presenting with retinal and choroidal neovascularization. Behavior and lifestyle modifications can be useful in controlling the rapidity and extent of damage in these diseases.

In the case of retinopathy of prematurity, preventative care and management can be effective in the treatment of infants that are born prematurely. Incidence and severity of ROP were inversely proportional to birth weight and gestational age (71). Clinical management of ROP has developed in complexity in the last two decades (72). The current standard of care involves careful management of oxygen levels that includes strict guidelines regarding the practices of increasing and weaning of fraction of inspired oxygen and the monitoring of O_2 saturation parameters in the delivery room, during in-house transport of infants to the newborn intensive care unit and throughout

hospitalization (73). These management practices have reduced the need for cryotherapy or laser surgery. The goal of eliminating ROP remains elusive however, since the management of extremely low birth weight infants still requires oxygen levels often conducive to development of ROP.

Many but not all patients diagnosed with early stage or non-proliferative diabetic retinopathy can prevent or significantly delay the far more damaging proliferative phase of the disease through careful management of their blood glucose levels. The high blood glucose levels are thought to be the initial insult in the small capillaries of the eye that leads to retinal ischemia. For Type I diabetics, this means frequent monitoring of glucose levels and adjusting by insulin injection. For Type II diabetics, changes in diet, exercise, and weight loss can aid in reducing many symptoms of diabetes and can result in remission in some cases.

Behavioral changes that can benefit patients with AMD include cessation of smoking and alcohol consumption, as well as reducing exposure to sunlight and wearing protective sunglasses. The management of patients with AMD has recently been advanced to include the dietary supplementation with antioxidants (vitamin C and E), beta carotene, and zinc as suggested by the AREDS study in 2001 (74;75). The thinking behind these studies is that the damage in AMD is due to oxidative damage subsequent to the generation of free radicals. The antioxidants vitamin C and E might act to scavenge these free radicals before they damage the retina. Other studies suggest that vitamin E supplementation alone is insufficient to protect against AMD (76). In that study, patients supplemented with vitamin E for four years showed no difference in incidence or progression of AMD when compared with placebo treated patients.

Surgical, laser, and photodynamic therapy (for AMD) techniques have been most commonly used to treat both PDR and AMD (77;78). Pan-retinal laser photo-coagulation has been used with relative success for a number of years(79;80). Unfortunately, laser photo-coagulation also damages healthy retinal cells adjacent to or underlying the treated area leading to a significant loss of peripheral and night vision. Laser photo-coagulation for retinal NV secondary to AMD often leads to an immediate significant reduction in visual acuity (81). A more recent development is the use of photodynamic therapy to treat CNV, which reduces collateral damage during laser therapy (34;82-84). As described above, photodynamic therapy involves the use of a photo-reactive dye to specifically target leaky endothelial vessels.

Surgical treatments include vitrectomy for removal of CNV membranes, foveal translocation, and removal or displacement of subretinal blood for AMD patients and removal of vitreous hemorrhage and scarring secondary to fibrovascular proliferation in PDR patients (33;85;86). Each of these surgical interventions carries intrinsic risks to the patient and can create further complications (77;87). All current treatment options provide solutions that result in some loss of vision and may have only temporary effects. Recurrence of symptoms is common and may ultimately result in loss of vision. Clearly the need exists for therapies that require minimal surgical manipulation, preserve existing vision, and provide long-term amelioration for any form of NV.

VEGF and the Hypoxia Signaling Pathway

A cytosolic heme protein may act as a sensor to detect decreased oxygen tension and to generate free radicals. This process, in turn, activates various transcription factors (88) including hypoxia inducible factor (HIF-1). HIF-1 stimulates transcription of multiple genes including VEGF in cell lines in response to hypoxia (89;90).

Subsequently, a hypoxia response element (HRE) for HIF-1 has been identified in the promoter region for VEGF receptor-1 and insulin like growth factor (IGF-1) (91). This suggests that HIF-1 signaling plays a role in VEGF mediated neovascularization in response to local retinal ischemia. VEGF acts as a major angiogenic stimulator early in the signaling cascade leading to retinal NV and it may also have a role in choriodal NV. Several new approaches attempt to modulate the VEGF signaling pathway to interfere with its angiogenic stimulation. Intravitreous injection of soluble VEGF receptors and antisense oligonucleotides for VEGF both reduce the retinal NV in a mouse model of ischemic retinopathy (47;48). Work in non-human primates has shown a reduction in NV of the iris following intravitreous injection of anti-VEGF antibody (46).

Current treatment options for patients with ocular neovascularization do not include antiangiogenic treatments, but these newer approaches hold promise. Recent reports have examined orally active drugs that inhibit the VEGF receptor kinase pathway and demonstrated that they can significantly reduce ocular neovascularization in mice.(92;93) Systemic inhibition of the VEGF pathway of angiogenesis raises safety concerns regarding the normal wound healing processes of the body that must be addressed before this could be applied clinically. To avoid concerns related to systemic angiogenic inhibition, local delivery of several agents is being investigated. Intraocular injections of an anti-VEGF antibody or an aptamer that binds VEGF have been tested for safety in phase I clinical trials and phase II-III trials are underway. Preliminary reports suggest that injection of the anti-VEGF antibody may induce a local inflammatory response, but it is not considered a severe enough problem to discontinue these approaches (94). Since the eye is an immune privileged site, it is unclear how this inflammation is occurring.

Another promising avenue of reducing the neovascular response is intraocular injection of endogenous proteins with known anti-angiogenic properties. Endogenous proteins are likely to be better tolerated than foreign antibodies or aptomers. Several proteins with purported anti-angiogenic activity have been identified (95-97), and intraocular injection of each of these alone or in combination could be considered. These large molecules all share the potentially limiting disadvantage of requiring repeated intraocular injection.

Inhibitors of VEGF-mediated NV

Pigment Epithelium-Derived Factor

Pigment epithelium-derived factor (PEDF) was first purified from human retinal pigment epithelial cultures as a member of the serine-protease inhibitor family (98) and as a factor that induces neuronal differentiation of cultured human Y79 retinoblastoma cells (95). PEDF is synthesized in retinal pigment epithelium (RPE) cells and secreted into the interphotoreceptor matrix (98). PEDF is found both intracellularly and extracellularly in the fetus and early adult eye but is lost at the onset of senescence (99;100). PEDF is a very potent inhibitor of corneal neovascularization (NV) in the rat eye. It also prevents endothelial cell migration towards a wide variety of angiogenic inducers exhibiting slightly greater activity than thrombospondin I, pure angiostatin, or endostatin in this in vitro assay (3). It is down-regulated by hypoxia and induced in the retina as a result of hyperoxia which suggests that the loss of this inhibitor may be central to the development of ischemia induced retinal NV. PEDF therefore appears to be a (the) major angiogenic regulator of the retinal vasculature and is an excellent candidate gene for therapy against ocular NV. As an intraocularly injected protein, PEDF delayed the loss of photoreceptors in the rd mouse (101). This implies that it can effectively disperse

throughout the retina, and, when expressed in a secretable form from a vectored gene, the effects of PEDF may be relatively independent of the retinal cell type supporting expression. Thus, one key experimental aim will be to test several promoter constructs regulating PEDF expression in different sets of retinal cells in order to maximize its level in vivo and availability to the retinal vasculature.

The crystal structure of glycosylated human PEDF was solved at 2.85 angstrom resolution in 2001 (102). This structural determination provides a basis for considering the many biologic roles of PEDF. The structure shows motifs of possible receptor sites as well as a heparin-binding site that might play a role in PEDF localization. Significantly, PEDF shares structural homology with other members of the serpin family but possesses an asymmetric charge distribution unlike any previously characterized serpin. It is not an active serine protease inhibitor despite structural similarities.

A putative 80-85 kDa receptor for PEDF has been isolated from retinoblastoma tumor cells (103) and is discreetly distributed on the surface of cells in the neural retinas of adult steers (104). These studies provide evidence for PEDF acting on photoreceptor and ganglion cell neurons and may provide insight into the neurotrophic and vascular functions of PEDF in the retina. However, it remains to be determined whether this receptor, or a related receptor, might be present on endothelial cells. PEDF seems to be selective in that it destroys newly forming vessels but does not harm existing vasculature. This selectivity makes PEDF a much more attractive candidate for anti-angiogenic therapy than non-selective therapies that inhibit endothelial growth factors systemically. Recent data suggest that PEDF discriminates between newly forming vessels and existing vessels by the same Fas ligand – Fas receptor system that is used in the immune system

to eliminate unwanted lymphocytes by apoptosis (105). This study also showed that the same mechanism is used by thrombospondin-1, another endogenous inhibitor of angiogenesis. Fas is a transmembrane receptor that binds to its ligand, Fas L, and initiates a caspase dependent apoptotic cascade leading to cell death. A more complete exposition of the Fas-FasL pathway can be found in the excellent review by Nagata & Golstein (106). PEDF induces the surface expression of the Fas ligand in endothelial cells. However, this effect alone is insufficient to confer the selectivity that PEDF seems to possess. In existing vessels, the Fas receptor is not present and survival signals such as survivin, Bcl-2, or FLIP are present at high levels. These factors protect such cells from PEDF induced apoptosis. By contrast, endothelial cells involved in new vessel formation display the Fas receptor due to the influence of angiogenic stimulators, such as VEGF. These migrating endothelial cells are therefore sensitive to PEDF-induced apoptosis. If the stimulators of angiogenesis are at sufficiently high levels, survival signals will also be present at levels that are capable of overriding the PEDF-stimulated Fas and endothelial cells will survive and go on to form new vessels (107). A delicate interplay of pro- and anti-angiogenic factors therefore controls the formation of new vasculature, and it is easy to imagine how this delicate balance could be disrupted by subtle biochemical changes and lead to pathologic neovascularization.

There are some experimental results suggesting that PEDF may be secreted preferentially from the apical surface of RPE cells (108). These data were derived from cultured RPE cells. If this is true *in vivo*, the apical secretion of PEDF may indicate that this factor has a greater role in controlling retinal vascular development than for choroidal vessels.

The gene for PEDF was localized to chromosome 17 by the analysis of 3 independent somatic cell hybrid panels (109). Fluorescence in situ hybridization showed localization at the terminal portion of 17p. The PCR analysis of somatic cell hybrids containing specific regions of 17 was subsequently used to sublocalize PEDF to 17pter-p13.1. Further studies used linkage analysis to narrow the localization of the PEDF gene to 17p13.3, the same region as that carrying the autosomal dominant retinitis pigmentosa locus (RP13) identified in a South African family (110).

Angiostatin

Angiostatin is a proteolytic fragment of plasminogen that possesses potent angiostatic properties. It is an endogenous regulator of vasculogenesis and, as a naturally occurring peptide, it is not likely to stimulate an immunogenic response (111;112). Neither plasminogen nor plasmin inhibits endothelial cell proliferation, nor does angiostatin affect coagulation. Although angiostatin is known to inhibit tumor growth *in vivo* by increasing apoptosis and inhibiting tumor associated angiogenesis, its precise mechanism of action is unclear. Apoptosis *in vitro* is induced in endothelial cells by multiple forms of angiostatin (113) and cells have been shown to be arrested at the G2/M transition interface (114). Administration of angiostatin to tumor bearing mice has not resulted in detectable systemic cytotoxicity; only angiogenic proliferation appears to be inhibited (115-117). Angiostatin therefore appears to be an effective and nontoxic inhibitor of NV that is worth evaluating in models of ischemic retinopathy. A recent study has indicated that Kringle 5 of angiostatin may induce PEDF and inhibit VEGF both in cell culture and a rat model of ischemic retinopathy (118).

Other Inhibitors of Ocular Angiogenesis

In addition to PEDF and K1K3 Angiostatin, other agents have been used to control ocular angiogenesis and need at least a mention. As is the case with many anti-angiogenic compounds, interferons were initially found to inhibit tumor angiogenesis in animal models and were suggested to be used as potential therapeutics in treating patients (119-121). Interferon alpha/beta also inhibits wound healing in another animal model (122). It was initially observed that patients undergoing systemic administration of interferon alpha for other disorders were presenting with various forms of retinopathy subsequent to the loss of their retinal vessels (123). At higher doses the systemic administration of interferon alpha was producing retinal ischemia by limiting or reducing the number of retinal vessels in the eyes of these patients. This same effect can be exploited by administering lower doses of interferon alpha to treat choroidal NV (124-127). Interferon alpha has also been successful in treating retinal NV in Behcet's disease (128) and has been suggested as a potential therapy for diabetic retinopathy (129). Interferon alpha failed to suppress corneal NV in animal model when applied topically or subcutaneously (130).

Endostatin, a proteolytic fragment of collagen XVIII, is an endogenous inhibitor of tumor angiogenesis. It has been suggested that vectored expression of this agent could be used to regulate pathologic angiogenesis in human diseases like cancer and various retinopathies (131-133). Since it is a naturally occurring inhibitor of angiogenesis, like PEDF, vectored expression should have minimal side effects. Recently endostatin has been demonstrated to inhibit VEGF-induced retinal vascular permeability, neovascularization, and retinal detachment when intraocularly delivered (134). It has also been effective in reducing choroidal NV when expressed from a systemically

administered adenoviral vector (135). Another recent study examined the correlation of VEGF and endostatin levels with the severity of diabetic retinopathy in human patients. The concentrations of VEGF and endostatin in aqueous humor and vitreous fluid were significantly correlated with the severity of DR. Specifically the levels of VEGF and endostatin differed significantly between active or proliferative DR and quiescent DR (136). This study suggests that ocular endostatin might be effective in controlling retinal as well as choroidal NV.

Biology of Adeno-Associated Virus

AAV is a non-enveloped virus of the family parvoviridae with a single-stranded 4681 base DNA genome and an icosahedral capsid composed of the three structural proteins VP1, VP2 and VP3. Adeno-associated viruses are termed dependoviruses meaning that they are not capable of autonomous replication. Instead they rely, in part, on the intracellular machinery from another concomitant viral infection to complete a lytic infection. AAV replication complexes have been isolated from cells coinfected with adenovirus, vaccinia, or herpes simplex virus as the helper (137;138). Without helper virus, AAV enters a latent phase, specifically integrating into the AAVS1 site on human chromosome 19 (139). Upon subsequent infection with a virus capable of providing helper functions, the AAV genome is excised from chromosome 19 and resumes the lytic phase. Site-specific integration is a characteristic not shared by recombinant AAV which is thought to remain largely unintegrated and occasionally integrate at random sites (140). Long-term stable integration during the latent phase of the AAV life cycle, is one of the attributes that makes this virus viable and attractive as a gene delivery system (141;142).

The AAV genome consists of two 145 base inverted terminal repeats (ITRs) and two overlapping reading frames that encode the Rep and Cap proteins. Rep transcripts

produced from the p5 and p19 promoters encode for Rep 78 and Rep 52 proteins respectively. Alternative splicing of both transcripts allows for the translation of smaller Rep proteins, Rep 68 and Rep 40. Rep 78 and 68 confer DNA excision and replication functions that are required for the lytic phase of the AAV life cycle. The capsid proteins (VP1, VP2, and VP3) are encoded from two alternatively spliced transcripts from the p40 promoter. The proteins VP2 and VP3 are translated from the same transcript using different initiation sites (138;142). These wild-type AAV proteins are provided in *trans* during the production of recombinant AAV. It was discovered that by removing the Rep and Cap genes it was possible to make AAV incapable of replication even in the presence of helper virus. Further, the removal of these viral genes accommodated the insertion of therapeutic genes and the development of rAAV as a viral vector.

Recombinant AAV Serotypes and Capsid Variants

Eight different serotypes of rAAV have been isolated and identified in primates (143-149). The different serotypes were isolated separately and have varying host ranges with some overlap. Serotypes 2, 3, and 5 have been characterized as deriving from human populations, whereas rAAV serotype 4 infects primarily non-human primates (143-148). The most recently isolated serotypes, 7 and 8, were derived from rhesus monkeys using molecular techniques (149). Most rAAV transduction experiments discussed here were performed with serotype 2 vectors. The various serotypes share a high level of homology on a genetic level with the exception of serotype 5 which is significantly divergent from other members of the group. The distinguishing characteristic among serotypes is the cell surface receptor to which each serotype will bind. The receptor for rAAV2 and rAAV3 is the heparin sulfate proteoglycan (150;151). Fibroblast growth factor receptor 1 (FGFR) and $\alpha_V\beta_5$ integrin also act as coreceptors for

rAAV2 (152;153). Serotypes 4 and 5 bind to N-linked sialic acid residues either directly as a receptor or as part of the receptor complex (154;155). Some unpublished data suggests that receptors for rAAV serotypes 1 and 6 may involve O-linked sialic acid. Various serotypes exhibit preferential transduction of target tissues. This tissue tropism is most likely due to the surface receptor displayed on the cells of that particular tissue type. Serotype 1 is more efficient than serotype 2 at transducing skeletal muscle cells (156). Within the eye, there seems to be increased transduction efficiency of the retinal pigmented epithelium by serotype 1 and 5 vectors over serotype 2 vectors.

Knowledge of the various receptor binding specificities of the different serotypes has led to methods of viral purification that can efficiently produce vectors for any of the serotypes 1-6 (145;148;151;157-159). The transduction efficiency of these variously serotyped and pseudotyped AAV vectors is being investigated by a number of groups.

Another potential method of conferring tissue or cell-type specificity for AAV vectors involves modification of the capsid proteins. AAV2 capsid proteins have been modified to expose alternate ligands on the surface of rAAV thus altering its cellular binding specificity (160). Another possibility for increasing or modifying viral specificity involves direct modification of the capsid protein through molecular manipulation. Either a specific ligand can be targeted or phage libraries, expressing different peptides on their surface, can be used to scan tissues for protein sequences that bind preferentially. The nucleotides encoding the specific ligand can be inserted into the capsid gene at a region which will expose the ligands on the outer surface of the viral particle. One group has modified VP3 in this manner to target AAV2 to cells expressing

integrins. This allows infection of cell types expressing integrins independent of the heparin sulfate proteoglycan, the virus's primary attachment receptor (161).

Adeno-Associated Virus as a Vector

The work presented in this dissertation will focus on the use of rAAV vectors as a means of delivering anti-angiogenic factors to the retina. I chose rAAV serotype-2 to deliver the therapeutic genes because issues regarding attainment of high vector titers have been resolved (162) and rAAV preparations free of contaminating replication competent rAAV are now routine(162;163). Recombinant AAV mediated gene delivery results in long term expression in a wide variety of tissues, including various cell types in the retina(164) and optic nerve(165). Finally, rAAV vectors have shown very little *in vivo* toxicity in a variety of tissues(166).

Gene Based Therapies

The use of gene based therapy for the treatment of ocular neovascular disease offers advantages over conventional methods. By using a viral vector with a selective promoter to express the anti-angiogenic protein or factor locally, expression can be limited to a specific cell type or subset of cell types within the retina. This reduces the safety concerns relative to systemic administration of anti-angiogenic agents. Delivery of the vector to discreet compartments within the eye by sub-retinal or intravitreous injection may allow additional control of expression to only those local vessels affected. Choice of the appropriate viral vector for delivery of the therapeutic gene allows modulation of the duration of expression. Adeno-associated viral vectors appear to provide extended, perhaps even life-long, expression of therapeutic proteins within the eye. This may obviate the need for repeated intraocular injections in the case of chronic NV disease such as PDR or AMD. One conceivable treatment scenario is that patients

seen for surgical or laser treatment of active neovascularization could receive concurrent vector treatment that would provide long-term protection from subsequent neovascular events.

In addition to the work presented here, several alternative virally-vectored approaches have been reported recently. An adeno-associated viral vector encoding the soluble VEGF receptor 1, sFlt-1, shows promise for long-term inhibition of two types of ocular neovascularization (167). This vector, when injected into the anterior chamber, resulted in expression in both the corneal endothelium and iris pigment epithelium and reduced corneal NV by 36%. Subretinal injection of the same vector reduced choroidal NV subsequent to laser lesions around the optic nerve. These results suggest that a secretable factor expressed in one or more transduced cell populations can be effective in the control of ocular NV occurring in a disparate cell population. Since AAV mediated gene delivery allows the long-term expression of transgenes, this therapeutic strategy may provide long-term protection from ocular NV.

Another gene based approach to treating neovascular disease involves the virally mediated intraocular expression of anti-angiogenic agents. Several factors that have been identified as potential angiogenic inhibitors could be delivered in a viral-vectored system rather than by direct injection. By expressing the angiogenic inhibitor directly where it is needed and for a longer duration than a single protein injection, greater efficacy in the control of disease may be possible. In addition to our studies, this strategy was tested by expressing several anti-angiogenic factors from AAV vectors: tissue inhibitor of metalloproteinase-3 (TIMP3), PEDF, and endostatin (168). Each of these factors successfully reduced the level of neovascularization in an ischemic mouse model

of retinopathy of prematurity. A similar strategy is also being tested in a phase I clinical trial using adenovirus to deliver PEDF as a potential treatment for wet AMD(169). Adenovirus vectors have a shorter expression period than that mediated by AAV, a difference that might be exploited depending on the exogenous factors being expressed and the target ocular disease.

CHAPTER 2
VECTOR PLASMID DNA CONSTRUCTION

The initial goal of this dissertation project was to develop a series of AAV vectors using different promoters to target expression of PEDF and K1K3 angiostatin to the retina. I aimed to target the widest variety of retinal cell types as is currently possible. Five promoters will be used that target expression of the potentially therapeutic genes to subsets of cells in the retina. I chose a set of promoters that restrict expression of genes to different specific subsets of retinal cells. The 11-cis retinaldehyde binding protein (CRALBP) promoter, spanning nucleotides -2265 to -1 (Figure 2-1), drives expression in retinal pigmented epithelium (RPE) cells (170). The CRALBP promoter was initially analyzed in vitro in three different RPE cell lines and other non-ocular cell lines. These data suggest that basal promoter elements in the *RLBP1* gene exist between -243 and +80 bp and that element(s) that enhance CRALBP expression in RPE cells exist between -2089 and -1539 bp (170). The proximal mouse rod opsin (MOPS) promoter, spanning -385 to +86 in (Figure 2-1), targets expression to the photoreceptor (PR) cells (164;171). The efficiency and specificity of this MOPS promoter in the retina was established by gene transfer of reporter genes from rAAV vectors (164). The platelet derived growth factor (PDGF) promoter (172), labeled as -1600 to -1, will direct expression primarily in the retinal ganglion cells (RGC). The chicken beta-actin (CBA) (173;174) and cytomegalovirus (CMV) (175) promoters are more ubiquitous, leading to expression in multiple retinal cell types including the RPE and PR, or RGCs. This ubiquitous expression has been shown from numerous studies with reporter and therapeutic gene

expression following injection of vectors (165;173-176). Figure 2-1 is a diagram of each promoter construct driving PEDF in AAV vectors. Each vector-promoter construct could be then tested by either intravitreal or subretinal vector inoculation and ELISA quantitation of ocular PEDF levels.

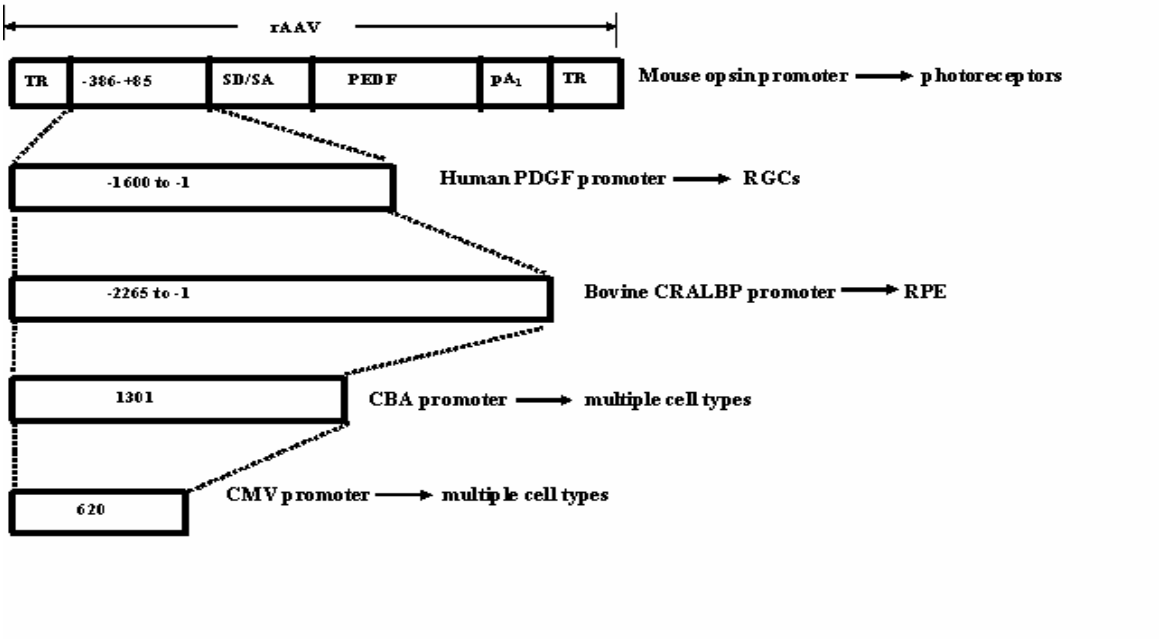

Figure 2-1. Diagram of rAAV vector constructs with PEDF gene. The basic rAAV is depicted with flanking terminal repeat (TR) sequences, followed by the promoter, and a splice donor/ splice acceptor from SV40 virus, the cDNA of either PEDF or K1K3, and a SV40 polyadenylation signal.

Plasmid Design

The work of constructing clones of K1K3 cDNA behind the promoters described above had been previously completed by Denis Beliaev in our group. These plasmids were used as the template for creating clones with PEDF as the transgene. The K1K3 angiostatin cDNA is shown in figure 2-2.

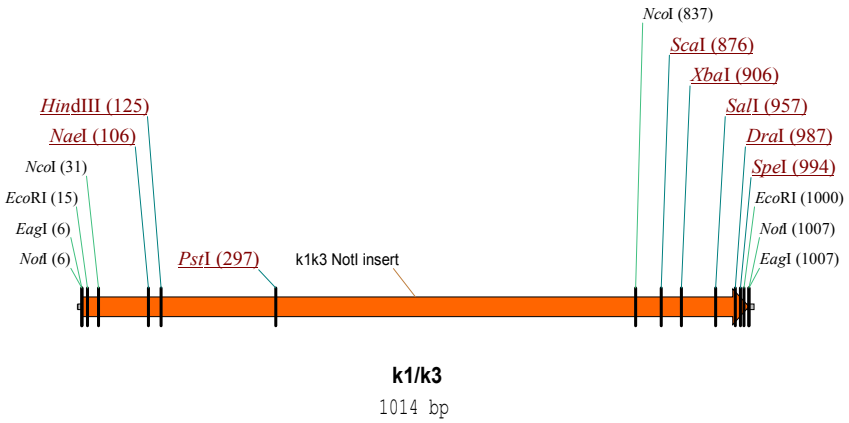

Figure 2-2. Map of the K1K3 cDNA insert with flanking NotI sites. The map was constructed from sequence in Vector NTI depicting the K1K3 Angiostatin insert flanked by NotI sites.

The above figure (2-2) is a map of the insert fragment containing the cDNA for K1K3 angiostatin and is 1014 base pairs in length. The flanking NotI sites allow insertion of the K1K3 fragment into the promoter-vector recipient fragment. An example of this kind of insertion is depicted in figure 2-3.

This map in figure 2-3 depicts a plasmid DNA that was cloned by Denis Beliaev. It served at the backbone for cloning CBA-PEDF as it already contains the chicken beta-actin hybrid promoter with the cytomegalovirus enhancer element. In order to clone in the cDNA for PEDF, it was a matter of digesting out the fragment containing K1K3, gel purifying the larger vector fragment, and religating with the complementary PEDF fragment.

The cDNA encoding human PEDF was received as a gift from Dr. Peter Campochiaro (Johns Hopkins University). The cDNA was initially in a vector called pT7T3-Pac PEDF. The PEDF cDNA was flanked by a 5' EcoRI and a 3' NotI site. Most other flanking sites in the polylinker would possibly cut within the PEDF cDNA. EcoRI

and NotI each occur only once in the vector and can therefore be used to excise the PEDF cDNA.

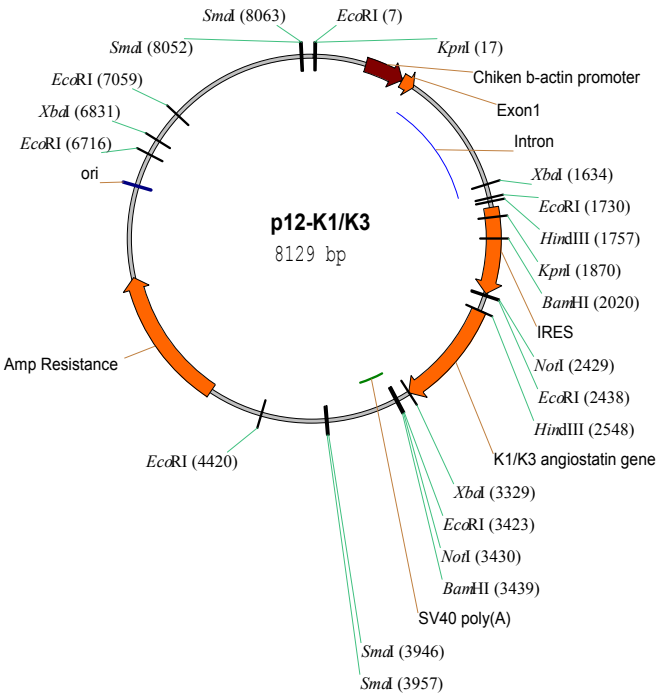

Figure 2-3. Example of a plasmid containing K1K3. Depicted in the map are the elements for the chicken-beta actin promoter/ cytomegalovirus enhancer, the coding region for K1K3 angiostatin, and a region coding for ampicillin resistance. A limited number of restriction sites are shown on the map. The repeats of SmaI sites at 8052, 8063 and 3946, 3957 are in the inverted terminal repeats needed for rAAV packaging.

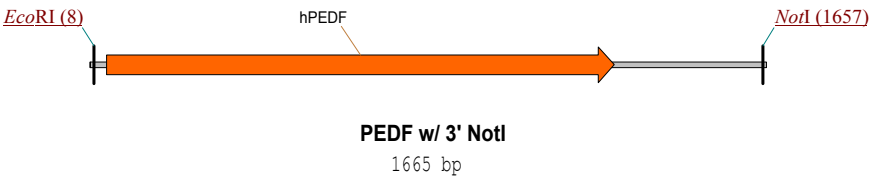

Figure 2-4. PEDF cDNA insert with a 3' NotI site

Following digestion with EcoRI is was necessary to insert a second NotI site at EcoRI site to allow the PEDF cDNA to be dropped out of its current vector and into the plasmid vectors in the place of K1K3. I chose to construct an oligo linker with EcoRI overhangs at either end and a NotI site in the middle. In order to provide proper annealing, I inserted a 10 base non-specific sequence 5' to the new NotI site in the oligo linker. The total sequence of the linker is depicted below:

EcoRI Non-Specific Insert NotI insert EcoRI

AAT TCA TAT GGG ATA GCG GCC GCG

GT ATA CCC TAT CGC CGG CGC TTA A

Insert Preparation

The oligos were mixed together at an equimolar concentration of 1 nmol/µl and heated to 65˚C for 3 minutes and then allowed to anneal together at room temperature. The original pT7T3-Pac PEDF vector was digested with EcoRI to open the plasmid. The vector was phenol:chloroform extracted, ethanol precipitated, and treated with alkaline phosphatase to limit auto-ligation. Two ligations were performed. One ligation was with a vector to insert ratio of 1 to 10, the other ligation was 1 to 1 ratio of vector to insert. The reactions were cleaned of the ligation reagents through phenol:chloroform extraction and ethanol precipitation.

Once reconstituted, this plasmid DNA was transferred into competent cells (XL10 Gold, Stratagene) by electroporation. The transformed bacteria were plated out in serial dilution onto LB ampicillin agar plates for selection. The ampicillin resistance conferred by transformation with the plasmid would be present whether the ligation included the insert or not. There is a chance that the vector simply auto-ligated despite treatment with phosphatase. Because of this, it was necessary to screen the colonies for incorporation of

the insert. Colonies were selected off the plates for the 1:1 and 1:10 vector to insert ligations and grown overnight in liquid Luria broth media at 37˚C. These cultures were used to extract plasmid DNA harvested from the ligation clones by miniprep protocol (Promega). This prepared plasmid DNA was then digested with NotI. If the insert had been incorporated the vector would now have two NotI sites creating two fragments that could be visualized on a 1% agarose gel. The auto-ligated vector would only have one NotI site.

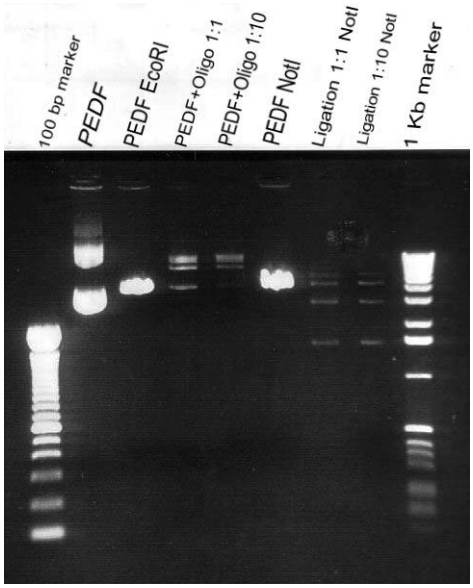

Figure 2-5. Digestions and ligations of pT7T3-Pac plasmid containing the PEDF cDNA. Samples were mixed with DNA loading dye and run on a 1% agarose gel at 120 volts for 1.5 hours. The running buffer was 0.5X TBE. The marker standards are 100 bp and 1Kb ladders from Promega.

As shown in figure 2-5, the original pT7T3-Pac PEDF plasmid was ligated with an oligo to add an additional NotI site to drop out PEDF. All samples were mixed with DNA loading dye containing 0.25% bromophenol blue, 0.25% xylene cyanol, and 30% glycerol in water and run on 1% agarose gel in a horizontal electrophoresis bed. The running buffer used was 0.5X Tris-borate EDTA (TBE). The gels were run at 120 volts

for approximately 1.5 hours. The DNA marker standards were 100 bp and 1Kb ladders from Promega (Madison, Wisconsin, US). The upper band in the lane labeled PEDF is genomic DNA from the bacteria. This band is not present in the next lane with EcoRI digestion. The next two lanes show the ligation reactions with the vector to insert ratios of 1:1 and 1:10. Again, the upper bands represent genomic bacterial DNA. The oligo insert is too small to increase the size of the plasmid to this degree. Next the vector and the ligation reactions were digested with NotI. In the case of the original vector, only one band is resolved indicating that the plasmid has been opened at the solitary NotI site. Each of the two ligation reaction colonies that were chosen has a similar banding pattern on digestion with NotI. There are four bands in each of these lanes. This pattern indicates a partial digestion by NotI. The uppermost, faintest band is likely partially digested ligated vector. The next band in each lane is ligated vector that has not been digested and remains as a closed, circular piece of DNA. Then the two lower bands represent the two fragments of the vector when NotI cuts at both sites. The lower band is the PEDF cDNA fragment now flanked by NotI sites and ready for cloning into our vector constructs.

The initial miniprep plasmid DNA yield was insufficient for our further cloning into each of our expression vectors. In order to obtain a larger amount of the PEDF fragment flanked by NotI sites, 100 µl of the culture of transformed bacteria were used to inoculate a larger volume (1L) of Luria broth containing ampicillin. Again this was grown overnight at 37˚C. Samples of this culture were processed by both the miniprep and maxiprep method (Promega) to extract the cDNA. The extracted plasmid DNA was digested with NotI and run on a 1% agarose gel to separate the bands.

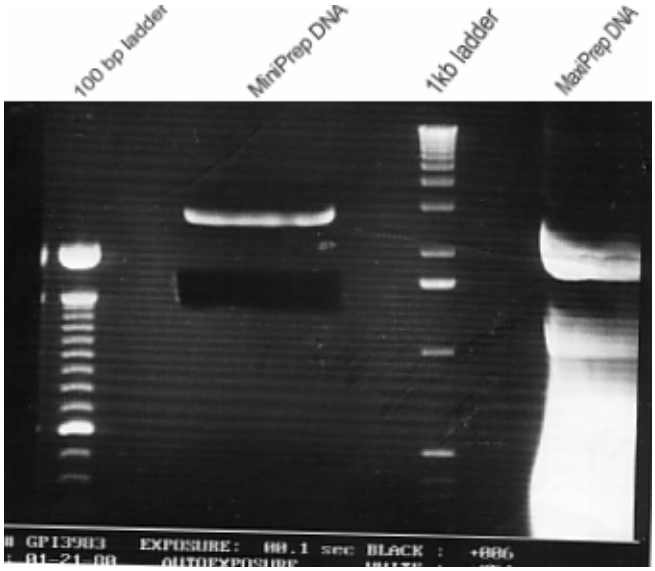

Figure 2-6. Example of a fragment separation gel of large scale plasmid preparation digested with NotI. The fragment with NotI flanked PEDF band has been cut out for purification. Samples were mixed with DNA loading dye and run on a 1% agarose gel at 120 volts for 1 hour. The running buffer was 0.5X TBE. The marker standards were 100 bp and 1Kb ladders from Promega.

In figure 2-6, the maxiprep lane was overloaded and did not produce clean bands. The miniprep lane did yield a clean, robust band for PEDF at 1.3 Kb. This band was excised and the insert fragment DNA extracted from the gel with a kit (Qiagen). In this way, the PEDF fragment was isolated in preparation for insertion into the vector plasmids.

PEDF Plasmid Assembly

As mentioned previously, the transgenes, K1K3 or PEDF, were each inserted between Not I sites in the vector plasmids. To replace the K1K3 insert with PEDF, each of the plasmids was digested with NotI to drop out the K1K3 insert. Then, the appropriate vector fragment of the plasmid was separated from the insert fragment by gel purification similar to the procedure used to separate the insert fragment containing PEDF. Finally, the plasmid vector fragment from the former digest was ligated with the

PEDF insert fragment with flanking NotI sites. In this manner, each of the plasmids containing PEDF and the promoters discussed above were constructed.

These plasmids were used to transform bacteria that were then screened to check for plasmids that contained the vector with the PEDF transgene. This procedure was conducted as discussed earlier in this section describing the addition of a NotI site to the PEDF cDNA. The colonies obtained from each of the transformations were screened first by digestion with NotI to determine if the PEDF transgene was present in the vector.

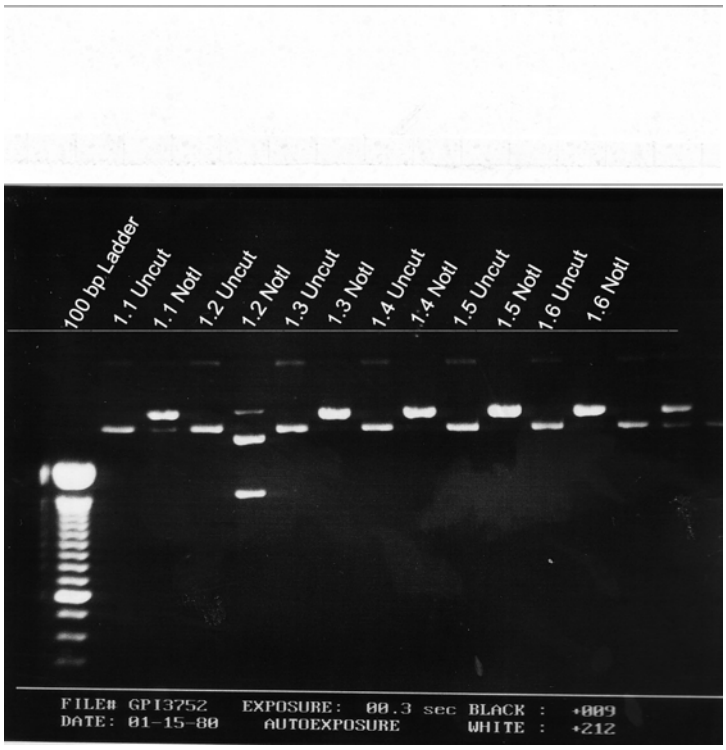

Figure 2-7. NotI digests of minipreps grown from colonies transfected with CMV-PEDF ligation product. Digest of colony 1.2 is the only one that shows a PEDF-containing fragment after digestion. Samples were mixed with DNA loading dye and run on a 1% agarose gel at 120 volts for 1.5 hours. The running buffer was 0.5X TBE. The marker standard was a 1Kb ladder from Promega.

As depicted in figure 2-7, colonies from the ligation reaction do not uniformly produce the expected ligation product. By digesting the minipreps from these colonies

with NotI I can determine which of the ligation products contains the insert. If the insert is present, two bands will be visible on the gel as seen for colony 1.2 in figure 2-7. If the vector ligated back on itself, the NotI digest would simply open the plasmid at this single NotI site producing a single linear fragment as seen in the other lanes in the same figure. A map depicting the new CMV-PEDF plasmid is shown in figure 2-8.

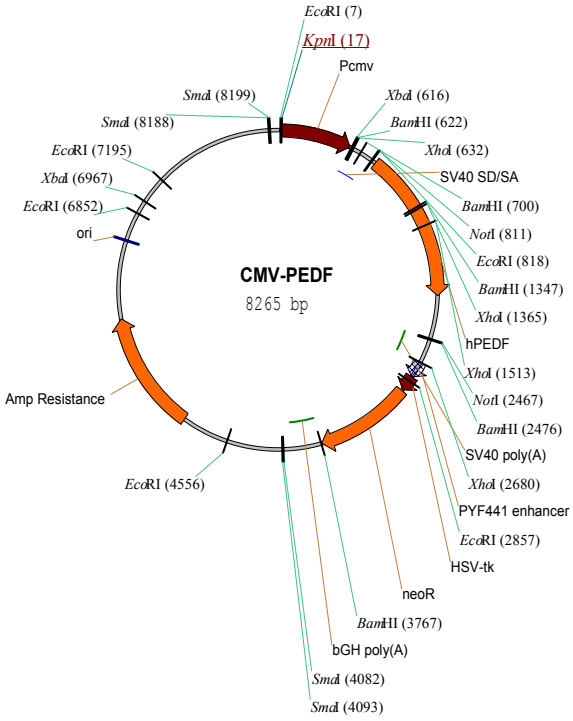

Figure 2-8. Plasmid vector with PEDF and CMV promoter. Depicted in the map are the elements for the cytomegalovirus promoter, the splice donor/splice acceptor site from SV40, the coding region for PEDF, the SV40 poly-adenylation signal, and regions coding for ampicillin and neomycin resistance. A limited number of restriction sites are shown on the map. The repeats of SmaI sites highlight the inverted terminal repeats needed for AAV packaging.

The other promoter vector constructs were prepared by a similar protocol to the first. For each vector construct, the K1K3 insert was dropped out by a NotI digest. The vector fragment retaining the promoter was gel purified and ligated with the PEDF insert fragment developed as described earlier in this chapter. The colonies produced from each

of these ligations were screened by NotI digestion to look for the 1.3 Kb band representing the PEDF insert. The next vector construct to be made after the initial CMV-PEDF plasmid was MOPS-PEDF. Following a similar procedure to that used for CMV-PEDF construction, the MOPS-K1K3 plasmid was digested with NotI to drop out the K1K3 insert. The promoter-vector fragment was gel purified and ligated to the PEDF insert. Plasmid DNA from individual colonies was screened by NotI digestion to determine which contained the complete MOPS-PEDF construct (Figure 2-9).

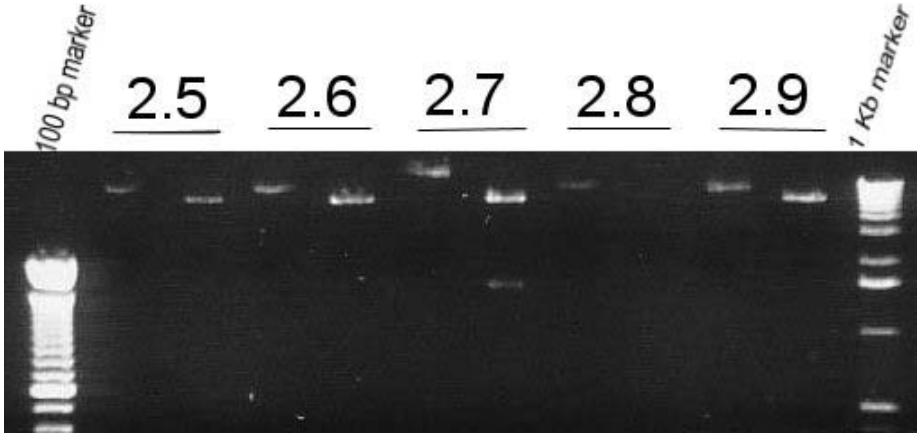

Figure 2-9. NotI digests of minipreps from colonies transfected with MOPS-PEDF ligation product. Digest of colony 2.7 shows a PEDF fragment at the expected size of 1.3 Kb. Samples were mixed with DNA loading dye and run on a 1% agarose gel at 120 volts for 1 hour. The running buffer was 0.5X TBE. The marker standards were 100 bp and 1Kb ladders from Promega.

A map depicting the MOPS-PEDF plasmid is shown in figure 2-10. Now that the cloning methods had been worked out sufficiently with the CMV-PEDF and MOPS-PEDF constructs, it was a matter of repetition to construct the other clones in a similar manner. CBA-PEDF, CRALBP-PEDF, and PDGF-PEDF promoter constructs were screened as discussed previously (Figures 2-11 and 2-12).

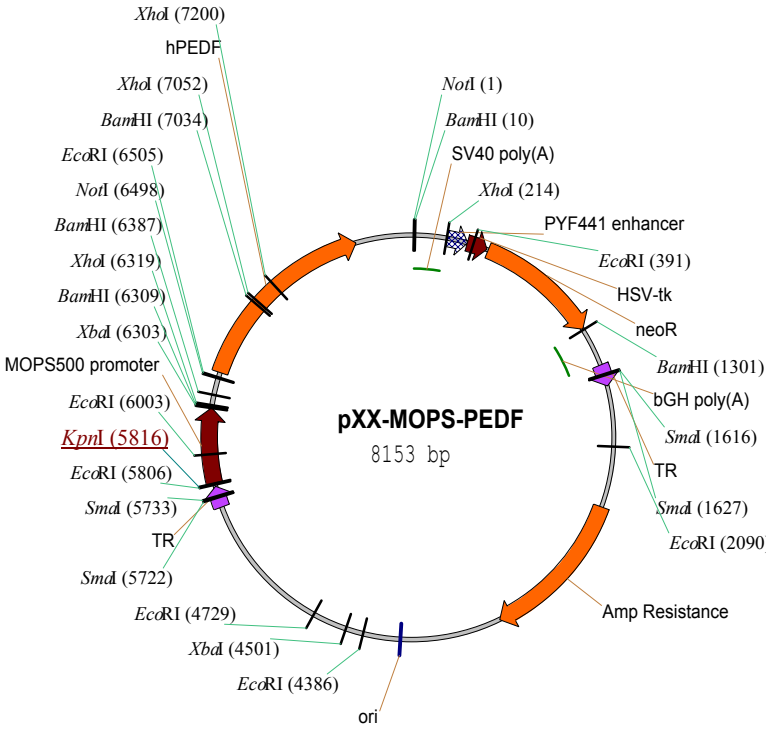

Figure 2-10. Plasmid vector with PEDF and MOPS promoter. Depicted in the map are the elements for the mouse rod opsin promoter, the coding region for PEDF, the SV40 poly-adenylation signal, and regions coding for ampicillin and neomycin resistance. A limited number of restriction sites are shown on the map. The repeats of SmaI sites highlight the inverted terminal repeats needed for AAV packaging.

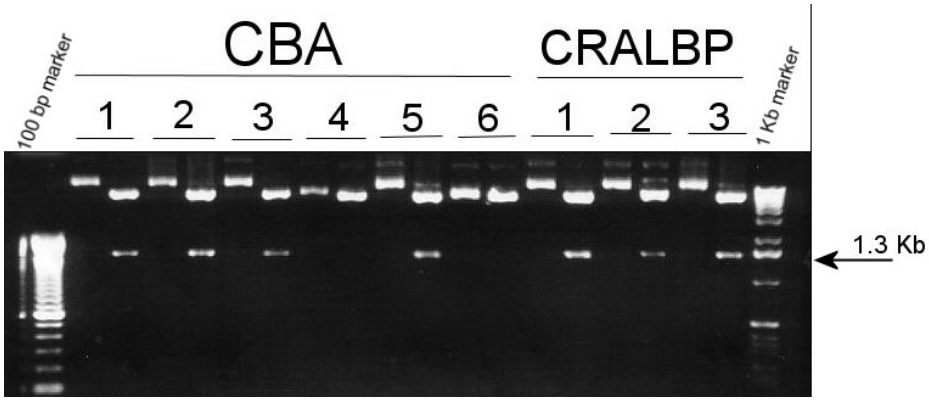

Figure 2-11. NotI digests of colonies transfected with CBA-PEDF and CRALBP-PEDF. Each colony is numbered and paired with an undigested sample in the left lane and a NotI digested sample in the right lane. CBA colonies 1, 2, 3, and 5 show 1.3 Kb band for PEDF. CRALBP colonies 1, 2, and 3 show 1.3 Kb band for PEDF. Samples were mixed with DNA loading dye and run on a 1% agarose gel at 120 volts for 1.5 hours. The running buffer was 0.5X TBE. The marker standards were 100 bp and 1Kb ladders from Promega.

As figures 2-11 and 2-12 depict, constructs for each of the remaining promoters were made according to the techniques discussed earlier in this chapter. I was able to select colonies for each of these constructs to grow as large cultures and submit for viral packaging. Maps for each of these constructs are in the following figures.

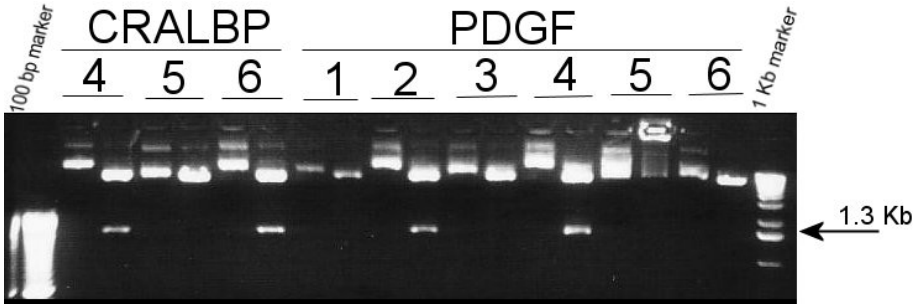

Figure 2-12. NotI digests of colonies transfected with CRALBP-PEDF and PDGF-PEDF. CRALBP colonies 4 and 6 show 1.3 Kb band for PEDF. PDGF colonies 2 and 4 show 1.3 Kb band for PEDF. Samples were mixed with DNA loading dye and run on a 1% agarose gel at 120 volts for 1.5 hours. The running buffer was 0.5X TBE. The marker standards were 100 bp and 1Kb ladders from Promega.

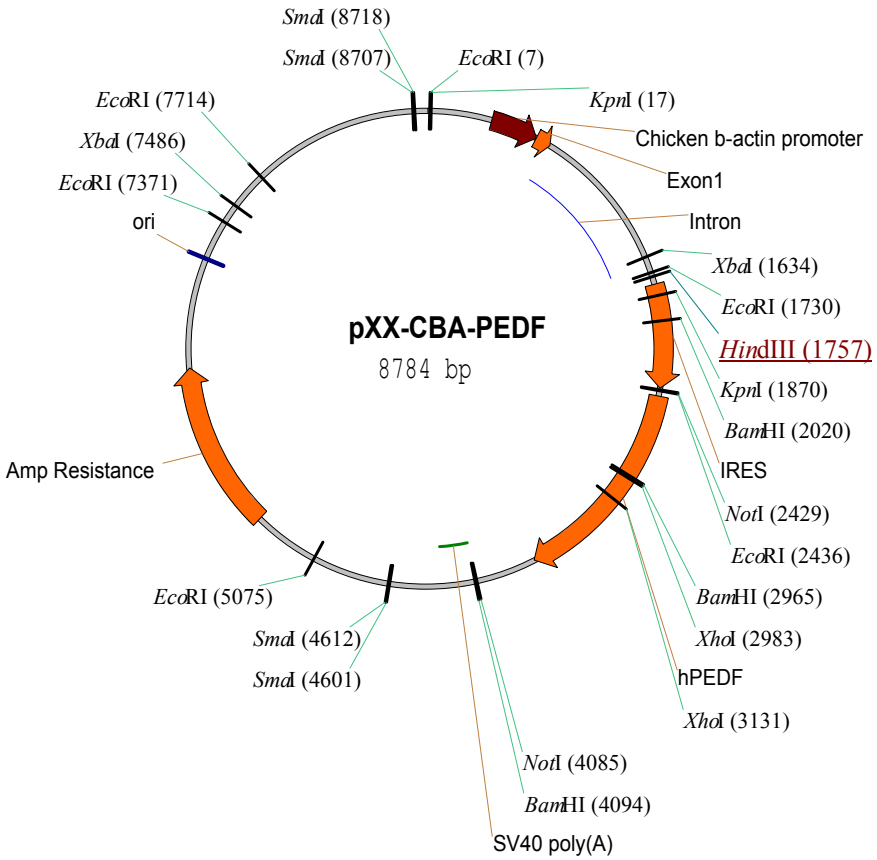

Figure 2-13. Plasmid vector with PEDF and CBA promoter. Depicted in the map are the elements for the chicken beta-actin promoter/ cytomegalovirus enhancer, the internal ribosome entry site, the coding region for PEDF, the SV40 poly-adenylation signal, and a region coding for ampicillin resistance. A limited number of restriction sites are shown on the map. The repeats of SmaI sites highlight the inverted terminal repeats needed for rAAV packaging.

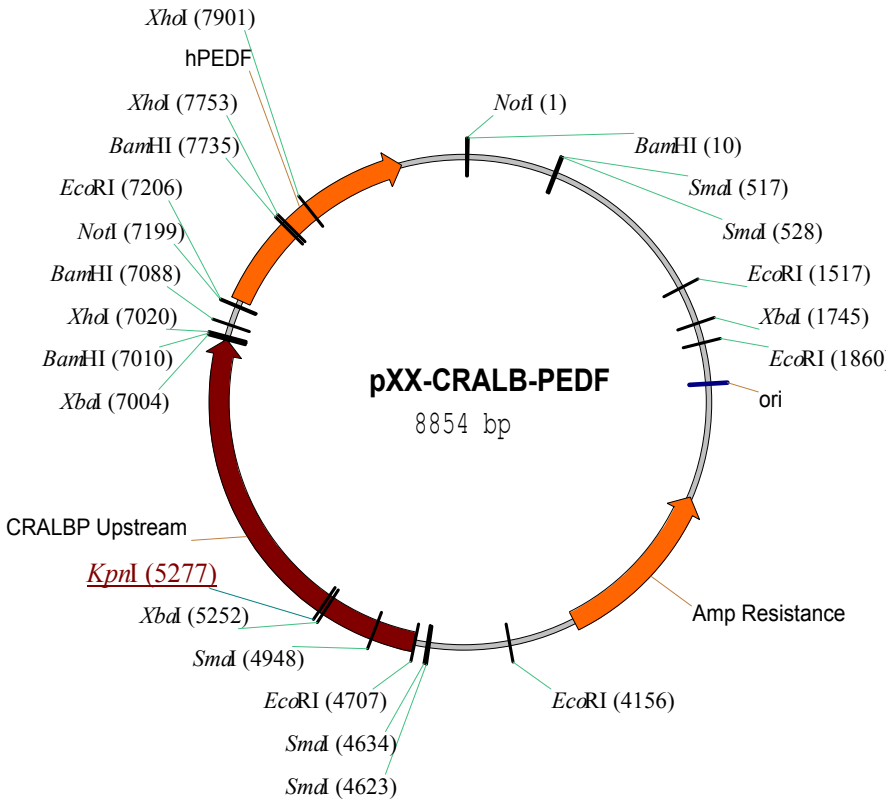

Figure 2-14. Plasmid vector with PEDF and CRALBP promoter. Depicted in the map are the elements for the 11-cis retinaldehyde binding promoter, the coding region for PEDF, and a region coding for ampicillin. A limited number of restriction sites are shown on the map. The repeats of SmaI sites highlight the inverted terminal repeats needed for rAAV packaging.

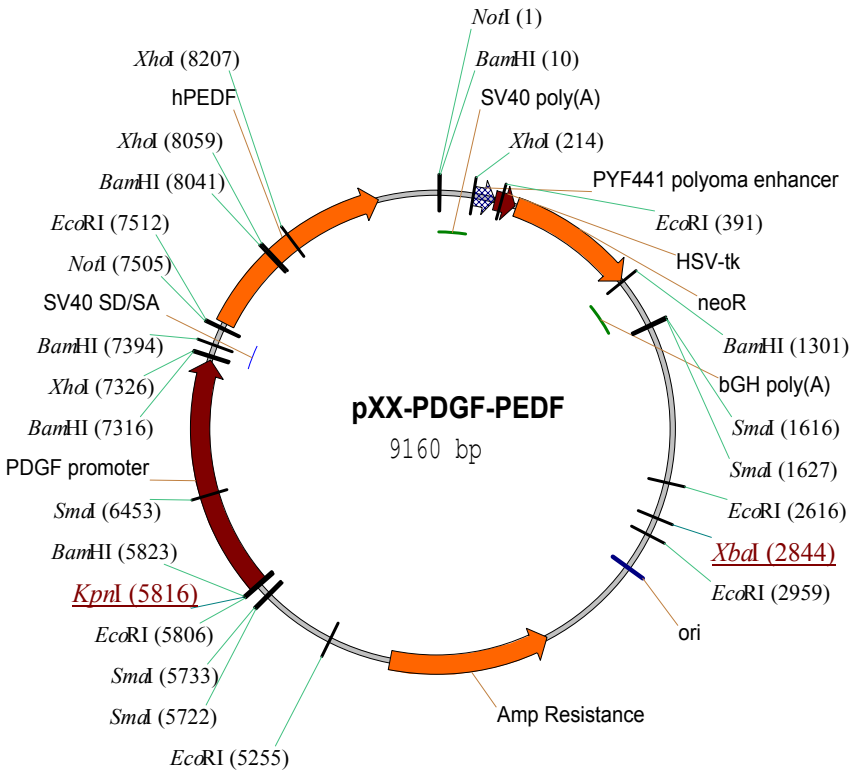

Figure 2-15. Plasmid vector with PEDF and PDGF promoter. Depicted in the map are the elements for the platelet derived growth factor promoter, the splice donor/splice acceptor site from SV40, the coding region for PEDF, the SV40 poly-adenylation signal, and a regions coding for ampicillin and neomycin resistance. A limited number of restriction sites are shown on the map. The repeats of SmaI sites highlight the inverted terminal repeats needed for rAAV packaging.

Orientation of PEDF cDNA

Our cloning method inserts the cDNA for PEDF between two NotI sites, leaving orientation of the insert in question. Colonies that show positive incorporation of PEDF cDNA may have the insert with the coding or non-coding strand following the promoter. Only the cDNA with the coding sequence properly oriented after the promoter will produce the desired protein. For this reason, it is necessary to perform an additional screening step on clones that possess the cDNA insert. By choosing a restriction enzyme that cuts once within the PEDF cDNA and at least once within the vector I can determine whether any particular clone has the cDNA in the correct or incorrect orientation. The

restriction enzyme KpnI cuts once in the PEDF cDNA as depicted in the map shown in figure 2-6. KpnI also cuts in the vector bearing the CBA promoter at two sites proximal to the insert site as shown in the map in figure 2-13. There should be three fragments resulting from a KpnI digest of the CBA-PEDF construct. The size of these fragments can determine the orientation of the insert.

Figure 2-16. KpnI digest of CBA-PEDF constructs for orientation. Colonies 19, 21, and 29 possess PEDF cDNA in the correct orientation. Minipreps of colonies were each digested with KpnI, mixed with DNA loading buffer, and run on a 1% agarose gel at 120 volts for 2 hours. The running buffer was 0.5X TBE. The marker was the 1 Kb ladder from Promega.

As shown in figure 2-16 each minipreps DNA from each colony was digested with KpnI resulting in three DNA fragments. If the insert is in the correct orientation, digestion with KpnI should yield fragments of 5700, 1850, and 1009 base pairs. In the incorrect orientation, the fragments should be 5300, 1800, and 1500 base pairs. While the two larger sized fragments would be difficult to distinguish, the smallest fragment tells the story quite effectively. The digests of miniprep DNA from colonies 19, 21, and 29 clearly show a band at approximately 1 Kb that corresponds to the smallest fragment expected from a construct with PEDF in the correct orientation. Similar tests for orientation could be designed for the other PEDF constructs.

Discussion

The vector that I wanted to use has NotI sites flanking the location where the therapeutic gene was to be inserted. The PEDF gene element that I received from the Campochiaro lab has a 3' NotI site and a 5' EcoRI site. I decided that the most straightforward way to solve this cloning problem was to add a 5' NotI site onto the end of the PEDF gene element. Oligos were designed that would anneal with the each other and leave a sticky end overhang that would match up with EcoRI site on the PEDF gene element. Embedded in these oligos would be the recognition site for NotI. Once the oligos annealed and matched up with the 5' EcoRI site, I would effectively have a PEDF gene element that was flanked by NotI sites and could be dropped into any of the vector constructs containing different promoters.

In retrospect, the cloning would have been more efficient had I modified the vector fragments to accommodate the EcoRI 5' site in the PEDF insert. This would have eliminated two problems. First, the orientation of the insert following ligation would never be in question. If the ligation of vector and insert was successful, then the product would have the insert in the proper orientation after the promoter. Second, neither the vector or the insert fragment would be self-ligating. As it was in our initial cloning strategy, both the vector and insert fragment terminate in matching NotI sites. If the insert closes on itself and is transfected into a bacterial cell, the Amp resistance gene is not present and the cell will not form a colony. However, if the vector fragment closes on itself, the resulting plasmid does confer Amp resistance to a transfected cell and a colony can be formed on Amp+ plates. I reduced the probability of self-ligation by phosphatase treating the vector fragment, but this also reduces the overall cloning efficiency. Even with the phosphatase treatment, many of the positive colonies were

confirmed to contain only self-ligated vector. However, overall, all promoter PEDF rAAV vector constructs were successfully made.

CHAPTER 3
VECTOR ANALYSIS

After reaching the initial goal of developing a series of rAAV vectors using different promoters to target expression of PEDF and K1K3 angiostatin to the retina, it was necessary to analyze the expression levels to determine the optimal candidate for therapeutic application. Five promoters will be analyzed for their ability to target expression of the potentially therapeutic genes to subsets of cells in the retina. As discussed in chapter 2, the CRALBP, MOPS, and PDGF promoters each target specific subsets of cells in the retina. The CBA hybrid and CMV promoters drive expression less specifically in many retinal cell types depending on the site of injection. Each vector-promoter construct was tested by either intravitreal or subretinal vector inoculation. Since PEDF is naturally secreted and K1K3 was engineered to be secreted, whole eye cups with the lens removed were analyzed for vector expression by ELISA. This does not differentiate expression by cell type, but provides a more rapid assessment of vector effectiveness. In the future it might be advantageous to localize and characterize the expression from various promoter vector constructs by in-situ hybridization or immuno-staining after a stringent wash to remove secreted proteins. However, the secreted nature of the transgenes is likely to make it difficult to localize expression confidently except by RNA analysis.

Protein Production

Before any determination of vector expression levels could be made, PEDF had to be expressed in a bacterial system, isolated, and purified to serve as an ELISA standard

for further measurements. A commercial source for purified PEDF was not available at the commencement of this dissertation project. Therefore I used a plasmid containing the cDNA for human PEDF with a C-terminal octa-histidine tag under the control of an IPTG inducible promoter (gift of P. Campochiaro). This plasmid was transfected into BL21 cells (Promega, Madison, WI) and grown overnight under selection with chloramphenicol (37 μg/ml) to an O.D. of 1.6 in a 1L volume of Luria broth. A 1ml sample of these cells was removed at this point and labeled as uninduced. IPTG was added to a final concentration of 0.6 mM to induce production of the PEDF protein. A 1ml sample of the cells one hour after induction was removed and labeled as induced. The remaining cells from the culture were harvested at two hours post-induction. The entire induced culture was pelleted by centrifugation at 2500 x *g* for 20 minutes at 4˚C. The supernatant from this step was discarded and the cell pellet resuspended in 50 ml STET buffer (0.1M NaCl, 10 mM Tris, 1 mM EDTA, 5% Triton X-100, pH 8.0) with 10 mg/ml lysozyme. The cells were then lysed by sonication of 10ml aliquots at a time on wet ice to disrupt the cells completely. Sonication involved alternating 15 second on/off intervals to prevent the cell suspension from overheating. The fully lysed cell suspension was separated by centrifugation at 10,000 x *g* for 20 minutes at 4˚C. The pellet of this separation was discarded and the supernatant was centrifuged again under the same conditions. The final supernatant of the centrifugation was retained. Two 1 ml samples were removed from both the lysed cell pellet and the retained supernatant and were labeled as crude pellet and crude supernatant respectively.

Protein Purification

Imidazole was added to the remaining crude supernatant to a final concentration of 10 mM. This solution was then mixed with a 2 ml slurry of NiNTA beads (Qiagen,

Valencia, CA) and incubated on a rotary shaker at 200 RPM for 1 hour. After this incubation, the lysate/bead mixture was centrifuged at 10,000 x *g* for 2 minutes to pellet the beads and all but 25 ml of the supernatant is removed. The NiNTA beads were resuspended in this remaining quantity of supernatant and loaded as a slurry to pack a column. The gravity flow-through column used only holds 15 ml volumes at a time, so multiple loadings onto the same column were needed. The finished column had a bed volume of approximately 2 ml.

The NiNTA system takes advantage of the C-terminal octa-histidine tag present on our expressed PEDF protein. The histidine residues have a binding affinity for nickel that causes the expressed protein to become attached to the agarose beads. When these beads are packed as a column, the expressed PEDF remains attached through the C-terminal His-tag. The column can be washed with relatively low molarity Imidazole (20 mM) to remove any contaminating unbound protein. Increasing concentrations of imidazole weaken the interaction between histidine residues and nickel conjugates. Imidazole concentrations of 100 mM, 250 mM, and 750 mM can be used to elute the bound PEDF off the column. Samples of each of these fractions were loaded into wells of a 12% Tris HCl polyacrylamide gel along with SeeBlue Plus 2 pre-stained standards (Invitrogen, Carlsbad, CA) and samples from the uninduced total cell and induced total cell. The PAGE analysis of these initial elutions off the NiNTA column is shown in figure 3-1.

In my first attempt at protein purification, I neglected to wash the column with lower concentrations (20mM) of imidazole to remove unbound proteins. I instead

proceeded from running the supernatant flow through the column directly to eluting with 1 ml fractions of 100 mM imidazole labeled as Elute 1.1-1.4 and 1 ml fractions of 250

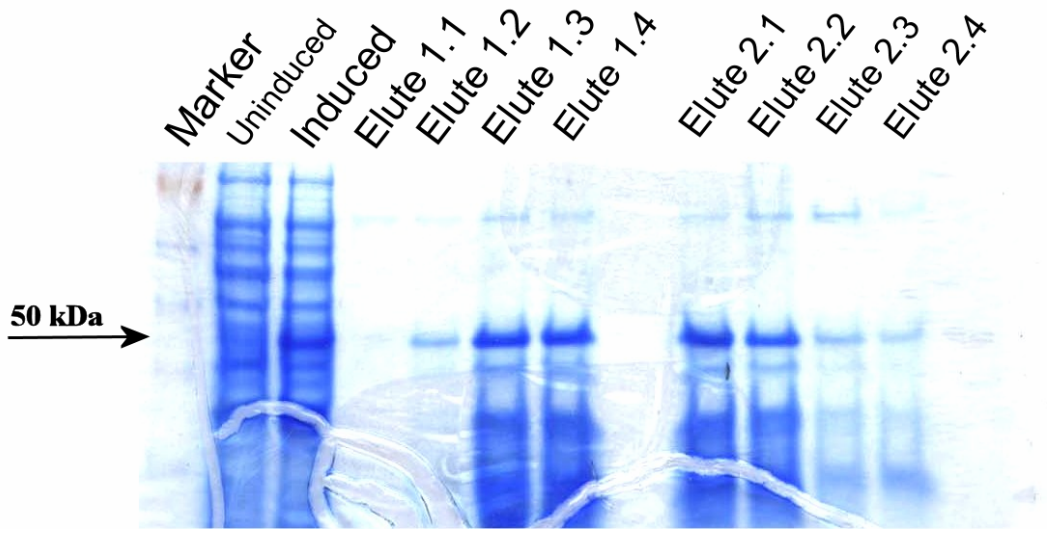

Figure 3-1. PAGE analysis of initial elutions of PEDF protein purification. Samples were loaded onto a 12% Tris-HCl polyacrylamide gel and run at 150 V for 1.5 hours. Marker lane contains pre-stained protein standards ranging from 4-250 kDa. Elute 1.1-1.4 are samples of the consecutive elutions at 100 mM imidazole. Elute 2.1-2.4 are elutions at 250 mM imidazole. The expected band for PEDF should be approximately 50 kDa.

mM imidazole labeled Elute 2.1-2.4 on the gel in figure 3-1. Additional 1 ml fractions at 750 mM imidazole were run in a separate PAGE, but there were no significant bands to be detected. There is a band at approximately 50 kDa present in the induced total sample that is not present in the uninduced total sample. In the samples from the purification elutions, this same band is visualized at the highest levels in the bands labeled Elute 1.3 through Elute 2.2. At this stage, the protein band representing PEDF is most definitely present, but many other lower molecular weight proteins are also present in these fractions. Further purification was needed in order to use this expressed PEDF in my experiments. To this end, these four fractions were collected and pooled together to repeat the protein purification step. These fractions were resuspended in STET buffer

and equilibrated to a final concentration of 10 mM imidazole. The pooled fractions were re-run through the NiNTA system with the same elution steps as described above. In this column, the bed of NiNTA beads (approximately 2 ml bed volume) was washed three times with 50 ml of 20 mM imidazole in denaturing buffer. A 1 ml sample of each of these washes was reserved and labeled as 20mM 1-3. The elution steps were very similar to the procedure used for the initial column elution discussed above. Consecutive 1 ml fractions (approximately 0.5 bed volume) were loaded onto the column, the flow-through was collected and labeled 1-4 according to the concentration of imidazole used in the elution. Samples of each of these fractions were loaded into wells of a 12% Tris HCl polyacrylamide gel along with pre-stained protein standards and samples from the uninduced total cell, induced total cell, crude supernatant, and lysed pellet. The PAGE analysis of these further purification elutions off the NiNTA column is shown in the figure 3-2.

Most of the purified PEDF protein eluted as a 50 kDa band at the 100 mM imidazole concentration. The subsequent elutions with 250 mM and 750 mM (not shown) imidazole produced weaker bands constituting progressively smaller fractions of the total purified protein.

Elution fractions 1-4 from the 100 mM imidazole were pooled together and placed into dialysis cassettes (Slide-A-Lyzer 10K, Pierce, Rockford, IL) to begin the process of reducing the imidazole and salt concentrations. The pooled fractions containing the eluted, purified PEDF protein in dialysis cassettes were placed in decreasing concentrations of imidazole in a diluting buffer containing 4M urea, 500 mM sodium phosphate pH 6.5, 1 mM benzamidine, 1 μg/ml pepstatin, and 4 mM EDTA.

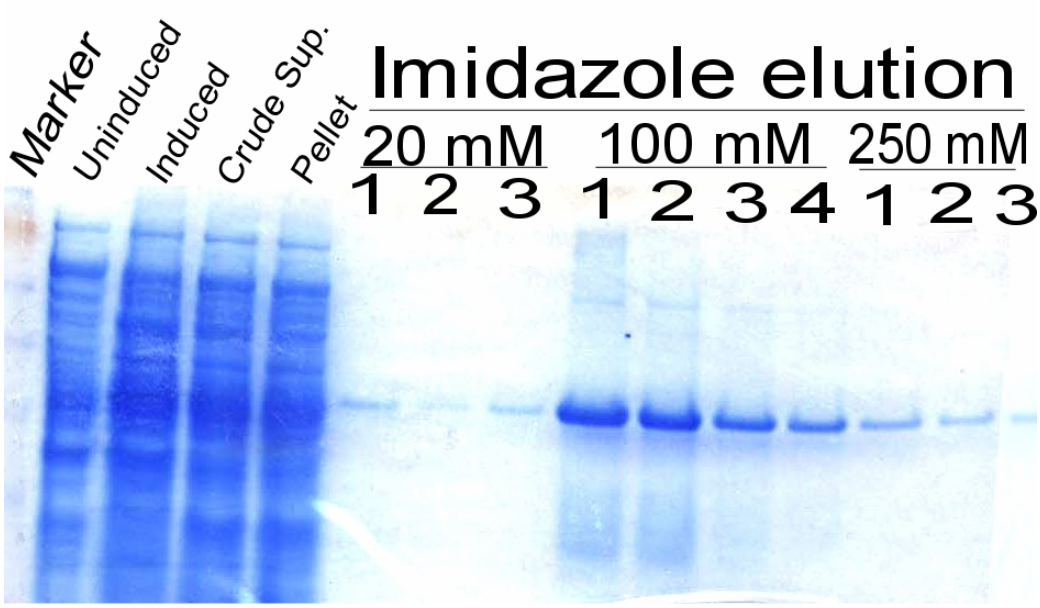

Figure 3-2. PAGE analysis of PEDF Ni-NTA purification. Samples were loaded onto a 12% Tris-HCl polyacrylamide gel and run at 150 V for 1.5 hours. Marker lane contains pre-stained protein standards ranging from 4-250 kDa. The expected band for PEDF should be approximately 50 kDa.

The dialysis cassette allows free movement of dissolved salts and other low molecular weight contaminants, but retains the higher molecular weight protein. The dialysis cassette containing the protein was stirred and allowed to equilibrate in the cold room with each 1 L volume of dilutant for a period of 1-2 hours. The series of diluting buffers started at 100 mM and progressed through 50, 20, 10, 5, and 1 mM imidazole solution. Then the dialysis cassette was transferred to the next lower dilutant in series until the final solution was equilibrated overnight in diluting buffer containing no imidazole. This final solution of PEDF was used to establish our standard curve for ELISA determinations. The purified protein was also used to generate a polyclonal mouse anti-PEDF antibody for use in the ELISA system.

ELISA Design

A PEDF ELISA was carried out on supernatants from disrupted whole mouse eyes with lens, comparing vector treated vs. control eyes in the same animal. Our collaborators at JHU supplied a C-terminal octa-his-tagged recombinant PEDF and a corresponding rabbit polyclonal antibody. The ELISA protocol is a standard indirect sandwich colorimetric assay. The 96 well plates are coated with the polyclonal antibody to PEDF (6µl in 12 ml PBS/10% FBS). The bound antibody captures any PEDF protein from the eye extract added in the next step of the protocol. Detection of bound PEDF employs an anti-His_5 monoclonal antibody (Qiagen) (5µl in 12 ml PBS/10% FBS) to detect the penta-His tail of recombinant PEDF followed by a biotinylated anti-mouse IgG antibody (5µl in 12 ml PBS/10% FBS) and streptavidin conjugated to horseradish peroxidase (HRP) (Invitrogen) (5µl in 12 ml PBS/10% FBS). To determine the levels of PEDF present in treated eyes, each whole eye was homogenized in PBS with 0.01 M PMSF added and the insoluble material spun down. Then, serial dilutions of the supernatant (in a volume of 100 µl) were added a 96 well ELISA plate. A standard curve was constructed using known amounts of purified recombinant PEDF to calibrate the signals. Based on our experience with other his-tagged proteins in the eye, 10-20ng of PEDF should be detectable per well, well within the range of expected therapeutic levels based on a recent report (177). This initial ELISA protocol, as depicted in figure 3-3, was demonstrated to effectively detect His-tagged PEDF in protein standard tests.

Due to a misunderstanding with our collaborators, the cloned PEDF vectors did not possess the terminal His tag necessary for detection in our ELISA system. It was

therefore necessary to either re-clone each of the vectors or to redefine the ELISA using a new antibody.

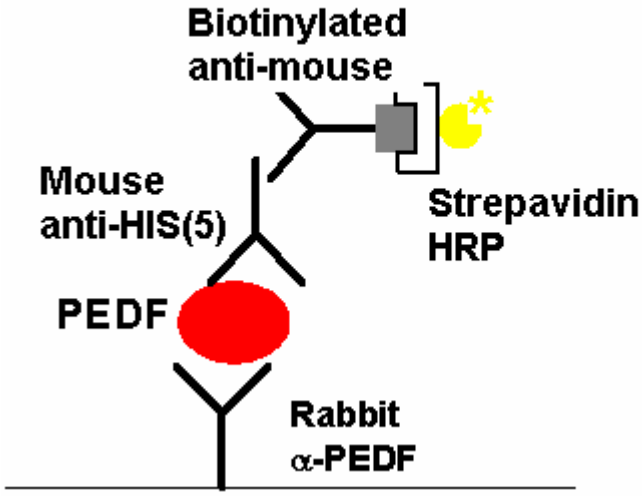

Figure 3-3. Diagram of PEDF ELISA using a penta-His antibody for detection.

The straightforward solution was to retool the ELISA to detect PEDF without the use of the His tag. Working with Dr. Paul Hargrave's lab at the University of Florida I raised a mouse polyclonal antibody against PEDF. This polyclonal antibody was used in place of the anti-HIS antibody as described in the above ELISA protocol. Since the polyclonal mouse antibody would also be detectable by the biotinylated anti-mouse IgG antibody, this was the only substitution necessary. PEDF was detected by a sandwich ELISA procedure using a biotin conjugated antibody and HRP conjugated avidin for detection. Rabbit α-PEDF (5µl in 11 ml 0.1 M $NaHCO_3$) was coated on 96 well Immulon flat bottom microtiter plate (Dynex Technologies, Chantilly, VA) incubated overnight at 4˚C. The wells were blocked with 10% fetal bovine serum in PBS pH 7.4 (blocking solution) for 2 hours at 37˚C. PEDF protein standards and eye extract samples were loaded as 100µl aliquots into wells and the plate was kept overnight at 4˚C.

Detection consisted of a secondary mouse polyclonal α-PEDF (6µl in 11 ml PBS/10% FBS) followed by a biotin conjugated rat α-mouse IgG (MP Biomedicals, Irvine, CA) (5µl in 11 ml PBS/10% FBS) and HRP conjugated avidin (BD Biosciences Pharmingen, San Diego, CA) (5µl in 11 ml PBS/10% FBS). The secondary mouse polyclonal antibody was not characterized by western blot. Since the primary antibody only captures PEDF, the secondary antibody should only be able to detect this captured protein. Further characterization of the secondary antibody should be conducted to confirm this. Each step of detection was conducted with plate agitation at room temperature for 1-2 hours and the plate was washed 5 times between steps. TMB peroxidase substrate system (Kirkegaard & Perry Laboratories, Gaithersburg, MD) was pipetted as 100 µl aliquots into all wells and allowed to reach fully developed color, usually 30 minutes, before stopping the reaction with 1 M H_3PO_4. The plates were read in an automated microplate reader at 450 nm. The revised PEDF ELISA is shown in figure 3-4.

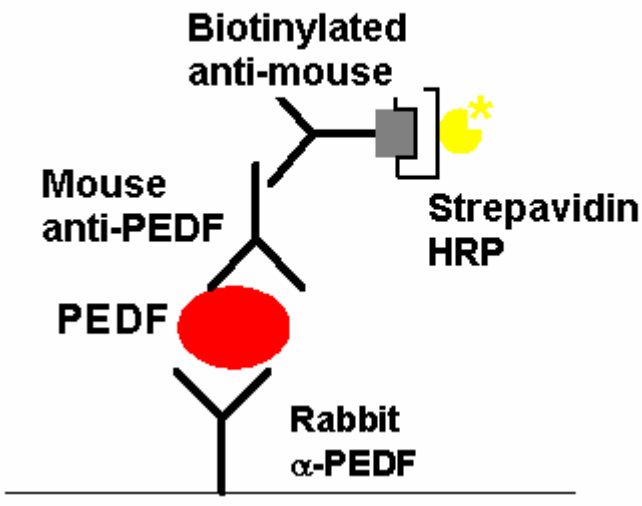

Figure 3-4. Diagram of revised PEDF ELISA.

The ELISA for detecting K1K3 is similar in design to the assay for PEDF. An antibody against angiostatin is coated onto 96 well plates. Protein standards or K1K3 in eye extracts are captured by the bound antibody in the next step of the procedure. Both the standard used for this ELISA and the expressed K1K3 possess a myc epitope as a tag for detection. Rabbit polyclonal α-plasminogen (Enzyme Research Laboratories, South Bend, IN) (3µl in 11 0.1 M $NaHCO_3$) was coated on 96 well Immulon flat bottom microtiter plate (Dynex Technologies) incubated overnight at 4˚C. The wells were blocked with 10% fetal bovine serum in PBS pH 7.4 (blocking solution) for 2 hours at 37˚C. K1K3 protein standards and eye extract samples were loaded as 100µl aliquots into wells and the plate was kept overnight at 4˚C. Detection consisted of a secondary α-myc biotin conjugated antibody (Invitrogen) (5µl in 11 ml blocking solution) followed by HRP conjugated avidin (Pharmingen) (5µl in 11 ml blocking solution). Each step of detection was conducted with plate agitation at room temperature for 1-2 hours and the plate was washed 5 times between steps. TMB peroxidase substrate system (Kirkegaard & Perry Laboratories) was pipetted into all wells and allowed to reach fully developed color, usually 30 minutes, before stopping the reaction with 1 M H_3PO_4. The plates were read in an automated microplate reader at 450 nm. A diagram of the detection of bound K1K3 employing the procedure described above is shown in figure 3-5.

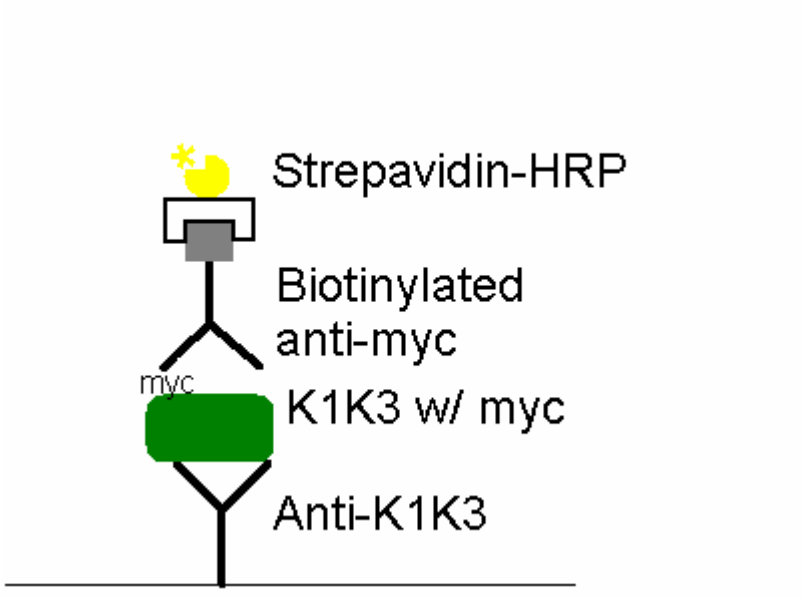

Figure 3-5. Diagram of K1K3 ELISA using myc epitope for detection

ELISA Standard Curves

The ELISA for both PEDF and K1K3 allowed us to construct standard curves for each of the proteins and to use these to analyze the expressed protein content of eyes treated with the various AAV vectors. The protein used as a standard is the bacterially expressed and purified human PEDF discussed earlier in this chapter and depicted in figure 3-2. The standard starts at the highest concentration of 68 ng loaded per well and is serially diluted 1:1 10 times in 10% FBS in PBS. The last standard then has a concentration of 0.067 ng loaded per well (not shown in figure 3-6).

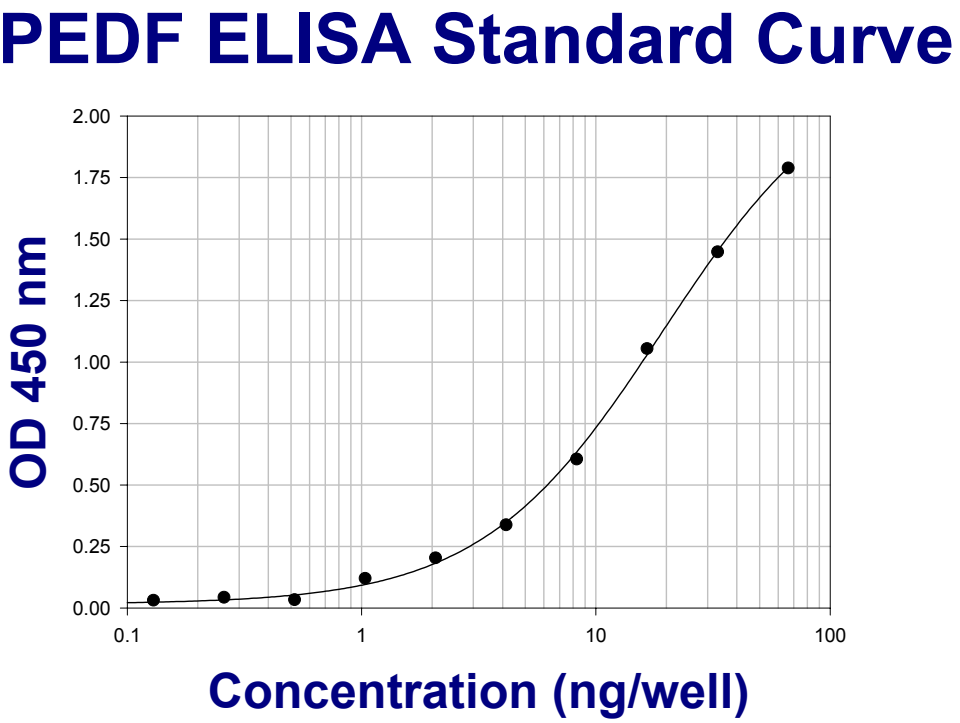

Figure 3-6. Example of a PEDF ELISA standard curve. The data is plotted as a semi-log plot with the concentration of PEDF in ng loaded per well on the x-axis and the observed OD 450 on the y-axis.

The PEDF ELISA standard curve is based on the procedure detailed in the preceding text and in Figure 3-4. The ELISA for PEDF in this example standard curve has a detection range of approximately 0.5-68 ng/well.

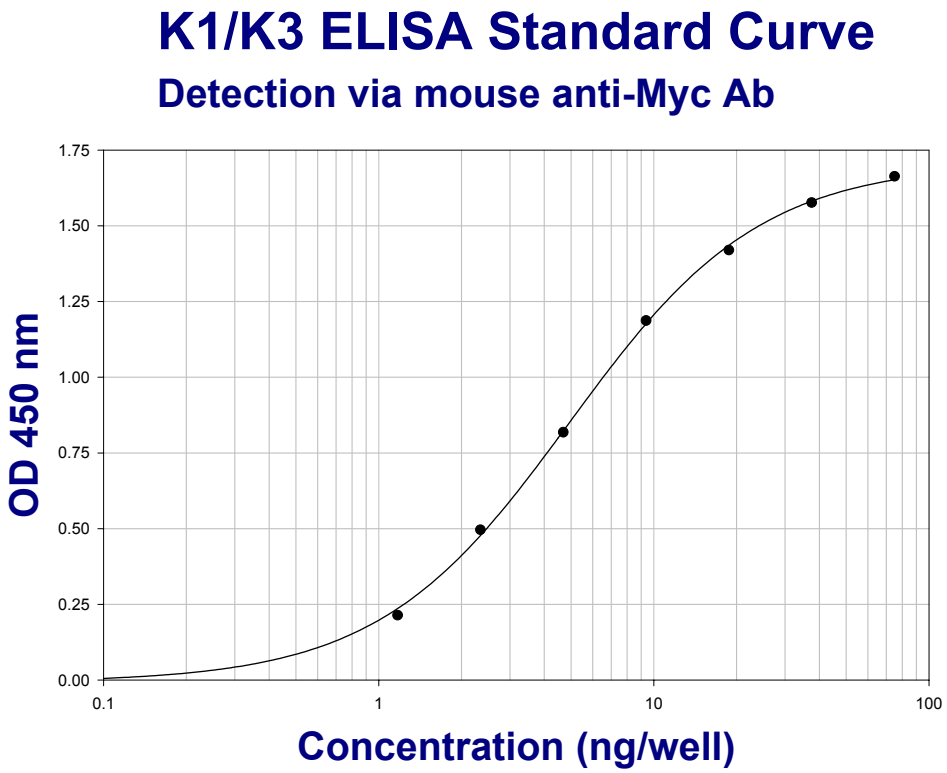

Figure 3-7. Example of a K1K3 ELISA standard curve. The data is plotted as a semi-log plot with the concentration of PEDF in ng loaded per well on the x-axis and the observed OD 450 on the y-axis.

The K1K3 ELISA curve derives from the procedure discussed above and diagrammed in figure 3-6. The protein used as a standard is the bacterially expressed and purified K1K3 with a c-myc epitope that was a generous gift of P. Meneses, Cornell University, and was purified by methods similar to those used for PEDF. The ELISA for K1K3 in this example standard curve has a detection range of approximately 2-75 ng/well.

Once the standard curves for both K1K3 and PEDF were elucidated, it was possible to use these ELISA systems to determine the intraocular level expressed for these proteins from each of our targeted vectors.

CHAPTER 4
GENE THERAPY IN A MOUSE MODEL OF ISCHEMIC RETINOPATHY

Background

The vasculature of the retina in healthy adults is normally quiescent. A delicate balance between pro-angiogenic signals, like VEGF (1;2), and angiogenesis inhibitors, like PEDF (3), maintains the vascular homeostasis in the retina. If this balance is upset, as might occur secondary to systemic disease or local injury, new vessel outgrowth can occur. This pathologic NV consists of new and rapidly forming vessels that are typically weak and may grow into inappropriate areas of the retina ultimately leading to loss of vision. As discussed in the chapter 1, this pathologic NV is common to several ocular diseases; diabetic retinopathy, age-related macular degeneration, and retinopathy of prematurity.

As also outlined in chapter 1, current clinical treatment options exist for patients presenting with retinal and choroidal NV. However, all current treatment options provide solutions that result in some loss of vision and may have only temporary effects. The inherent risks to the patient make the currently available treatments less than optimal therapies for these conditions. An alternative therapy that minimizes the risk to the patient and provides long-term protection from pathological NV has yet to be developed.

K1K3 angiostatin and PEDF are two of the most potent inhibitors of neovascularization. In this chapter, I test whether either PEDF or K1K3 can provide therapeutic control of retinal NV. The putative therapeutic genes will be delivered by rAAV serotype-2 vectors. As previously mentioned this method provides for long-term

expression of passenger genes, has limited immunogenic potential, and efficiently transduces a variety of tissues. I examine the effect of expression of these anti-angiogenic factors in a mouse model of ischemic retinopathy. This system serves as a model for retinopathy of prematurity and as a surrogate model for diabetic retinopathy. Both disease states are characterized by pre-retinal neovascularization and share a similar pathophysiology.

Materials and Methods

Animals

All animals were treated in accordance with the ARVO Statement for the Use of Animals in Ophthalmic and Vision Research. C57BL/6 mice were obtained from Jackson Laboratory (Bar Harbor, ME). Breeding pairs of mice were housed in the University of Florida Health Science Center Animal Resources facilities. Females were examined daily for signs of pregnancy and isolated in individual cages for confirmation. Timed-pregnant dams were also occasionally obtained from the same vendor. Animals were euthanized by an overdose of ketamine/xylazine mixture given subcutaneously (10 µg/g body weight of ketamine HCl, 2µg/g body weight of xylazine in an appropriate volume of 0.9% NaCl).

Vector Design, Packaging and Delivery

The rAAV vector cassette consists of a selected promoter upstream of an SV40 early splice donor/splice acceptor site, the expressed gene, and an SV40 polyadenylation sequence. PEDF cDNA was a gift of P. Campochiaro and K1K3 cDNA was a gift of P. Meneses. K1K3 has an IgK leader peptide secretory sequence upstream of the expressed gene. At its carboxy-terminus K1K3 also has a myc epitope for ELISA detection. The entire expression cassette containing either cDNA is flanked by AAV2 terminal repeats

required for viral packaging. Viral vectors were packaged and purified as previously described (163;178). Briefly, plasmid DNA containing the vector cassette is transfected into human 293 cells along with helper plasmid DNA containing the two rAAV genes and Adenovirus helper functions. The cells are harvested in PBS with EDTA, pelleted and resuspended in a low salt buffer, and lysed by freeze-thaw. The virus is purified on an iodixinol gradient followed by cation exchange column chromatography (Q-HiTrap, Amersham, Piscataway, NJ). Recombinant AAV vector is eluted from the cation exchange column on FLPC with 500 mM NaCl. The fractions corresponding to the elution peak for the virus are pooled, concentrated, and buffer exchanged into 300µl Lactated Ringers solution. Initial viral titer is calculated by quantitative competitive PCR and a final titer is determined by infectious center assay.

In order to determine the optimum promoter to drive expression of the therapeutic gene, I designed and made five promoter constructs. Each promoter regulates expression in a subset of cells in the retina. Chicken β-actin (CBA) is a ubiquitous strong promoter composed of a CMV immediate early enhancer (381 bp) and a CBA promoter-exon1-intron1 element (1352 bp), cis-Retinaldehyde Binding Protein (CRALBP) promoter is a retinal pigment epithelium (RPE) specific promoter (2265 bp) when administered subretinally in an rAAV vector (A. Timmers and W. Hauswirth, unpublished), mouse rod opsin (MOPS) is a photoreceptor specific promoter (372 bp) (164), platelet derived growth factor (PDGF) is an endothelial promoter (1600 bp) that regulates expression in retinal ganglion cells (RGC) when delivered intravitreally in rAAV vectors (A. Timmers and W. Hauswirth, unpublished), and the cytomegalovirus (CMV) promoter (620 bp), like CBA, is also relatively ubiquitous in the retina but expresses at a lower levels than

CBA (179). I inserted each of these promoters upstream of the therapeutic genes, PEDF or K1K3. For the purpose of determining in vivo expression levels, each vector was injected into the subretinal or intravitreal space of adult mice. For anesthesia a Xylazine/Ketamine mixture (Xylazine 5 mg/Kg, Ketamine 100 mg/Kg) was administered by intraperitoneal injection. Topical anesthetic, given in addition, consisted of 1 drop of proparacaine (1%) per eye. Approximately 10^{10} particles (2 X 10^{8} infectious units) in a volume of 1µl of therapeutic vector were injected into the right eye either subretinally or intravitreally. The contralateral eye was injected with the same volume of PBS. Mouse pups were injected intraocularly with 0.5µl on postnatal day (P0) with one of the experimental vectors in the right eye and PBS in the contralateral eye. The neonatal pups (less than 1 day old) do not respond to normal anesthesia. I therefore sedated neonatal pups by hypothermia by placing them in a plastic weigh boat on wet ice. The pups are monitored closely for slowing of motor activity deemed to be the anesthetic threshold. Following ocular injections, the pups were placed on a 37 degree animal warming tray to bring them back to appropriate temperature prior to returning them to the dam's care.

ELISA

Eyes from age-matched animals were enucleated and frozen quickly in 100 µl of PBS pH 7.4 with 0.05% PMSF, and homogenized manually on ice using a ground glass tissue homogenizer followed by three freeze thaw cycles on liquid nitrogen and wet ice. The homogenate was centrifuged in a refrigerated desktop centrifuge to pellet the insoluble material. The resulting whole eye extract was loaded into sample wells for detection by ELISA. I determined the ocular levels of PEDF protein by an indirect sandwich ELISA procedure using a biotin conjugated final antibody and HRP conjugated avidin for detection. Rabbit anti-PEDF (gift from P. Campochiaro) was coated on 96

well Immulon flat bottom microtiter plate (Dynex Technologies) in 0.1 M NaHCO3 overnight at 4˚C. The wells were blocked with 10% fetal bovine serum in PBS pH 7.4 for 2 hours at 37˚C. PEDF protein standards and eye extract samples as 100µl aliquots were then loaded into the wells and incubated the plate overnight at 4˚C. Detection consisted of a secondary mouse polyclonal anti-PEDF (gift of P. Hargrave) followed by a biotin conjugated rat α-mouse IgG (ICN Biomedicals) and HRP conjugated avidin (Pharmingen). Each step of the detection was conducted with plate agitation at room temperature for 1-2 hours and the plate was washed 5 times between steps. TMB (3,3',5,5'- tetramethyl-benzidine) peroxidase substrate system (Kirkegaard & Perry Laboratories) was pipetted into all wells and allowed to reach fully developed color, usually 30 minutes, before stopping the reaction with 1 M H3PO4. The plates were read by absorbance at 450 nm in an automated microplate reader. A similar method was employed to determine K1K3 levels. Rat anti-K1K3 (Enzyme Research Laboratories) was coated onto plates, and K1K3 samples loaded as described. I used a biotinylated secondary antibody to the myc epitope (Invitrogen) on the expressed K1K3 to detect bound protein. HRP conjugated avidin followed by TMB peroxidase substrate completed the detection step as described above.

Hyperoxia Treatment

Mouse pups, with their nursing dam, were placed in a chamber at 73% oxygen at P7 and maintained in this environment for 5 days until P12. The chamber used in the OIR model is a plexiglass box with a hinged front door. Holes in the top of chamber allow for gas tubing and sensor wires to run into and out of the chamber. The oxygen level is monitored and gas delivery controlled by a ProOx 110 oxygen controller using an E-700 sensor (Reming Bioinstruments, Redfield, NY). At P12 the pups and nursing dam

were returned to normal room air and maintained for another 5 days. At P17, the pups were euthanized as described and their eyes enucleated and fixed for embedding and sectioning. Representative pups from each group were anesthetized and perfused through the left ventricle with 4% paraformaldehyde in 0.1 M sodium phosphate (pH 7.4) containing 5 mg/ml FITC-dextran for visualizing the retinal vasculature (see below).

Quantitative and Qualitative Assessment of Retinal NV

Both eyes of each P17 pup were enucleated and fixed for paraffin embedding and serially sectioned at 5μm thickness as described by Smith et al.(180). Representative sections (every 30th section) through the full eyecup were stained with hematoxylin and eosin to visualize cell nuclei. Investigators masked to the identity of the treatment groups counted neovascular endothelial cell nuclei above the internal limiting membrane in every 30^{th} section through each eye. These representative sections provide a basis for comparing the effect of expression of therapeutic factors without the need for enumerating every section through the eye. In sections containing any portion of the optic nerve, endothelial cell nuclei directly above or associated with the optic nerve head were not counted as neovascular nuclei. Any endothelial vessels above the optic nerve head or within one ONH diameter distance may have arisen from persistent hyaloid vessels and were not included in our data analysis. Vascular cell nuclei were considered to be associated with neovascularization if they were on the vitreous side of the internal limiting membrane. Only endothelial cell nuclei that were clearly part of a vessel structure with a discernable lumen in any plane were included in our analysis. All such cells were counted unless they were clearly associated with hyaloid structures. Single nuclei or clumps of nuclei not defining a vessel were not counted as they may represent sectioning artifacts. Data were analyzed by a paired t-test with vector treated and

contralateral uninjected eyes serving as determinants. For qualitative assessment of retinal NV both eyes of each perfused P17 pup were enucleated and the retina dissected and flat-mounted as described by D'Amato et al. (181). Flatmounted retinas were photographed by fluorescence microscopy using a Zeiss Axioplan2 microscope, Zeiss Plan-Fluar 10X lens, Sony DXC-970MD camera with tile field imaging and MCID software (Imaging Research Inc., Ontario, Canada). At least three eyes from each treatment group were examined in this way.

Results

Optimizing Ocular Expression from the Vector Construct

To determine the optimal promoter construct for use in anti-angiogenic experimental therapies I initially assayed the amount of ocular vectored protein in adult mice expressed from each of five vector constructs containing different promoters. To a first approximation the level of PEDF or K1K3 protein expression in the eye should correlate with how well that vector performs in reducing aberrant NV. I chose a set of promoters that restrict expression of genes to different specific subsets of retinal cells. Each vector-promoter construct was tested by either intravitreal or subretinal vector inoculation. I measured ocular protein expression levels by ELISA 6 weeks following vector injection. Only the nature of the promoter regulating the PEDF or K1K3 or the site of intraocular injection was changed. ELISA has several advantages over other methods to examine the protein expression in the eye. PCR based methods of determining promoter efficiency only reflect the amount of mRNA made and may not accurately reflect protein levels. ELISA provides a protein quantification that is more precise than Western blotting. The results are summarized in Table 3-1 and indicate that for both PEDF and K1K3 the CBA hybrid promoter produces the most consistently

robust ELISA measurements of protein expression. Interestingly, subretinal or intravitreal routes of vector delivery generated approximately equivalent levels of ocular protein. For purposes of maximizing protein expression in the retina, I therefore conclude that rAAV-CBA-PEDF and rAAV-CBA-K1K3 vectors are best suited for therapeutic evaluation in a retinal NV setting. Further experiments following expression of PEDF or K1K3 using the CBA promoter in neonatal pups demonstrated that I could obtain levels of 6-36 ng and 6-113 ng of protein for PEDF and K1K3 respectively between 2 and 17 days after injection of vector at P0.

Table 4-1. Ocular K1K3 or PEDF levels for various viral vector constructs. Intraocular protein levels for K1K3 and PEDF were measured in whole eye homogenates from adult mice by ELISA. Consistently high levels of both K1K3 and PEDF were observed in eyes injected with vectors bearing the CBA promoter driving expression.

Promoter	**PEDF ng/retina**	**K1K3 ng/retina**
CBA Subretinal	20-65	6-40
CBA Intravitreous	25-70	8-60
CRALBP Subretinal	3-4	<1
MOPS Subretinal	1-2	<1
PDGF Intravitreous	2-3	3-4
CMV Subretinal	<1	<1
CMV Intravitreous	<1	<1

Expression of K1K3 or PEDF was determined by ELISA from whole eye homogenates in adult mice. The rAAV vectors with the CBA promoter produced the highest levels of K1K3 or PEDF expression from either intravitreal or subretinal inoculations. There was no significant difference between intravitreal and subretinal

injection for either K1K3 or PEDF. Neonatal expression levels measured between P2 and P17 for the CBA promoter for both K1K3 and PEDF are comparable to the adult and still above the estimated therapeutic threshold for each protein. More significantly, the levels attained from neonatal eyes exhibited a much more rapid onset of expression relative to the adult. In the adult animals I measure protein expression levels 6 weeks following the initial interocular injection because ocular protein rises only slowly during the first 4 weeks following vector injection. In our work with neonatal mice, I have been able to detect protein expression by ELISA as early as one day following injection (see below and chapter 5).

Vector Behavior in the Oxygen Induced Retinopathy (OIR) Mouse Model

In order to functionally test whether PEDF or K1K3 vectors reduced NV in vivo, I chose to examine their performance in a mouse model of ischemic retinopathy. Retinal neovascularization is induced in a modification of a previously described protocol (180;181). However, before analysis of any therapeutic effects, I needed to know what levels of each agent were produced in the eyes of P1 to P17 neonatal mice since our initial survey of intraocular levels of passenger gene expression was in adult mice with a mature retina. P1 neonatal mice were injected intraocularly with rAAV-CBA-PEDF or rAAV-CBA-K1K3 as described above. Levels of PEDF and K1K3 expression were followed by ELISA after injection. Expression of PEDF was detectable as early as P2 and persisted at levels well above contralateral uninjected eyes to the last time point at P17. The PEDF levels measured in the neonatal mice (6-36 ng/eye) were not as high as those measured in adult mouse eyes (20-70 ng/eye), however they were well above levels in the untreated contralateral eyes and estimated therapeutic thresholds (see below). K1K3 levels measured in injected eyes of neonatal mice were 6-113 ng/eye. Quantitative

differences between PEDF and K1K3 levels achievable in adults vs. neonates may be related to size, developmental differences, and the time after injection.

Assessment of Anti-Neovascular Effects

To qualitatively assess retinal NV after vector treatment I viewed the retinal vasculature in flat-mounted FITC-dextran perfused whole retinas. Whole mounts were imaged using tile-field mapping fluorescent microscopy which allows the whole retina to be examined at relatively high resolution. Such visual assessment of full retinal vascular beds provides a useful initial comparison between treatment groups. The patterns of NV observed in the FITC dextran perfused retinas were consistent with what has been reported previously using this model (180-182) (Figure 4-1). Retinas of neonatal mice exposed to hyperoxia exhibit increased tortuosity of radial vessels accompanied by increased perfusion of peripheral vessels and central vaso-obliteration (Figure 4-1a). For comparison, a whole mount from normoxic age matched animal shows the normal pattern of retinal vasculature (Figure 4-1b). The uninjected, hyperoxia exposed retina in Figure 4-1a can be directly contrasted with the contralateral PEDF (Figure 4-1c) or K1K3 (Figure 4-1d) vector treated retinas. PEDF or K1K3 vector treated retinas showed a qualitative decrease in the number of neovascular tufts with a relatively uniform perfusion pattern over the full retina. The overall vasculature pattern appeared much more like that in the normal animal (Figure 4-1b). However, these sorts of images do not lend themselves readily to a quantitative analysis of NV, and are subject to several preparation artifacts(183). Therefore an independent and more quantifiable additional analysis of the treatment groups was performed.

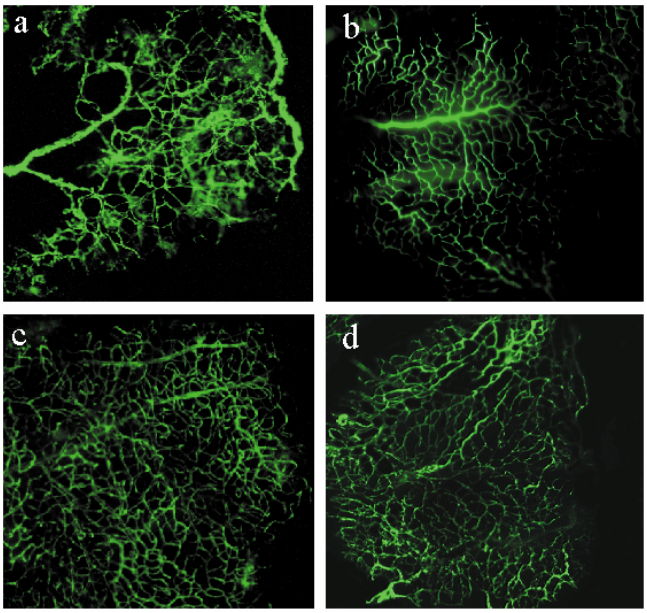

Figure 4-1. Qualitative determination of neovascularization from composite tile-field mapped 10X photomicrographs of whole-mounts of retinas from 17 day mouse pups. The pups were perfused with FITC-Dextran in 4% formaldehyde to visualize the retinal vasculature. Each panel shows one quadrant of the retinal whole-mount oriented with the central retina on the left and the peripheral on the right. (a)An untreated control pup exposed to 5 days of hyperoxia followed by 5 days at room oxygen exhibited the expected abnormal retinal vasculature. Note the increased peripheral perfusion, the dilated, tortuous radial vessels, and the largely avascular central retina. (b)A normoxic age matched animal shows the normal pattern of retinal vasculature. Animals injected with either PEDF vector(c) or K1K3 vector(d) exhibited a vasculature much closer to that seen in a normal age-matched animal, with uniform perfusion over the retina and fewer areas of apparent vascular leakage.

In order to gain better insight into the efficacy of treatment with rAAV-CBA-PEDF or rAAV-CBA-K1K3, direct enumeration of endothelial cells in the retinal vasculature was assessed as previously described (180). I enucleated and fixed both vector-treated and control eyes from P17 pups for paraffin embedded sectioning. These representative sections provide a reliable method for quantitatively assessing the total level of retinal NV in each eye. Two individuals masked as to the identity of the treatment groups quantified NV by enumerating all endothelial cell nuclei found in the vitreous space

above the inner limiting membrane (ILM). Comparisons were made between one eye of each animal injected with therapeutic vector and the contralateral uninjected eye serving as an internal control (Figure 4-2). In tissue sections, uninjected control eyes typically showed abundant longitudinal and transverse aberrant microvessels in the vitreous space above the ILM (Figure 4-2c). Eyes injected with K1K3 or PEDF vectors had a dramatically reduced number of aberrant vessels (Figure 4-2a &b, respectively). Vehicle injected eyes and eyes injected with rAAV-CBA-GFP did not significantly differ from uninjected eyes in this assay (data not shown). Control eyes injected with rAAV-CBA-GFP demonstrate that the therapeutic effect is due to the expressed genes and not due to the vector itself.

Treatment with either rAAV-CBA-PEDF or rAAV-CBA-K1K3 significantly reduced the neovascular response (both $p<0.0000002$) when compared with the paired uninjected control eye (Figure 4-3). Average endothelial cell counts in PEDF-treated eyes was reduced by 74% compared to paired controls and 78% compared to paired controls for K1K3 treated eyes.

Discussion

Diabetic retinopathy, like other retinal neovascular disorders, remains a persistent and problematic malady that begs long-term treatment options. A steady and alarming increase in the number of patients diagnosed with diabetes worldwide is projected to continue its upward course (184). As discussed in chapter 1 of this dissertation, proliferative diabetic retinopathy (PDR) is a common complication in diabetic patients. The model of neonatal ischemic retinopathy used here shares similar features with the angiogenic patho-physiology of PDR. Retinal NV can also occur secondarily to

choriodal NV in AMD (185;186). The successful use of vectored expression of PEDF and K1K3 to control NV

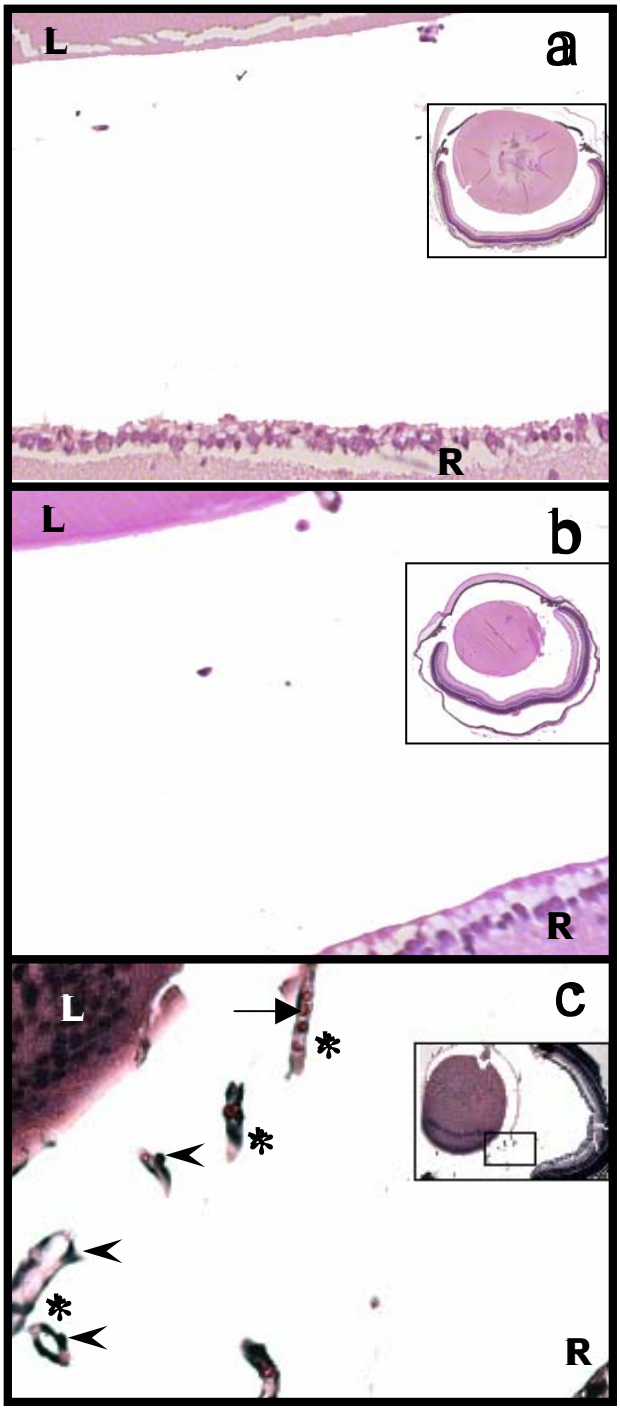

Figure 4-2. Composite photomicrographs showing transverse sections of whole eyes from hyperoxia treated mouse pups. Tile field mapped photomicrographs at 20X of representative whole eyes are inset in each panel. The arrowheads indicate representative vascular endothelial cell nuclei and the arrow indicates a red blood cell within a longitudinal section of an abnormal microvessel (indicated by asterisks) that have penetrated the inner limiting membrane. The vitreal space into which new blood vessels have penetrated is defined anteriorly by the lens (L) and posteriorly by the retina (R). Assessment of neovascularization requires quantitation of endothelial cell nuclei occurring on the vitreous side of the ILM (see Fig. 4-2). Eyes injected with rAAV-CBA-K1K3 had fewer endothelial cell nuclei in representative sections (a) than uninjected control eyes (c). Similarly, rAAV-CBA-PEDF treatment resulted in a reduced number of endothelial cell nuclei (b) than uninjected control eyes (c).

in this model may translate well to use of similar vectors to successfully treat chronic retinal NV in human patients.

In earlier experiments, I measured PEDF intraocular concentrations of 20-70 ng in the adult mouse and 6-36 ng in the neonatal mouse. Similar measurements of animals injected with a rAAV vector expressing K1K3 angiostatin produce levels of 6-60 ng/eye in the adult or 6-113 ng/eye in the neonate. I have calculated estimate therapeutic threshold levels for both of these compounds based on their systemic administration. The details of these calculations will be discussed in greater detail in chapter 6. The threshold levels for either K1K3 or PEDF in the eye are approximately 2 ng/eye. Therefore it appears that the vectors can achieve and maintain intraocular levels of either PEDF or K1K3 angiostatin in neonatal and adult mice sufficient to expect significant reduction of retinal NV.

The use of rAAV vectors for expression of therapeutic anti-angiogenic compounds offers several significant advantages over the systemic or ocular administration of anti-angiogenics.

1. Local production and secretion of PEDF and K1K3 limits the anti-angiogenesis effects to the area where they can have the most benefit and do the least harm.

Systemic administration of these compounds might leave the patient vulnerable to aberrant wound healing and could lead to unanticipated toxicity.

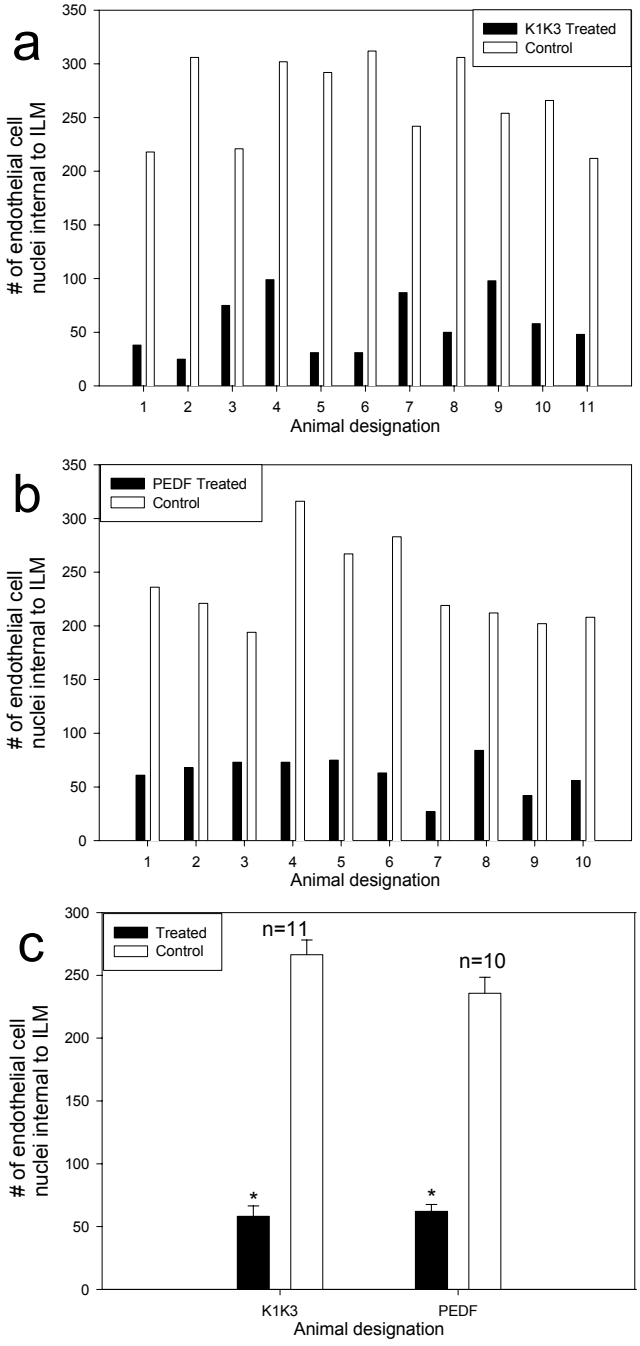

Figure 4-3. Enumeration of endothelial cell nuclei above the ILM in sections of whole eyes from hyperoxia treated P17 mouse pups. These quantitative results agree with the qualitative assessment (see Fig. 4-1), that vector-mediated expression

of PEDF (a) or K1K3 (b) reduces the level of oxygen-induced neovascularization. (c) Statistical analysis of the average endothelial cell counts in the paired eyes shows a significant difference between control and treated eyes for both PEDF and K1K3 ($P < 0.0000002$)

2. Recombinant AAV vectors support a sustained level of passenger gene expression in the eye that allows for long-term control of NV. I have observed nanogram levels of expressed protein in rat eyes for at least 21 months (B. Raisler and W. Hauswirth, unpublished). This provides the advantage of eliminating the need for repeated injections of anti-NV compounds that might be required with other systemic or local therapies.

3. PEDF and K1K3 expression from rAAV vectors is sufficiently robust to treat retinal NV. The persistent expression of anti-NV agents locally reduces concerns related to the pharmacological half-life of these factors in the eye. Periodic administration of non-vectored anti-NV agents may prove insufficient for long-term control of the disease.

Since rAAV vectors support long-term expression of passenger genes, the anti-NV agents PEDF and K1K3 are likely to be present in the eye for an extended period. In order to confirm the safety of long-term expression of these factors in the eye, I examined adult mice that were injected with PEDF and K1K3 in rAAV vectors. Six months following intravitreal injection, the animals were anaesthetized and perfused with the FITC-dextran solution as described in the Materials and Methods section of this chapter for the visualization of retinal vasculature. The eyes were removed and the retinas flat-mounted and examined for any changes in the vasculature that might be attributed to long-term expression of PEDF or K1K3 (Figure 4-4). In particular, I was interested to know whether there was any reduction in the vessel density in the retina or other gross vascular pathology. Injected adult mouse eyes had comparable vessel densities to uninjected eyes and showed no gross pathology. This indicates that injection of vectors expressing PEDF or K1K3 inhibits neovascularization while not affecting normal angiogenesis. While this finding alone does not address all aspects of the safety of rAAV

vectored gene therapy in the eye, it does provide evidence that long-term expression of PEDF or K1K3 is not producing deleterious effects in the vasculature of the mouse eye.

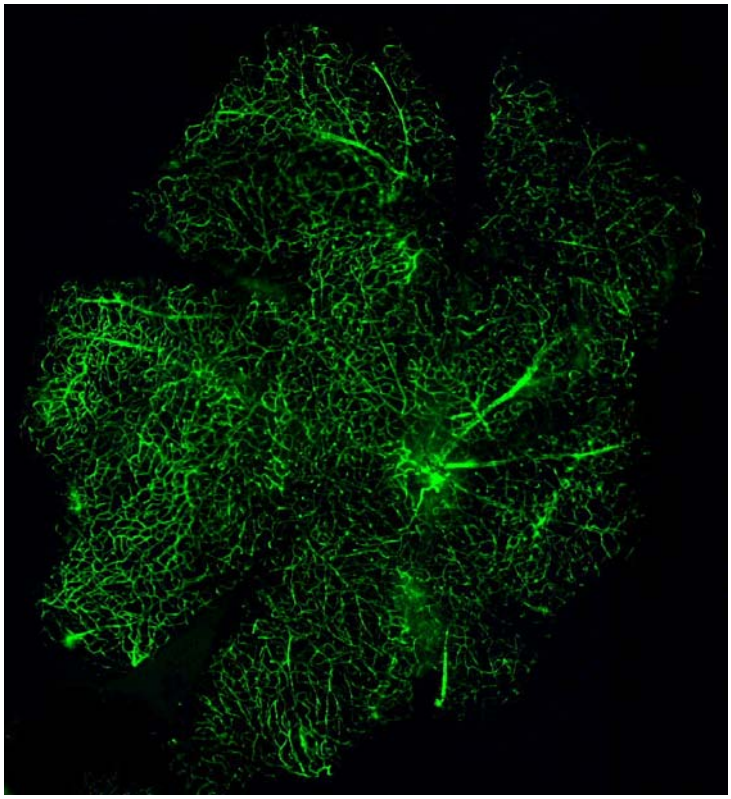

Figure 4-4. FITC-Dextran flat mount of a retina from PEDF vector treated adult mouse. The vector was injected intravitreally 6 months prior to this flat mount. There is no aberrant reduction in vessel density and no observable gross pathology.

Following the publication of the findings discussed the results section of this chapter we were contacted regarding the persistence of hyaloid vessels in the OIR model. The hyaloid vasculature nourishes the developing lens early in development, through P14, and spontaneously regresses, between P14 and P30, as the lens reaches maturity (187;188). Evidence suggests that in a neonatal rat model of ischemic retinopathy, also employing a hyperoxic chamber, the hyaloid vasculature persists beyond when it would have normally regressed (189). It was therefore reasonable to be concerned that some of

the endothelial cells that I counted in our experiments as neovascularization may have been hyaloid in origin.

It can be fairly debated whether some vessels between the retinal surface and the lens are truly neovascular or persistent hyaloid in origin. Our experience suggests that it is common for neovascular vessels to become detached from the retinal surface as an artifact of fixation and sectioning. Not wanting to preclude any possible neovascular cells from analysis, I initially included these vessels in our data sets for both control and experimental animals. I concede, however, that using this methodology may have also revealed the ability of PEDF or K1K3 to inhibit persistence of hyaloid vasculature.

In order to further address these issues, I re-masked and recounted all sections through all eyes used in the data set for publication. In this count, I used more stringent counting criteria that included only those vessels that are directly in contact with the inner retinal surface. Again, the area of any section surrounding the optic nerve head was left uncounted and vessels that clearly originated from this area but extended outside of it were also not included in the new data set. It is important to note that these vessels were also not included in our original counts for the data published in the paper. In this new count, any vessel structure in the vitreous space or in contact with the lens was not included in the data set. As all slides were masked to the investigator, the counting criteria were held constant for control and experimental groups. The outcome still demonstrates a reduction of number of endothelial cells comprising vessels attached to the inner limiting membrane: 78% reduction ($p<0.00002$) for K1K3 treated eyes and 66% reduction ($p<0.0005$) for PEDF treated eyes (Figure 4-5). This method of counting did produce a larger variance among individual eyes for both groups and between

experimental and control groups. However, the differences between treated and control eyes for each group are still highly statistically significant.

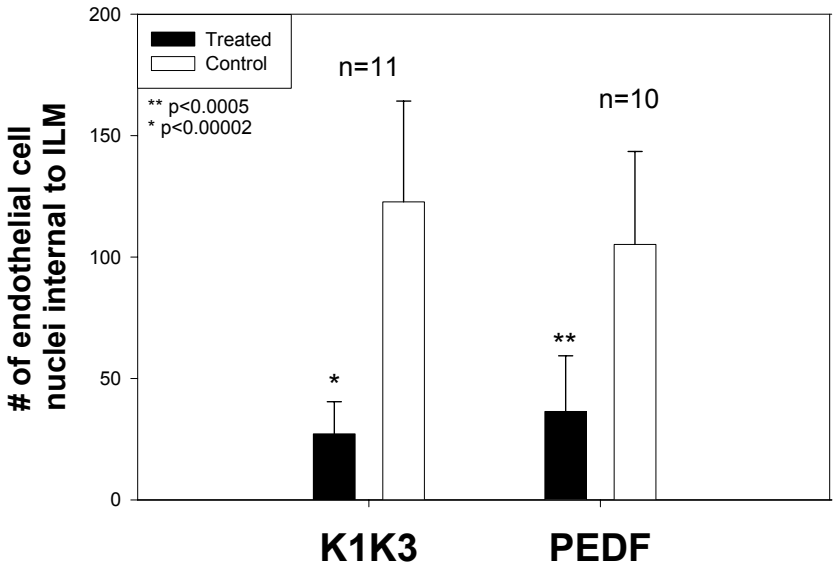

Figure 4-5. Enumeration of endothelial cell nuclei in contact with the ILM in sections of whole eyes from hyperoxia treated P17 mouse pups. Statistical analysis of the average endothelial cell counts in the paired eyes shows a significant difference between control and treated eyes for both PEDF and K1K3 ($P < 0.00002$ and $P < 0.0005$)

Of interest, I was able to isolate at least one section in a P17 mouse with a clearly visible persistent hyaloid vessel (artery) entering the vitreous space (Figure 4-6). The endothelial nuclei in this vessel would not have been included in the data sets using either counting protocol. Since this section is from a post-natal day 17 animal that went through the hyperoxia protocol, but received no therapeutic treatment, our data clearly agree with earlier findings that hyaloid vessels do persist in hyperoxia models.

In summary, I have demonstrated that rAAV vectors incorporating a CBA promoter are capable of producing sustained therapeutic levels of PEDF and K1K3 in the mouse eye. Intraocular injection of rAAV-CBA-PEDF or rAAV-CBA-K1K3

significantly reduced the level of retinal NV in a neonatal mouse model of ischemic retinopathy.

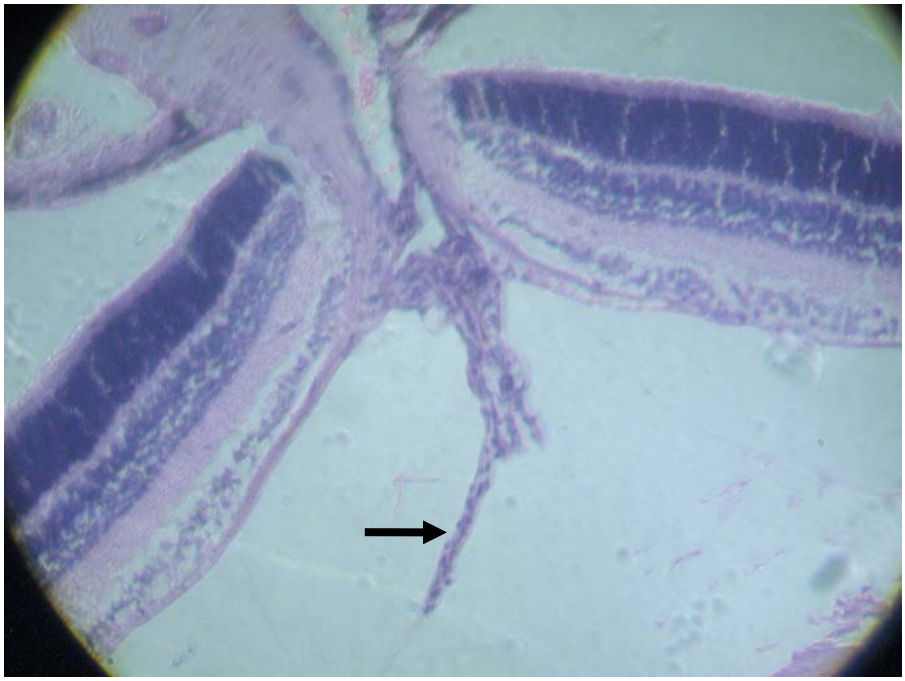

Figure 4-6. Transverse section of eye from a hyperoxia treated neonatal mouse. The arrow indicates a persistent hyaloid vessel at P17.

With this advance, the concept of efficient and well-targeted gene-based approaches for treating neovascular diseases of the eye coupled with the potential of rAAV vectors for persistently delivering anti-angiogenic proteins to the retina is being realized.

CHAPTER 5
SHORT-TERM IN VIVO EXPRESSION OF PEDF AND K1K3

Introduction

Background

As summarized in chapter 4, expression of the anti-NV agents K1K3 or PEDF by rAAV vectors is effective in controlling retinal NV in the OIR mouse. Some initial work had been done to demonstrate that these vectors would express sufficient levels of these proteins in the neonatal eye. In this chapter, I will examine the short-term *in vivo* expression profile of both PEDF and K1K3. I will estimate the intraocular dose delivery of each of these anti-NV agents in order to better understand how their temporal expression impacts the retinal vasculature in the OIR model. Previous studies have demonstrated that systemic injections of K1K3 consecutively administered in the period immediately following hyperoxic exposure in the OIR mouse model were effective in reducing retinal NV (190). Another group examining the anti-NV effects of PEDF in the same model also injected the protein systemically in the period from P12 through P17 with similar effects (191). These results together suggest that administration of an anti-NV agent in the period following the return to room air is sufficient for the control of NV. If my findings confirm this elevated late expression profile for K1K3 and PEDF, it would lend credence to this concept.

Experimental Design

In order to expand our understanding of the mode of action of PEDF and K1K3 and their potential interactions with each other, I conducted experiments to determine the

short-term expression profiles of both therapeutic proteins. Initially, the time period to be examined was from day 1 postnatal to day 17 postnatal; the period of the ischemia induced retinopathy model.

If PEDF is a major player in the control of neovascularization, I should be able to detect modulation in PEDF levels between normoxic and hyperoxic neonatal mice. Further, if viral mediated expression of PEDF or K1K3 is operating to reduce the level of neovascularization in this model, there should be some evidence confirming higher or earlier levels of these anti-angiogenic compounds in vector injected eyes compared to uninjected controls.

Material and Methods

Vector Delivery

On postnatal day (P0), mouse pups were sedated by hypothermia and injected intraocularly with 0.5µl with one of the experimental vectors, rAAV-CBA-PEDF or rAAV-CBA-K1K3 in the right eye and with 0.5µl PBS in the contralateral eye. Once it was established that PBS injection in contralateral eyes did not modulate expression levels, both eyes of the neonatal mice were vector injected in order to facilitate data collection.

Hyperoxia Treatment

Mouse pups, with their nursing dam, were placed in a chamber at 73% oxygen at P7 and maintained in this environment for 5 days until P12. At this time the pups and nursing dam were returned to normal room air and maintained for another 5 days. At P17, the pups were euthanized as described and their eyes enucleated and snap frozen in 100 µl of PBS pH 7.4 with 0.05% PMSF and homogenized manually on ice using a ground glass tissue homogenizer and processed as described in chapter 4.

ELISA

The homogenized whole eye extract was loaded into sample wells for detection by ELISA. I determined the ocular levels of K1K3 and PEDF protein by an indirect sandwich ELISA procedure as previously described in chapter 4. Briefly, a polyclonal antibody detecting either K1K3 or PEDF was coated onto 96 well plates, the eye extract samples were loaded following the washing and blocking steps. Detection consisted of a secondary mouse polyclonal anti-PEDF followed by a biotin conjugated rat α-mouse IgG (ICN Biomedicals) and HRP conjugated avidin (Pharmingen). Or, in the case of K1K3, detection was through a secondary mouse biotinylated anti-myc antibody (Invitrogen) on the expressed K1K3 to detect bound protein. HRP conjugated avidin followed by TMB peroxidase substrate completed the detection of these proteins by ELISA.

Results

Data Collection

Obtaining samples for each of the time points during the experimental period presented a challenge. In order to obtain statistically significant results, it was necessary to take four eyes (two from each of two animals) each day during the period. Given the average litter size of six to eight pups, this meant that each litter could only provide enough data for 3-4 days during the period. Given this limitation, it was not possible to collect data for the entire experimental period from the same litter of mice. Some litters are larger than other litters and some dams nurse or mother their pups better than other dams. These variations that introduce potential nutritional difference between litters and will necessarily be part of the experimental uncertainty. These uncertainties are not likely to be greater than that caused by variations in the intraocular volume of vector delivered in this model. The volume of an injection in a neonatal mouse eye is 0.5 µl.

Small variability may exist in the volume delivered through the syringe (losses to dead volume) or some volume might reflux out of the eye upon removal of the needle. If this volume was 0.1 µl, this would constitute a 20% variance in the amount of vector delivered.

The first set of experiments involved injecting either rAAV-CBA-K1K3 or rAAV-CBA-PEDF into one eye of neonatal mouse pups. The contralateral eye remained uninjected to serve as an internal control and to check that the expression driven by the vector was restricted to the injected eye. Once it was confirmed that no expression was seen in the contralateral eye, replicate experiments were done in which both of the eyes of the pups were injected with therapeutic vector. The first portion of the experiment involved housing the pups and their nursing dam at normoxic conditions in room air. Pups were then removed from their nursing dam and sacrificed on each day subsequent to the injection. The eyes were enucleated, snap frozen, and homogenized according the protocol discussed in chapter 3. The ocular extract was then analyzed for protein content by ELISA as in chapter 4.

Data Analysis

Significant levels of PEDF (Figure 5-1) and K1K3 (Figure 5-2) were observed as early as day 1 post-injection. These levels were above the calculated anti-NV thresholds, as discussed in chapter 7, for both of the therapeutic compounds and persisted for 17 days following the injection.

Figure 5-1 depicts the expressed levels of PEDF in eyes of neonatal mouse pups that were injected intraocularly with rAAV-CBA-PEDF on post-natal day one. Endogenous PEDF levels are not at zero, but the scale of this graph compresses the values in uninjected eyes so that they appear close to zero. The actual values for the

endogenous levels of PEDF range from 0.3-1.2 ng/eye. These levels are below the estimated therapeutic threshold for PEDF of 2 ng/eye as discussed in chapter 7.

Figure 5-2 depicts the expressed levels of K1K3 in eyes of neonatal mouse pups that were injected intraocularly with rAAV-CBA-K1K3 on day one of life. There is no reference line depicting endogenous levels of K1K3 control eye similar to that depicted in figure 5-1 for PEDF because the ELISA for K1K3 relies on the expressed protein bearing a myc epitope tag. Therefore, even if endogenous angiostatin were present it would not possess this tag and would not be detected by our ELISA procedure.

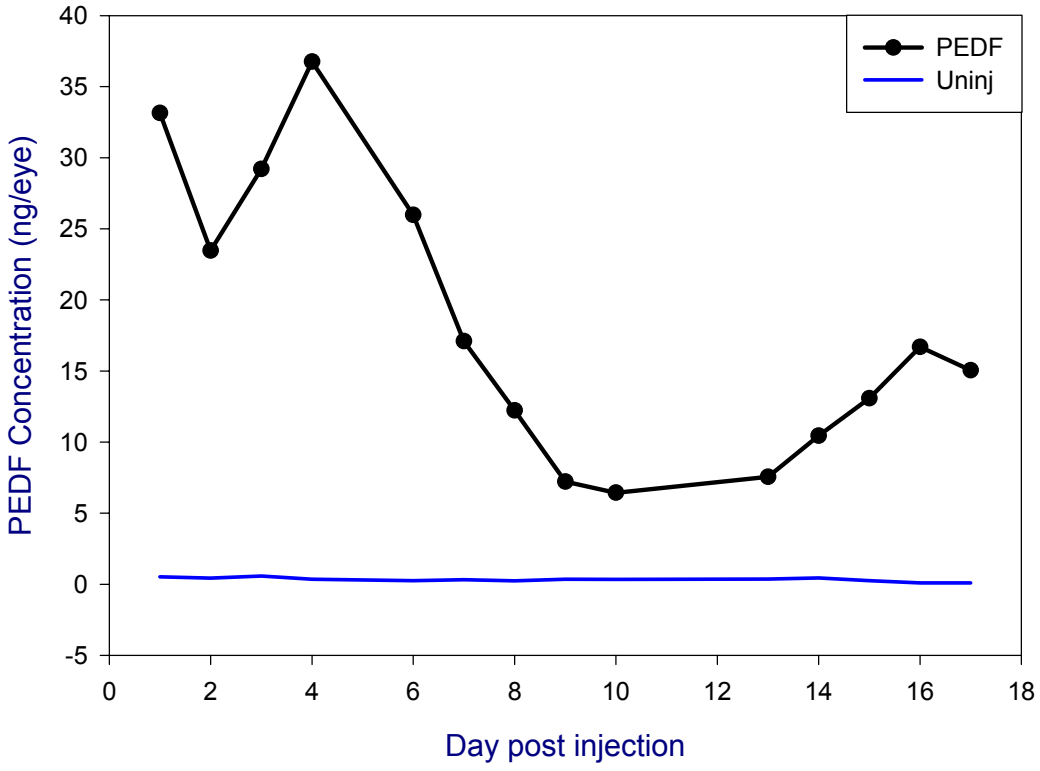

Figure 5-1. Short-term expression of PEDF in neonates. Pups were injected P0 with vector expressing PEDF or remained uninjected. PEDF ocular concentration was measured by ELISA on days P1-P17. The black line with data points as closed black circles depicts the average level of PEDF in eyes on day 1

through day 17 of life in normoxic housed animals. The lower blue line tracks endogenous levels of PEDF in the eyes of these normoxic housed mice.

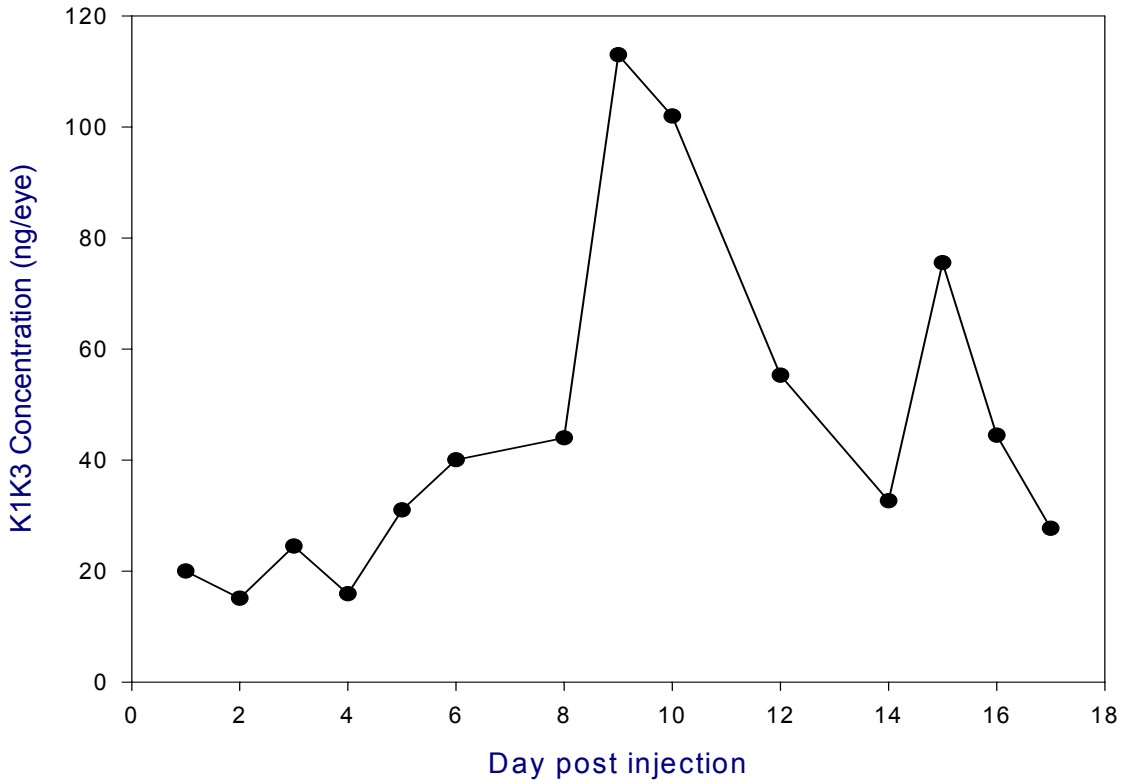

Figure 5-2. Short-term expression of K1K3 in neonates. Pups were injected P0 with vector expressing K1K3. K1K3 ocular concentration was measured by ELISA on days P1-P17 in normoxic housed mice. The black line with data points as closed black circles depicts the average level of K1K3 in eyes on day 1 through day 17 of life.

Interestingly, as seen in figure 5-1 and figure 5-2 there was a peak of expression for both vector products. In the case of PEDF, this peak comes early around day 2-4 post-injection. For K1K3, the peak comes later, around day 9-10 post-injection. One potential explanation for this peak in expression is related to the mitotic index of the cells in the retina. The cells are undergoing a much more rapid division early in the development of the retina (192). It would make sense that the cells undergoing cell division, would also

have the cellular machinery ready to make substantial amounts of our viral-mediated therapeutic protein as well, and this behavior of rAAV vectors is well documented (193-195). This argument sounds reasonable for the expression profile seen with the PEDF vector, but fails to explain the somewhat delayed profile observed with K1K3. Clearly a more complex mechanism is at work here.

Potential PEDF Regulation by K1K3 Expression

In an attempt to elucidate the potential relationship between angiostatin-K1K3 and PEDF I used the same eye extract samples to determine PEDF protein levels in eyes that were injected only with vector expressing K1K3. Sufficient eye extract remained after the ELISA determination of expressed K1K3 in each eye to also determine the level of endogenous PEDF in these same eyes. By conducting this assay I was able to correlate ocular PEDF levels with the virally-mediated expression of K1K3.

Short-term Expression in Neonates

As the bulk of the work in this dissertation focuses on the OIR mouse model, I began my experimental approach by examining expression in eyes from neonatal animals. Figure 5-3 shows that when K1K3 expression is high, around day 9-10 post-injection, endogenous PEDF levels are also high. When K1K3 levels decrease later in the experimental time frame, endogenous PEDF also decrease. However, the endogenous PEDF measured in these eye extract samples followed a similar pattern to the expression pattern of K1K3. This suggests that there is a positive correlation between expression of ocular K1K3 and regulation of endogenous ocular PEDF levels.

These measurements shown in figure 5-3 are all derived from animals housed at normal oxygen levels. Importantly, the levels of PEDF measured here are still above the estimated therapeutic threshold for efficacy. It may be that early expression of PEDF

prior to the time frame of the experimental challenge of hyperoxia followed by return to room air may be essential to the success of the therapy.

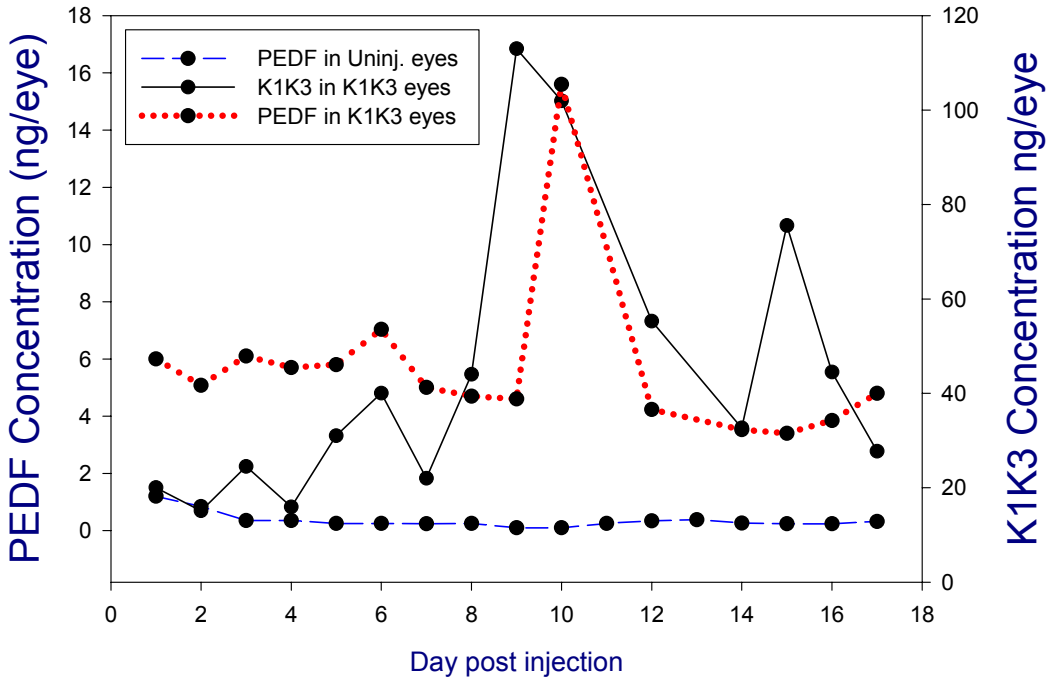

Figure 5-3. PEDF and K1K3 levels in K1K3 P0 injected eyes measured between day 1 and 17 in normoxic housed neonatal mice. The dashed blue line is the level of PEDF in uninjected eyes and tracks on the PEDF scale on the left side of the graph. The solid black line follows K1K3 levels in K1K3 injected eyes and tracks on the K1K3 scale on the right side of the graph. The red dotted line is PEDF levels measured in K1K3 injected eyes and tracks on the PEDF scale on the left side of the graph.

In fact, it is possible that K1K3 is exerting its anti-angiogenic effects largely through the modulation of endogenous levels of PEDF and possibly VEGF, although the latter has yet to be monitored.

Additional data was collected from neonatal pups that were housed according to the OIR protocol. The neonatal pups were housed in hyperoxic conditions (73% O_2) from P7 to P12. This hyperoxic exposure will impact the levels of endogenous PEDF expressed

in these neonatal mice and it may also affect the expression of vectored genes. The K1K3 vector injected and uninjected eyes from these animals were collected as described earlier and the ocular concentrations of K1K3 and PEDF were measured by ELISA. The hyperoxic measurements are depicted in figure 5-4.

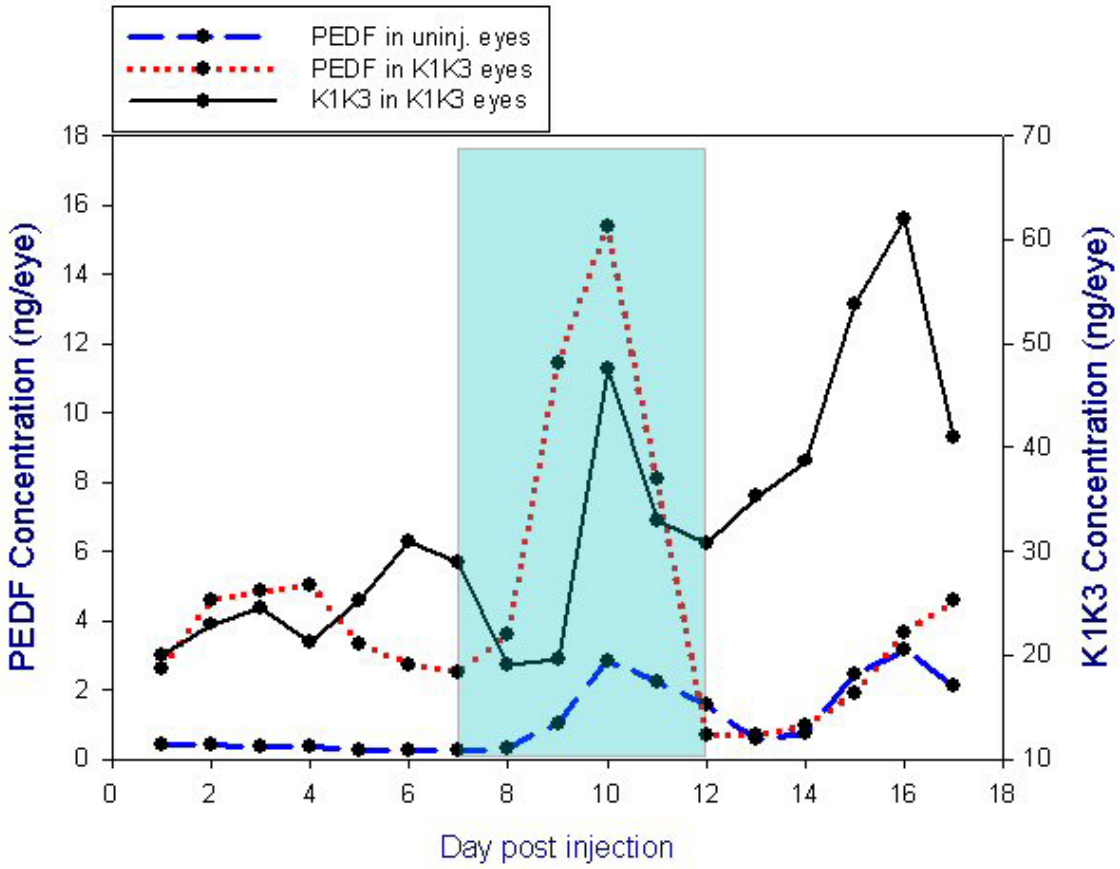

Figure 5-4. PEDF and K1K3 levels in K1K3 P0 injected eyes measured between day 1 and 17 in neonatal mice housed according to the OIR protocol. The dashed blue line is the level of PEDF in uninjected eyes and tracks on the left y-axis PEDF scale. The solid black line follows K1K3 levels in K1K3 injected eyes and tracks on the right y-axis K1K3 scale. The red dotted line shows PEDF levels measured in K1K3 injected eyes and tracks on the left y-axis PEDF. The cyan rectangle overlays days 7-12 indicating the period of 73% O_2 exposure.

The PEDF levels measured here subsequent to K1K3 vector injection are less than those measured from direct expression from a vector bearing the PEDF cDNA.

However, the levels are still well above the endogenous levels seen in age matched mouse eyes. If we overlay the graph of PEDF levels from injection of rAAV-CBA-PEDF with the above graph, we can see that in the case of either therapeutic vector the levels of PEDF were elevated before the hyperoxic exposure (Figure 5-5).

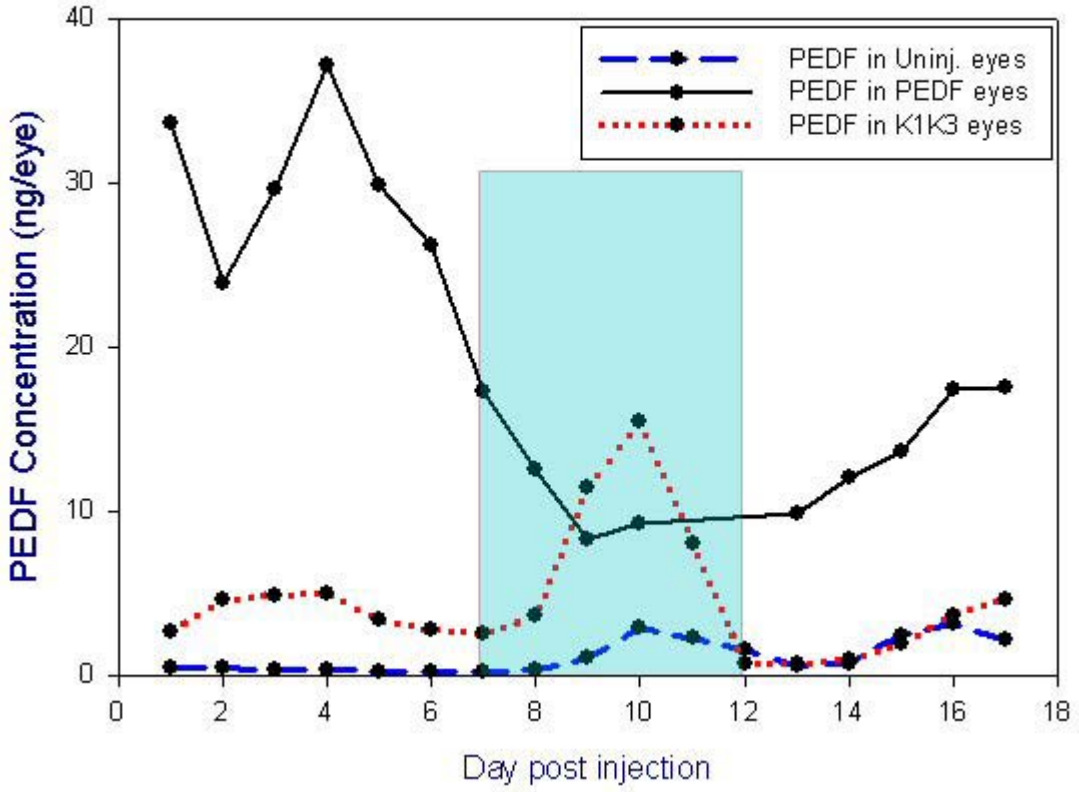

Figure 5-5. Comparison of PEDF levels in K1K3 vector injected, PEDF vector injected, and uninjected eyes from neonatal mice housed according to the OIR protocol. As the figure legend indicates, the long-dashed blue line is the level of PEDF in uninjected eyes. The solid black line follows PEDF levels in PEDF vector injected eyes. The red dotted line is PEDF levels measured in K1K3 injected eyes. The cyan rectangle overlays days 7-12 indicated the period of 73% O_2 exposure.

As figures 5-4 and 5-5 depict, PEDF levels are elevated before the hyperoxic period by both PEDF and K1K3 expressing vectors peaking at approximately day 4. In chapter 4, we saw the efficacy of both of these vectors in controlling the retinal

neovascularization response in the OIR model. The upregulation of endogenous PEDF by the K1K3 expressing vector provides a possible common mechanism by which these vectors might be providing their protective effect. It is potentially significant that the levels of PEDF were elevated before the period of hyperoxia. This initial insult, the transition from room air to 73% oxygen, forms the basis for the later aberrant retinal NV in this model. It seems reasonable for levels of endogenous PEDF to increase in response to this increase in oxygen because the developing retinal vasculature responds to this increase in O_2 tension by inhibiting vascular development. Then when the animals return to room air on day 12 of life, the relative hypoxia causes a sudden suppression of endogenous PEDF followed by an increase in neovascularization almost certainly due to up-regulation of VEGF and/or down-regulation of PEDF. Perhaps having PEDF expressed before the period of hypoxia alters the effect on the oxygen induced modulation of endogenous PEDF so that VEGF-mediated NV is blunted.

Through our collaboration with Dr. Peter Campochiaro at Johns Hopkins, the same vectors used in this study have been shown to be effective in the control of choriodal NV (CNV) in their laser-induced mouse model. (As I was not the individual responsible for the experiments conducted, the data will not be presented in my experimental chapters. Instead some of the findings of that work are discussed in chapter 6 and are summarized here to lend context.) The only data published to date on this effect features the PEDF expressing vector (196). Although both PEDF and K1K3 vectors were used in the study, the PEDF expressing vector was effective in controlling CNV with an injury occurring just 4 weeks after vector injection. The K1K3 expressing vector was not effective at controlling CNV at 4 weeks following vector injection. Further work demonstrated that

the K1K3 expressing vector was effective at controlling CNV if the period between vector injection and laser injury was extended from 4 weeks to 6 weeks. Optimal expression of any gene from serotype 2 rAAV vectors takes 3-4 weeks. This would lead to the expectation that K1K3 may not have been fully expressed until 4 weeks post injection. Alternately, if K1K3 exerts anti-neovascular activity, at least partially, through modulation of endogenous PEDF, it is reasonable to expect that it might take a period longer than 4 weeks to yield a fully functional anti-NV effect. In an effort to better understand the dynamics of PEDF regulation by K1K3, I measured PEDF levels in adult mouse eyes injected with rAAV-CBA-K1K3. The results are shown in figure 5-6.

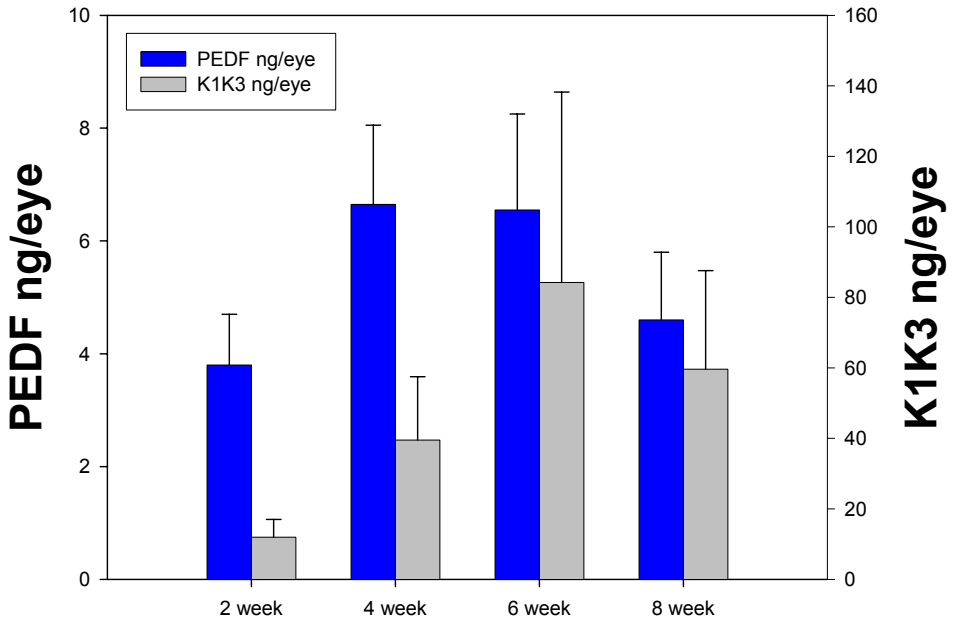

Figure 5-6. K1K3 and endogenous PEDF levels in adult eyes treated with K1K3 vector. As the figure legend indicates, the grey bars represent average K1K3 levels and correspond to the right y-axis. The blue bars are average PEDF levels in the same K1K3 vector injected eyes and track on the left y-axis. PEDF levels for uninjected adult eyes are not shown on this graph and are lower than 1 ng/eye at all time points.

These data indicate that K1K3 can be measured as early as 2 weeks post injection in an adult mouse eye, but that peak expression levels are not reached until about 6 weeks

post injection. The level of endogenous PEDF at 2 weeks is an average of 3.8 ng/eye and has reached 6.65 ng/eye by 4 weeks. The level of endogenous PEDF in K1K3 vector treated eyes remains near this level at 6 weeks measuring 6.55 ng/eye on average. It is not possible from this data to conclude that PEDF is the causative agent in preventing CNV in the laser induced CNV model. But, the anti-angiogenic effects of PEDF provide the mode of action for the K1K3 expressing vector as might be inferred based on the OIR mouse data. These data lend credence to the idea that PEDF levels must reach a certain level or be extant for a certain period of time prior to the experimental injury. Clearly further work must be done in these areas before truly significant conclusions can be reached about the regulatory relationship between K1K3 and PEDF.

Discussion

In summary, rAAV vectors expressing either PEDF or K1K3 are capable of substantial expression of their passenger genes within the time frame of the OIR model. PEDF expression shows an early peak of 24-38 ng/eye around day 3-5 following a P0 injection of rAAV-CBA-PEDF vector. Injection of K1K3 vector also produces a peak of expression, but in this case, the level of expression is more robust and the peak occurs days later than seen with PEDF. K1K3 expression peaks around day 9-10 post injection and reaches levels of 116 ng/eye. The vectored expression of K1K3 seems to increase endogenous levels of PEDF in the eyes of animals housed either in normoxic or hyperoxic conditions as in the OIR protocol. I speculate that this modulation of PEDF levels by vectored K1K3 expression may be part of the mechanism through which K1K3 control the NV response in the OIR mouse.

The day 3-5 peak in vectored gene expression for PEDF and the accompanying mitotic theory does not hold well with the data for K1K3 short-term expression.

However, for K1K3 treated eyes, there is a K1K3 peak seen around day 9-10 for eyes injected with rAAV-CBA-K1K3 (Figure 5-4). At this point, we are not able to arrive at a reasonable explanation for why this is the case except to note that K1K3 levels rise slower than PEDF levels when their respective vector is administered in adult mice. However, it is also important to note that in terms of absolute magnitude, K1K3 expression is at a higher level than PEDF expression. K1K3 levels are measurable at 30-40ng/eye around day 4-6 and peak at over 100ng/eye at day 9-10 in normoxically housed neonates. This indicates that K1K3 expression may be observed at a much higher level than PEDF expression, but that both proteins reach levels of 30-40ng/eye early in their expression period. It is possible that K1K3 has a higher level of expression in the neonatal eye because it is not affected by the same feedback mechanisms that expressed PEDF might be affected. As a normally occurring regulator of NV in the eye, the vector expressed PEDF might be similar enough in form to endogenous PEDF to be recognized by feedback pathways that cause PEDF to be degraded or sequestered. Another possibility to explain the higher levels of K1K3 might be more efficient secretion of K1K3 versus secretion of PEDF. While both genes are encoded with secretory signals and are expressed from the same promoter, it is possible that, due to folding structure or post-translational modification, K1K3 might be more readily secreted from the cell. A last possibility to consider is that there could be some cellular toxicity associated with overproduction of PEDF. While no gross histopathologic changes were observed in sections from PEDF vector injected, it is possible that after a period of early intense production of PEDF cellular toxicity might become a factor. This would imply that no similar toxicity issues are present with K1K3 expression.

The short term expression experiments conducted here reflected the period of the OIR mouse model, from P1-P17. This time period may be later revised to include time points out to 28 days postnatal. The ischemia induced retinopathy model is known to be spontaneously reversible. Unlike the human disease that causes life-long visual impairment, the induced neovascularization in the mouse resolves completely by day 28 postnatal (16 days post removal to room air). In order to understand the behavior of viral mediated expression of PEDF and K1K3 and the corresponding endogenous levels of PEDF following hyperoxic exposure, the time period of the experiment may be increased to include these later time points.

CHAPTER 6
FUTURE DIRECTIONS

Vector Refinement

The initial rAAV vectors used in the work discussed here were broadly expressing vectors that yielded the maximum amount of therapeutic protein from the expression of their cDNA. This modality is not perfect or even desirable if the eventual goal is for this research to progress to human trials. While the passenger gene in both vectors is the human cDNA, the promoter used is possibly too ubiquitous to be used in human trials for ocular NV. It would be far better to control the expression more tightly, either by limiting the target range of the virus or by targeting the promoter to express in only certain cell types within the eye. Optimal control of expression might involve some combination of the two concepts.

Viral Targeting

As discussed in the introduction, AAV serotype 2 targets to cells partially through a heparin sulfate proteoglycan receptor complex, common on many cell types but not present on endothelial cells. It might be advantageous for us to target viruses carrying our therapeutic genes more specifically to endothelial cells. These cells bear unique surface markers that might be exploited to allow specific viral entry. Lineage specific markers might be used to distinguish existing vasculature from pathologically formed angiogenic vessels (197-199), although a recent study suggests that adult hematopoetic stem cells may function as hemangioblasts (200) making such a distinction more difficult. There is evidence that endothelial cells participating in NV can be distinguished

from quiescent endothelial cells. Integrins $\alpha_v\beta_3$ and $\alpha_v\beta_5$ are present on endothelial cells participating in angiogenesis, but are absent on normal retinal endothelial cells (201;202). Through manipulation of the viral capsid, modifications might be made to the virus allowing it to bind to, and gain entry through, these particular cell surface receptors (203;204). Work currently underway in our group is focusing on several such viral capsid modifications. Insertion of ligands such as E-selectin, Apolipoprotein E, or the endothelial cell specific peptide ligand SIGYPLP (205) into various positions in the viral capsid are being tested for more efficient viral targeting of endothelial cells. Initial experiments will determine whether these modifications can reproducibly target *gfp* expression to endothelial cells in the retina. If these experiments are successful, it will be possible to proceed with capsid modified vector expressing therapeutic genes to test for efficacy in the OIR model. Another approach that might show promise is the use of bridging antibodies to increase viral transduction of endothelial cells. CD105 is an angiogenesis-associated protein that is strongly expressed in activated and proliferating endothelial cells. Antibodies to CD105 show highly selective binding to newly formed vessel, but react weakly or not at all with the existing vasculature. Nettelbeck *et al*. (206) have developed a recombinant bispecific antibody that binds to both the adenovirus capsid and to the CD105 protein on the surface of endothelial cells thus targeting adenovirus vectors to endothelial cells. This kind of bispecific antibody strategy could be adapted to targeting adeno-associated viruses to endothelial cells as well by coinjecting the antibody along with the rAAV vector. The bispecific antibody would be mixed with the viral vector preparation prior to local or systemic administration thereby conferring specificity for proliferating endothelial cells. If viral vectors can be re-targeted to a sub-

set of cells within the eye, the potential of serious or harmful side-effects of anti-neovascular treatment should be greatly reduced.

Vector Promoter Selection

Uncontrolled expression of any gene might be deleterious to the cell supporting the expression. Even if the expression was limited to a particular cell type, injury to one cell type could lead to bystander damage in the retina as a whole. Though no cellular toxicity has been observed to date in any of the work discussed in this dissertation, the potential for long-term toxicity in human patients still remains a legitimate concern. For example, if RPE cells are damaged by infection with a rAAV anti-NV vector and became unable to normally process the all-*trans*-retinal back to its 11-*cis* form photoreceptors that depend on a steady supply of 11-cis retinal might degenerate. Alternately if existing normal retinal vasculature was damaged and lost its integrity, the vessels could become leaky leading to edema or to the pathologic formation of new vessels. It is simple to see how, over an extended period of time, relatively subtle cellular toxicity from an inappropriately targeted gene therapy vector might be worse for the patient than the original pathological condition. It is therefore important to control vector expression within the cell type infected to prevent such potential damage.

The promoter used in the studies discussed here is the robust and ubiquitous CBA promoter. While this promoter was ideal for initial studies because it produces a maximal level of the expressed protein, this expression level may not be ideal for future studies, particularly if any of these therapies are to move toward human clinical trials. Alternative promoters might limit expression to the particular cell type involved in the disease state. For example, the *tie* gene encodes a receptor tyrosine kinase that is expressed only in the endothelium of blood vessels. Reporter gene studies suggest that

the *tie* promoter expresses primarily in endothelial cells undergoing vasculogenesis and angiogenesis (207). The β-3 integrin promoter would be another candidate promoter to target expression to endothelial cells specifically.

One of the driving forces in establishment of retinal NV in diabetic retinopathy and retinopathy of prematurity is a relative hypoxia experienced in part of the eye. In the developing retina in premature infants, the high oxygen therapies used to overcome their lack of proper lung function can sometimes translate to a poorly vascularized retina. When the infant is returned to room air areas of the eye that are under-vascularized may experience a relative hypoxia and respond by sending out signals, such as VEGF, to recruit new blood vessels to the area. In diabetic patients, the breakdown of vessels due to sheering stress may cause distal areas along these vessel tracks to be poorly oxygenated. Again, this relative hypoxia in this area of the eye could be the driving force behind the retinal NV. Another alternative therefore would be to take advantage of the hypoxia response element (HRE) mechanism to allow a direct promoter response to the insult of hypoxia in the eye. Using HRE elements to control the expression of anti-NV agents could limit their expression temporally and spatially. As a potential treatment for coronary artery disease, which frequently involves repeated bouts of myocardial ischemia, a hypoxia response element-incorporated promoter was used as a switch to turn on the gene expression in response to hypoxic signal (208). This system, using multiple HRE elements to modulate expression, has successfully expressed GFP reporter gene in retinal and choriodal NV models (209). Future work replacing the reporter gene with anti-angiogenic factors will adapt this system for the treatment of ocular NV disease.

Serotype Selection

Another aspect of our research is to examine rAAV vector serotypes to determine expression levels and in some cases expression profiles with regard to cell type specificity. Here I undertook the question of short-term expression of PEDF from serotype 5 rAAV-CBA-PEDF relative to the serotype 2 vector used throughout our previous experiments. The outcome is shown in figure 6-1.

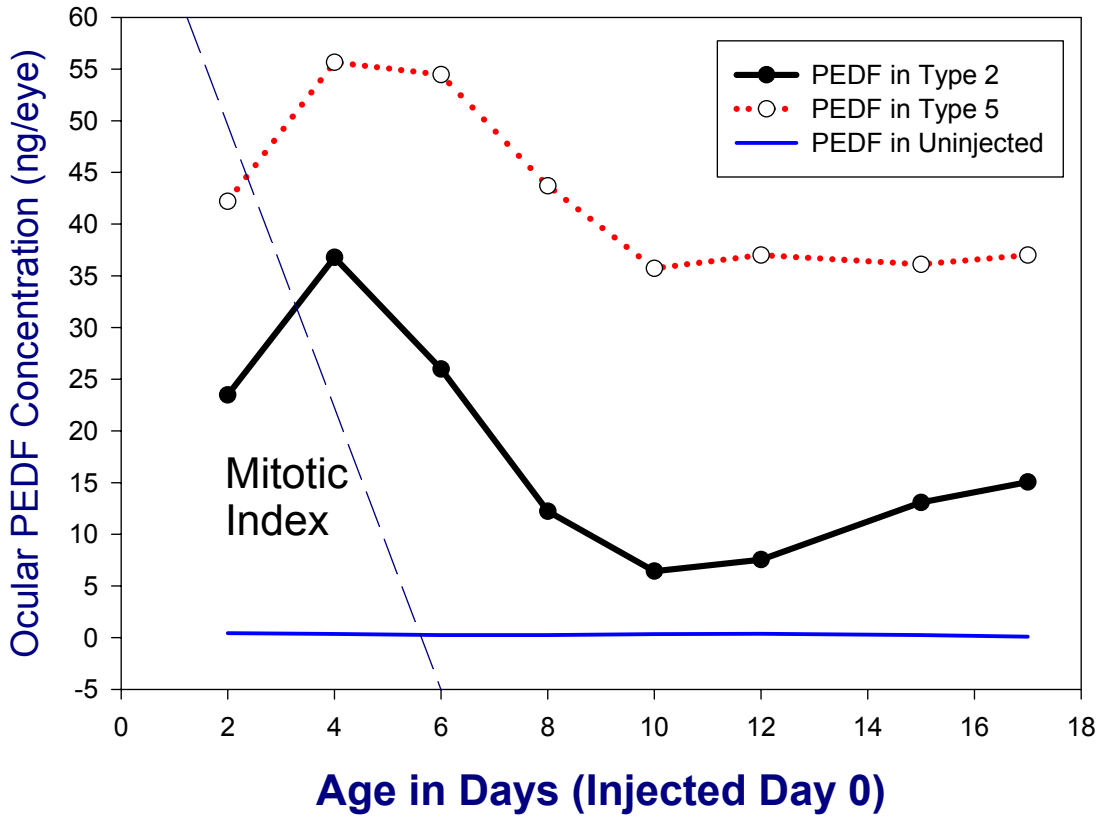

Figure 6-1. Serotype 2 vs. serotype 5 short-term expression of PEDF in normoxic housed neonatal eyes. The red dotted line refers to the expression levels of PEDF from the serotype 5 vector. The black line is PEDF from the type 2 vector and the blue line indicates PEDF levels in uninjected eyes. The diagonal blue dashed line depicts the approximate mitotic index of cells in the retina. This line is unitless and does not correspond to the y-axis on the graph.

Figure 6-1 is similar to figure 5-1 with the addition of data representing ocular PEDF expressed in eyes injected with serotype 5 vector. The diagonal line referring to the mitotic index depicts the concept that early in the developing retina, day 1-2 of life, the cells are rapidly dividing. By day 6-7 of life, the retina is more mature and the cellular machinery used in differentiation and division are nearly quiescent. As has been previously shown (193-195), rAAV vectors make use of the cellular replication machinery in order to express their passenger genes. Therefore, it makes sense that we might see more expression early in the developing retina that would decrease as the retina becomes more mature. This is entirely consistent with a peak early around day 4 followed by a decline to lower, stable levels around day 10. It is difficult to say with certainty, but the levels of PEDF toward the end of the experimental period may be rising slightly. This trend is more apparent in the serotype 2 treated group.

Understanding the Anti-neovascular Mechanism of PEDF and K1K3

I have determined that endogenous levels of PEDF are modulated during and after exposure to hyperoxia in the neonatal mouse between P7 and P17. It is also possible to increase or augment this endogenous response by vector mediated expression of PEDF or K1K3 angiostatin during this same period. In order to better understand the role of PEDF in the control of vascular retinopathy, it will be necessary to look further into this model and examine how PEDF and VEGF levels are modulated during the hyperoxic exposure.

Although different in magnitude, endogenous PEDF increases following hyperoxic exposure in both vector injected and uninjected eyes. Therefore a mechanism other than any related to the vector must be operative. The NV protective effect seen in vector treated eyes may be due to PEDF levels significantly higher than in uninjected eyes following hyperoxia, or to even higher PEDF levels seen prior to or during the period of

hyperoxia. If the latter is the case, the early, elevated PEDF levels might confer a protective effect against the NV insult upon return to room air. I have already determined that there is an increase of endogenous PEDF at both P1-P7 and P7-P12 in response to injection of rAAV-CBA-K1K3 as discussed in Chapter 5. These experiments are summarized in tables 7-1 and 7-2.

Table 6-1. Endogenous PEDF levels and NV response in the uninjected control. The red dashed line indicates the estimated therapeutic threshold for PEDF to have anti-NV effects. The solid black line indicates the trend of endogenous PEDF during each time frame as measured by ELISA.

Uninjected Control Eye

Hyperoxia	Pre (P1-P7)	During (P7-P12)	Post (P12-P17)
PEDF Levels	Below threshold 	Below threshold to just above threshold at P10-P11 	Below threshold directly after then recovering slightly 
NV Response	Normal development of retinal vessels	Fewer vessels formed due to high O_2	Lack of vessels leads to hypoxia and hyper-proliferation

Table 6-2. Endogenous PEDF levels and NV response in the therapeutic vector treated eye. The red dashed line indicates the estimated therapeutic threshold for PEDF to have anti-NV effects. The solid black line indicates the trend of endogenous PEDF during each time frame as measured by ELISA.

Therapeutic Vector Treated Eye

Hyperoxia	Pre (P1-P7)	During (P7-P12)	Post (P12-P17)
PEDF Levels	Low but above threshold 	Highly elevated 	Below threshold directly after then recovering 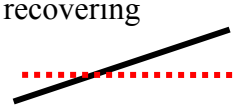
NV Response	???	???	Lower levels of NV measured

To place PEDF levels relative to the NV response in a clear perspective, tables 6-1 and 6-2 have been constructed. It seems unlikely that a small increase over the endogenous-uninjected PEDF levels following hyperoxia could account for a reduction in NV response. We also know from earlier work that PEDF is induced in therapeutic vector injected eyes as early as day 1 and persists through day 17 post-injection. This elevated level of endogenous PEDF was observed whether the animals were housed under normoxic or hyperoxic conditions. Since PEDF is induced in hyperoxia and repressed in hypoxia, I would expect endogenous PEDF levels to be higher during the period inside the hyperoxic chamber. In fact, this is the case. The common threads observed in neonates injected with either therapeutic vector are an early, elevated level of PEDF before the period of hyperoxia (P1-P7) and a highly elevated level of PEDF during the period of hyperoxia (P7-P12). These vector injected pups were equally reduced in their level of retinal NV in the OIR model. It remains to be determined whether this early PEDF expression is necessary and sufficient for control of NV in the OIR model. Administration of purified PEDF protein prior to the hyperoxic exposure is one way that this hypothesis might be tested. It would also be interesting to test whether rAAV-CBA-PEDF injection at time points later than P1 would be effective in controlling retinal NV. Through this type of testing, it might be possible to determine the optimal period, method, and concentration preventing retinal NV.

VEGF Levels During the OIR Model

It would be an interesting follow-up to this experiment to determine if vector expression also represses VEGF during the experimental period. This determination could be easily accomplished as an ELISA for VEGF is commercially available. Remaining samples of eyes injected with either therapeutic vector could be tested by

ELISA. If VEGF is repressed in vector treated eyes either prior to or during the hyperoxic period, we might be closer to understanding how these vectors exert their therapeutic effect. If VEGF is unchanged, the anti-NV effect may operate by a post-translational mechanism, perhaps by inhibiting VEGF receptor binding.

PEDF or Angiostatin Protein Treatment

If elevated levels of PEDF early in the OIR model yield a protective effect against the hyperoxia related angiogenesis, it might be possible to translate these effects to a therapy for premature human infants with or at risk for ROP. Due to potential toxicity concerns, it is unlikely that a gene therapy approach would be used in treating ROP infants. If I can demonstrate that an injection or a series of injections of PEDF or K1K3 angiostatin protein can have a similar prophylactic effect to that seen with the gene therapy approach, protein administration would be a preferable method of treating ROP in humans. The challenge here lies in finding the correct level of PEDF and the correct time before/during the hyperoxia/hypoxia challenge to treat in order to gain an optimal protective effect. Initial efforts testing this theory are underway. This will involve the injection of purified PEDF (BioProducts of Maryland, Middletown, MD) into the eyes of neonatal pups at time points preceding entry into the hyperoxic chamber. Preliminary experiments with 100ng of PEDF injected on P7 just before hyperoxic exposure did to produce the hoped for results in the OIR model. This preliminary experiment did show a NV reduction in the injected eye. However, the contralateral uninjected eye often had a lower level of NV than the matched injected eye. This made it difficult to draw conclusions regarding the efficacy of PEDF protein injections. It is possible that the contralateral eye is affect through some regulatory mechanism stemming from the injection of PEDF in the partner eye. Obviously, we need a better understanding of the

pharmacokinetic parameters of PEDF in the mouse eye. To this end, eyes from neonates injected with varying concentrations of PEDF at varying time points pre-hyperoxia will be screened by ELISA on subsequent days. In this way we can determine the intraocular half-life of injected PEDF protein. This information might guide us to more effective ocular PEDF dosing regimens in which one or several repeated PEDF protein intraocular injections might produce the desired effect of reducing NV in the OIR mouse model.

Some of our data suggest K1K3 exerts anti-angiogenic effects through the regulation of PEDF levels. Future work will determine if injection of K1K3 angiostatin protein will lead to the up-regulation of PEDF as does the injection of the K1K3 expressing vector. Once we are able to determine the appropriate timing and concentration of protein to administer, it might be possible to translate a protein-based approach to effective therapy for premature infants. A physician able to make an appropriately timed ocular injection of PEDF, angiostatin, or some other anti-angiogenic protein might be able to preserve vision in neonates who would otherwise be severely affected by ROP.

Other Models of Ocular Neovascularization

The bulk of the work in this dissertation focused on the use of rAAV vectors expressing K1K3 and PEDF in the ischemia induced retinal NV model in the neonatal mouse. Through our collaborations, the same vectors used in the OIR model were also effective against CNV in the laser-induced adult mouse model, as summarized in chapter 6. Similar laser CNV models in the pig (210) and monkey (211) are available and more closely approximate the size and structure of the human eye. The monkey CNV model has the further advantage of possessing a macula, a central retinal feature that other non-human species lack. Testing vectors in these larger eyes may provide additional insight

into their potential as therapeutics for humans. Alternative ocular neovascular models exist that might be used to further test these vectors and may reveal important issues about the generality of the vector and/or the therapeutic genes PEDF and K1K3. Some of these models are discussed below.

VLDL-receptor Knockout Mouse

Mice that lack the very low density lipoprotein receptor (VLDLR) as knock-out animals were originally reported to exhibit little or no observable phenotype (212), with the possible exception that the animals had lower body weight and appeared leaner than their wild-type counterparts. When the ApoE receptor 2 gene was also disrupted in these mice, they exhibited neurological abnormalities (213). Upon closer examination, when the low density lipoprotein receptor was disrupted, abnormal lipid metabolism was noted (214). Partial correction of this hyperlipidemia in mice with familial hypercholesterolemia was subsequently achieved using an rAAV vector expressing VLDLR (215). Recently it has been found that these VLDLR deficient mice also suffer a spontaneous retinal NV and late CNV (Xiaohua Gong, U. C. Berkeley, personal communication) that might make these mice useful models for both CNV and retinal NV treatment with our rAAV anti-NV vectors.

Macrophage Chemotactic Protein-1 Knockout Mouse

Macrophage chemotactic protein-1 (MCP1) is involved in inflammatory corneal neovascularization (216), but is not involved in bFGF mediated corneal neovascularization. This correlates with findings that interleukin-10, secreted by macrophages, exhibits anti-angiogenic effects (217;218). Thus, MCP1 may be a major player in initiating/maintaining CNV. The hypothesis was recently tested by showing

that disrupting the gene for MCP1 leads to a model of spontaneous NV (Jay Ambati, University of Kentucky, personal communication).

Diabetic Mouse Models

Diabetes has been modeled in the mouse for a number of years. Some strains of mice are genetically diabetic such as C57BL/KsJ db+/db+ mice or the non-obese diabetic (NOD) mouse. Other mice can be rendered diabetic by treatment with streptozotocin (STZ) which destroys beta-cells in the pancreas. Only recently have researchers turned to diabetic mice as a potential model for studying diabetic retinopathy. Several retinal metabolic abnormalities were noted in the diabetic mouse retina (219) including increased oxidative stress, protein kinase-C activity, and elevated levels of nitric oxides. These metabolic changes are likely to be a precursor to cellular damage that could lead to vascular retinopathy. Thus, older diabetic mice may be promising animal models in which to study the pathogenesis of diabetic retinopathy.

Summary

The refinement of the vectors discussed in this dissertation will provide a therapeutic vehicle to deliver anti-NV factors to the eye safely, effectively, and with the potential for long-term correction of NV response in diabetic patients. Targeting of the virus by capsid modifications or serotype specificity may increase the efficiency of transfecting particular cell types. Variations in the promoter used to drive expression of the anti-NV factors in the eye may limit expression temporally, by cell type, or conditionally to respond to hypoxia. Further understanding of interplay between anti-NV like PEDF and K1K3 and pro-angiogenic factors like VEGF will provide a solid basis for developing additional therapies. By applying the therapeutic vectors developed in this

dissertation to other animal models of NV, additional insight may be gained moving these therapies toward clinical application.

CHAPTER 7
CONCLUSIONS

Effective, long lasting treatment of retinal neovascular disorders, including diabetic retinopathy and proliferative AMD, remains one of the greatest challenges in ophthalmology today. The number of individuals suffering from diabetes has increased worldwide in recent years and is projected to continue to rise (184). Proliferative diabetic retinopathy (PDR), characterized by a hyper-proliferation of microvessels in the retinal vasculature, is a common complication in diabetic patients. PDR shares a patho-physiology with our model of ischemic retinopathy, the OIR mouse. The initial ischemic insult and the subsequent pathologic outgrowth of new vessels from the retinal vasculature occur in both PDR and ROP and ultimately lead to blindness in either disease. Retinal NV can also occur secondarily to choriodal NV in AMD (185;186). Gene-based therapies, predicated on the type summarized in this dissertation, could offer long-term control of proliferative retinopathy. Vector refinement through continuing research is likely to produce even safer and more efficacious treatment options that may be used in conjunction with current treatment methods.

Modeling Choriodal Neovascularization

While the focus of this dissertation has been the treatment of retinal NV in the OIR mouse model of ischemic retinopathy, the therapeutic vectors discussed here could also

be applied against CNV. This hypothesis was tested in collaboration with the laboratory of Peter Campochiaro at Johns Hopkins. They work with a model of CNV in which a laser is used to rupture Bruch's membrane at discrete locations. Following this injury new vessels grow through this hole in Bruch's membrane and invade the retina. This mimics the progression of the disease seen in human patients with advanced AMD.

Adult mice were injected with rAAV-CBA-PEDF or rAAV-CBA-K1K3, the same vectors used in my work in the OIR mouse model. The eyes of these mice were lasered either 4 or 6 weeks following the vector injection. Two weeks after laser injury, the size of CNV lesions were measured in choriodal flatmounts or in frozen transverse sections. The results for PEDF vector injected eyes are shown in figure 7-1.

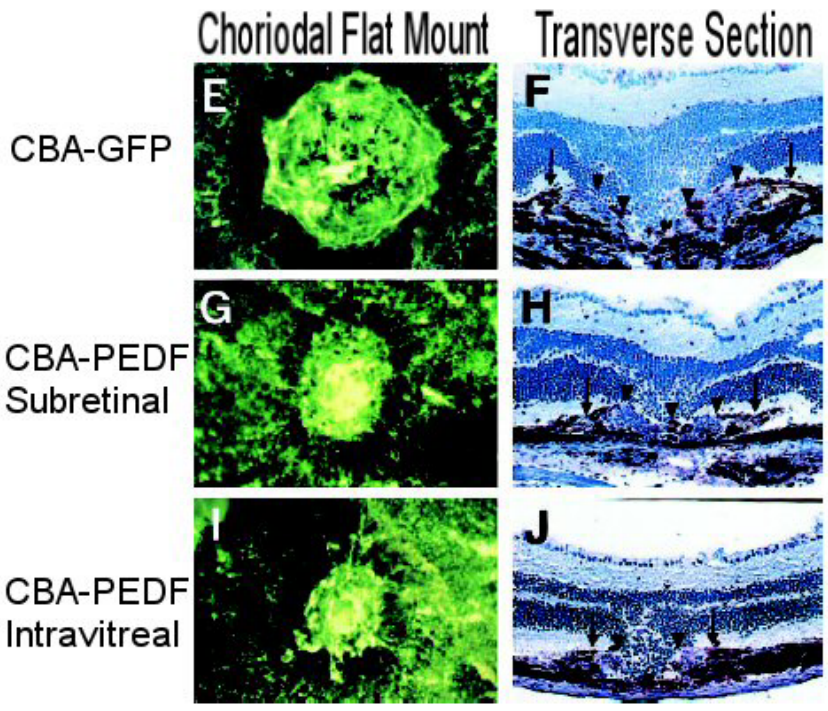

Figure 7-1. CNV lesion size reduced in eyes treated with CBA-PEDF vector. Adult mice were injected with rAAV-CBA-PEDF and laser treated 6 weeks later to induce CNV. Two weeks after the rupturing of Bruch's membrane CNV lesion size is determine in choriodal flatmounts (E, G, I) or frozen transverse sections (F, H, J). (E) Fluorescence microscopy shows a large CNV lesion at

the rupture site of Bruch's membrane in an eye that was injected with the control vector. The transverse section through another control vector treated eye (F) had a large diameter (*arrows)*. Much smaller areas of CNV were observed in choriodal flat mounts eyes that received intravitreal (I) or subretinal (G) rAAV-CBA-PEDF. This correlates with the small diameters seen in frozen transverse sections in similarly treated eyes (J and H).

Injection of rAAV-CBA-PEDF, either subretinal or intravitreal, showed a reduction in the size of CNV lesion in this model. A significant reduction in size of CNV lesion was reproduced in a larger number of animals treated with the PEDF expressing vector (196). Similar results were seen in eyes laser treated six weeks after they were injected subretinal with rAAV-CBA-K1K3 (Fig. 7-2).

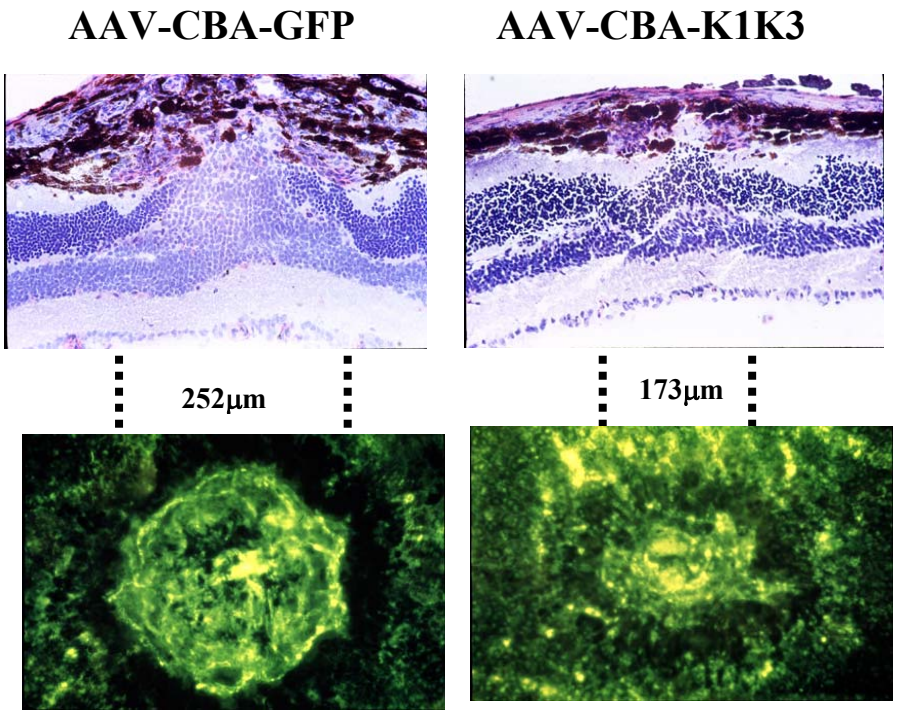

Figure 7-2. CNV lesion size reduced in eyes treated with CBA-K1K3 vector. Adult mice were injected with rAAV-CBA-K1K3 and laser treated 6 weeks later to induce CNV. Two weeks after the rupturing of Bruch's membrane CNV lesion size is determine in choriodal flatmounts or frozen transverse sections. Fluorescence microscopy shows a large CNV lesion at the rupture site of Bruch's membrane in an eye that was injected with the control vector (lower left) which is aligned to the

diameter measure of 252μm in the transverse section (upper left). Smaller areas of CNV were observed in choriodal flat mounts eyes that received subretinal rAAV-CBA-K1K3. This aligns with a smaller diameter of 173μm in a transverse section.

The efficacy of PEDF or K1K3 expressing vectors in controlling CNV was independent of the intraocular location of injection. This is somewhat surprising as we might expect a subretinal injection of an anti-NV agent to be more effective in the control of local choriodal vascular injury. However, both PEDF and K1K3 are produced at robust levels from the CBA promoter and are secreted from the cell where they are produced. PEDF and K1K3 therefore appear to freely diffuse through the eye and act on remote cell types.

Interestingly, PEDF expressing vectors were effective in reducing CNV lesion size whether the vector was administered four or six weeks before the laser injury. This was not the case for K1K3 expressing vectors. Experiments in which rAAV-CBA-K1K3 was injected four weeks prior to laser rupture of Bruch's membrane showed this vector to be ineffective in controlling CNV in this model. It was only when K1K3 expressing vector was injected six weeks before laser injury that reduction in CNV lesion size was observed. This effect may be related to the mechanism of action of K1K3. As noted in chapter 5, K1K3 may function partially through modulating endogenous levels of PEDF and/or VEGF. In figure 5-5, I show that endogenous PEDF is upregulated in the eyes of adult mice injected with K1K3 expressing vector. In those experiments, endogenous PEDF levels were measurable as early as 2 weeks post injection of rAAV-CBA-K1K3, but never exceeded 8 ng/eye. This is a much lower level of PEDF than that achieved by injecting rAAV-CBA-PEDF vectors (20-70 ng). It is possible that the delay in reaching significant levels of PEDF or the lower levels of PEDF over the experimental time frame

is responsible for the delayed efficacy of the K1K3 expressing vector in the laser-induced CNV model.

Increasing Incidence of Adult Retinopathy

Current data suggests that our medical community will be faced with increasing numbers of patients suffering from PDR and proliferative AMD. Increases in the prevalence of diabetes, particularly adult-onset diabetes, and the advancing age of our population will be accompanied by parallel increases in cases of proliferative retinopathy.

Prevalence of Diabetes

Type II diabetes incidence is highly correlated with obesity (15;220). Both obesity and the prevalence of type II diabetes have increased during the period from 1990 to 1998 in the United States (221). In 1990 the total percentage of the US population affected by diabetes was 4.9%. By 1998, that percentage had increased to 6.5%. In 1990, a total of 43.6% of respondents were classified as either overweight or obese by BMI (Body Mass Index) calculations. By 1998, this had increased to 53.9%. It is important to note that this study of both obesity and diabetes incidence was based on telephone surveys of self-reporting adults. Because of this, the study is likely to underestimate the total number of diabetic patients as the self-reporting criteria focused on the answer to the question, "Have you been told by a doctor that you have diabetes?" Since the incidence of increased weight gain precedes the onset of diabetic symptoms by several years, it is likely that the incidence of adult-onset diabetes will continue to rise. More recent data estimates the number of patients with diagnosed or undiagnosed diabetes or with impaired fasting glucose at 29 million in the US (14). PDR is just one of the potential complications and can affect patients with either Type I (juvenile) or Type II diabetes. With the large increases in the prevalence of Type II diabetes, there will be a

commensurate increase in the number of patients with PDR. Current therapies for PDR include laser photocoagulation or surgical vitrectomy. As discussed earlier, these can be effective in preserving vision immediately following surgery, but carry inherent risks and often result in an immediate decrease in visual acuity. Most importantly, neither clinical treatment addresses the underlying angiogenic stimuli. Clearly the need exists for effective alternative therapies to preserve the long-term vision of diabetic patients.

Impact on PDR Therapies

Diabetic retinopathy being a chronic condition is difficult to treat. Many sufferers are unaware that they have diabetes until their ophthalmologist diagnoses diabetic retinopathy. By this time, it is too late for preventative care. Gene therapy approaches to treating PDR, such as those discussed here, could provide a much needed adjunct to current therapeutic techniques. Vitrectomy or laser photocoagulation could easily be coupled with intraocular injection of vectors expressing anti-NV agents such as PEDF or K1K3. This additional therapy could re-establish a balance between angiogenic inducers and inhibitors and prevent future NV events. This could benefit the patient by preserving what vision they have remaining thereby significantly enhancing their quality of life. It may also benefit society by ultimately reducing repeated health care costs and the economic impact of working age persons losing their vision.

In cases where a diabetic patient has not yet developed PDR, it is possible that gene therapy might be used preventatively. PEDF operates, at least partially, by inducing apoptosis in newly forming vessels (222). Treatment with PEDF expressing vector or with K1K3 expressing vector that upregulates endogenous PEDF may effectively reduce the NV response in diabetic patients before it becomes clinically significant. It is clear,

however, that preventative gene therapy is much more controversial than palliative therapy.

Prevalence of Age-related Macular Degeneration

AMD is the principal cause of visual impairment in those over the age of 65. Advanced AMD can be classified into two types: non-neovascular or "dry" AMD or neovascular or "wet" AMD. Dry AMD can lead to visual impairment due to loss of the photoreceptors. Although less than 20% of patients with AMD have the neovascular form, severe vision loss occurs predominantly in patients with this form of the disease. The principle and unavoidable risk factor in AMD is age (223). Other risk factors include exposure to sunlight (224;225), genetic influences (226-229), smoking (230-232), alcohol consumption (233;234), among other factors. Some of these factors, like cigarette smoking or exposure to sunlight, are behavioral components that can be minimized or eliminated. Other contributing factors, such as genetic predisposition are more difficult to address. Because the most significant risk factor for AMD is age, the changing demographics that will lead to an increase in the number of elderly persons, will also increase the incidence rate for AMD in the future.

Impact on AMD Therapies

The mechanism underlying the CNV in patients suffering from wet AMD remains to be fully elucidated. However, the problems associated with treating PDR are also common in treating advanced AMD. Namely, the current therapies available, laser photocoagulation, surgical intervention, or photodynamic therapy, fail to address the long-term recurrence of NV. Due to their advanced age, patients suffering from AMD also suffer from additional conditions that can limit treatment options. While not all patients with "dry" AMD will develop CNV, genetic studies may identify subgroups of

disease and thus help provide a selective approach to treatment (235). It may be possible to preempt any NV event from ever occurring in predisposed patients by a subretinal injection of a rAAV vector expressing PEDF or K1K3. It is likely that a subretinal injection would be more effective in treating CNV as it localizes the virus to the area where the initial NV stimulus is likely to occur. As with PDR, similar ethical problems may exist with pre-symptomatic gene therapy for AMD.

Effective Anti-angiogenic Intraocular Dose

Although the minimum effective intraocular dose of PEDF or K1K3 for controlling ischemic retinopathy is unknown, previous studies following administration of PEDF protein in the same model I employ here show the therapeutic threshold to be approximately 5-11 μg/day (191) when administered systemically. If we make the simplest and most conservative assumptions, that PEDF is stable and partitioned into the eye from the systemic vasculature based simply on the volume of the eye versus the volume of the whole animal, the concentration of ocular PEDF needed to inhibit retinal NV is estimated to be 1-2 ng/eye. This conservative calculation does not consider any pharmacokinetic stability parameters of PEDF or the existence of the blood-retinal barrier, both of which would tend to reduce further the amount of PEDF reaching the eye from the circulation. It is therefore possible that the true intraocular therapeutic threshold for PEDF is much lower than this rough estimate. I demonstrated here that rAAV vector expressed PEDF produces intraocular concentrations of 20-70 ng in the adult mouse and 6-36 ng in the neonatal mouse. This is at or considerably higher than our estimated therapeutic threshold. Similar calculations based on another study in which one dose of K1K3 angiostatin administered systemically was able to effectively reduced retinal NV in

the OIR mouse (190) yield an estimated maximum intraocular therapeutic threshold of 1.6 ng/eye for K1K3. Our rAAV vector expressing K1K3 angiostatin produces levels of 6-60ng/eye in the adult or 16-160 ng/eye in the neonate; again above our estimated maximum threshold. Therefore it appears that we can achieve and maintain intraocular levels of either PEDF or K1K3 angiostatin in neonatal and adult mice sufficient to expect significant reduction of retinal NV. However, the minimum effective intraocular dose remains to be established by careful vector titration experiments in the OIR mouse.

Controlling Vector Expression

Administration of rAAV vectors expressing cDNAs for anti-angiogenic proteins can therefore be as effective as administration of the corresponding proteins systemically, but without the requirement for repeated injections. In addition, use of rAAV vectors offers several potentially important advantages over systemic administration of anti-angiogenics. Local production and secretion of PEDF or K1K3 through vector gene delivery is likely to restrict any anti-neovascular activity to an area specific to the pathological angiogenesis in the subject. Proteins produced in the posterior ocular compartment are not likely to interfere with the normal angiogenic processes necessary for wound healing or tissue repair elsewhere in the body, and perhaps not even in the anterior segment of the same eye, although this remains to be tested. Further, rAAV vectors have demonstrated long-term, sustained high-level expression in the retina (165), and we observe nanogram levels in rat eyes for at least 21 months (B. Raisler and W. Hauswirth, unpublished), indicating that a single injection of rAAV bearing a therapeutic gene could provide durable inhibition of NV. This could obviate the need for repeated injections of anti-angiogenic compounds systemically or intraocularly.

Maximizing Therapeutic Levels

For the purposes of maximizing protein expression in the retina, I found that rAAV-CBA-PEDF and rAAV-CBA-K1K3 vectors produced the highest levels of ocular protein. The lower levels of expression seen for vectors with mouse opsin (MOPS), CRALBP, and PDGF promoters may be due to the different cell specificity of these promoters compared to CBA or, in the case of CMV, to a generally lower ability to support transcription in the same set of retinal cell types. When subretinally injected, CBA supports expression well in both RPE cells and photoreceptors (236). In contrast, the MOPS promoter is largely rod photoreceptor specific (164) and yields much lower intraocular expression, thus suggesting that the key source of secreted PEDF or K1K3 from vectors injected subretinally is the RPE cell. When injected into the vitreous, CBA-containing rAAV vectors express very well predominantly in RGC's (196). Since there was no significant difference in the anti-neovascular effectiveness of subretinally or intravitreally administered PEDF or K1K3 vectors with the CBA promoter, it appears that the potentially less traumatic intravitreal route of vector delivery may be favored. However, whether either vector has toxicity in either RPE cells or retinal ganglion cells remains to be determined.

Limiting and Localizing Expression

For optimizing the safety of ocular gene therapy for NV diseases it may be important to limit expression of a therapeutic protein even more specifically, either to just a single retinal cell type or to a more defined topographic area. By altering the promoter used to drive PEDF or K1K3 expression it may be possible to fine tune therapeutic gene expression to a pharmacologically significant but highly localized cellular pattern. The CBA promoter drives expression in multiple cell types whereas a more specific promoter

could be employed to target expression selectively. Alternatively, delivering the vector specifically to the intravitreal or subretinal space in a larger human eye may also define better localization of expression. Advanced stages of AMD are characterized by a neovascularization of the chorocapillaris within or adjacent to the macula where treatment might be most effective if the therapeutic vector is administered subretinally near potentially active CNV regions. This type of subretinal administration effectively limits the lateral spread of vector-mediated expression (237) whereas vitreal administration may allow less constrained vector diffusion to a wider and less controlled retinal area. Full testing of these ideas will require development of an animal model with a retinal area closer in size to that in humans than the mouse. A recently developed CNV model where lesions are induced by intense laser photocoagulation in a cynomolgus monkey has greatly assisted researchers in developing such therapies (238;239).

K1K3 Expression Modulates Endogenous PEDF

One of the more interesting findings in my dissertation work is the potential regulatory relationship between K1K3 angiostatin and PEDF. This part of my work was initially undertaken in response to a research report suggesting that the Kringle 5 (K5) fragment of plasminogen upregulates PEDF and downregulates VEGF (118). Kringle 5 is known to be potently anti-angiogenic in a rat model of retinal NV (240). It occurred to me that K1K3 angiostatin might have similar effects to K5 with regard to the regulation of PEDF. I had at my disposal an ELISA that was capable of measuring endogenous, as well as vector expressed, PEDF. It therefore seemed a logical extension of my research to determine if expression of K1K3 from a rAAV vector would modulate endogenous PEDF. Indeed vectored expressed K1K3 was capable of increasing levels of endogenous PEDF in both adult and neonatal mice. These data point to a possible mechanism of

action for the anti-angiogenic effects of K1K3, namely through the increase of the angiogenesis inhibitor PEDF.

Early PEDF Levels Are Critical in the OIR Model

From all of the work discussed in this dissertation, it is apparent that it is critical for levels of PEDF to be elevated before and/or during the hyperoxic exposure period in the OIR mouse. These PEDF levels can be derived from the expression of rAAV-CBA-PEDF vector or alternately in response to expression of K1K3 from rAAV-CBA-K1K3 vector. However, based on the consistent upregulation of endogenous PEDF during the hyperoxic period in uninjected neonatal mice, it seems likely that PEDF is the central player and that the levels of PEDF must be elevated early on in this experimental model. Since this model most closely mimics the pathology of ROP in human neonates, this provides insight into possible therapy for these patients. Even though rAAV vectors have been demonstrated to have low or no toxicity, it would still be unlikely that approval for injecting a long-term expressing viral vector into the eye of a child would be granted in the foreseeable future. Because there is no way that the potential toxicity of life-long expression could be known, the risks of that therapeutic approach are too great. If I could optimize treatment with PEDF protein at a discrete time and level before hyperoxic exposure, it could be prophylactic against the development of ROP and would be an important new therapy for preserving vision in premature infants. The experimental systems developed in this dissertation would allow testing of this important therapeutic hypothesis.

Summary

I have demonstrated that rAAV vectors incorporating a CBA promoter are capable of producing sustained therapeutic levels of PEDF and K1K3 in the mouse eye.

Intraocular injection of rAAV-CBA-PEDF or rAAV-CBA-K1K3 significantly reduced the level of retinal NV in a mouse model of ischemic retinopathy. Through our collaboration with Dr. Peter Campochiaro's group at Johns Hopkins, the same vectors are efficacious in reducing CNV lesion size in a laser-induced mouse model. Other studies have recently demonstrated effective gene therapy approaches for controlling ocular angiogenesis. Expression of PEDF from either rAAV (196) or adenovirus (241) vectors were effective in reducing choroidal NV in rodent models. Adenoviral vectors expressing endostatin (135) or plasminogen activator inhibitor-1 (242) were also effective in inhibiting retinal NV. Together with our present report, the generality of efficient and well-targeted gene-based approaches for treating neovascular diseases of the eye coupled with the potential of rAAV vectors for persistently delivering anti-angiogenic proteins to the retina is becoming apparent.

APPENDIX
TERMS AND DEFINITIONS

This appendix will provide definitions and expansions of acronyms used in this document.

AAV- Adeno-associate virus

AMD – Age-related macular degeneration

bFGF – Basic fibroblast growth factor

CBA – Chicken beta-actin (used to refer to the chicken beta-actin hybrid promoter)

cDNA – Coding deoxy-ribonucleic acid

CMV – Cytomegalovirus

CNV – Choriodal neovascularization

CRALBP – Cellular retinaldehyde binding protein (used to refer to a promoter)

DR – Diabetic retinopathy

EDTA – Ethylenediaminetetraacetic acid

ELISA – Enzyme linked immunosorbent assay

FGF-2 - Fibroblast growth factor 2

FGFR – Fibroblast growth factor receptor

GFP – Green fluorescent protein

HIF-1 – Hypoxia inducible factor

HRP – Horseradish peroxidase

IGF-1 - Insulin-like growth factor-1

K1K3 – Kringle domains 1-3 of angiostatin

MCP-1 – Macrophage chemotactic protein

mRNA – Messenger ribonucleic acid

NOD – Non-obese diabetic

NV – Neovascularization

OIR – Oxygen induced retinopathy

PBS – Phosphate buffered saline

PDGF – Platelet derived growth factor (used here to refer to a promoter)

PDR – Proliferative diabetic retinopathy

PDT – Photodynamic therapy

PEDF – Pigmented epithelium derived factor

PMSF – Phenylmethanesulfonyl fluoride

rAAV – Recombinant adeno-associated virus

ROP – Retinopathy of prematurity

RPE – Retinal pigmented epithelium

STZ – Streptozotocin

SV40 – Simian virus 40

TIMP-3 – Tissue inhibitor of metalloproteinase 3

TMB - 3,3',5,5' - tetramethylbenzidine

TR – Terminal repeat

VEGF – Vascular endothelial growth factor

VLDLR – Very low density lipoprotein receptor

LIST OF REFERENCES

1. Ferrara, N., Davis-Smyth, T. (1997) The biology of vascular endothelial growth factor. *Endocr.Rev.* 18, 4-25

2. Shweiki, D., Itin, A., Soffer, D., Keshet, E. (1992) Vascular endothelial growth factor induced by hypoxia may mediate hypoxia-initiated angiogenesis. *Nature* 359, 843-845

3. Dawson, D. W., Volpert, O. V., Gillis, P., Crawford, S. E., Xu, H., Benedict, W., Bouck, N. P. (1999) Pigment epithelium-derived factor: a potent inhibitor of angiogenesis. *Science* 285, 245-248

4. Urgena, R. B. (1972) Oxygen toxicity: basic and clinical considerations. *J.Iowa Med.Soc.* 62, 583-587

5. Faris, B. M. (1972) Retinopathy of prematurity. I. Etiology, pathology, clinical course, diagnosis and treatment. *J.Med.Liban.* 25, 373-377

6. Yeh, T. F., Lin, Y. J., Hsieh, W. S., Lin, H. C., Lin, C. H., Chen, J. Y., Kao, H. A., Chien, C. H. (1997) Early postnatal dexamethasone therapy for the prevention of chronic lung disease in preterm infants with respiratory distress syndrome: a multicenter clinical trial. *Pediatrics* 100, E3

7. Bancalari, E., Flynn, J. T. (1988) Respiratory physiology, oxygen therapy, and monitoring: report of a clinical trial of constant monitoring. *Birth Defects Orig.Artic.Ser.* 24, 41-52

8. Johnson, L., Schaffer, D., Quinn, G., Goldstein, D., Mathis, M. J., Otis, C., Boggs, T. R., Jr. (1982) Vitamin E supplementation and the retinopathy of prematurity. *Ann.N.Y.Acad.Sci.* 393, 473-495

9. Tasman, W. (1988) Multicenter trial of cryotherapy for retinopathy of prematurity. *Arch.Ophthalmol.* 106, 463-464

10. Palmer, E. A. (1988) Cryotherapy: indications, methods, and current status. *Birth Defects Orig.Artic.Ser.* 24, 255-263

11. Palmer, E. A. (1986) The multicenter trial of cryotherapy for retinopathy of prematurity. *J.Pediatr.Ophthalmol.Strabismus* 23, 56-57

12. Dobson, V., Quinn, G. E. (1996) Retinopathy of prematurity. *Optom.Clin.* 5, 105-124

13. Paysse, E. A., Lindsey, J. L., Coats, D. K., Contant, C. F., Jr., Steinkuller, P. G. (1999) Therapeutic outcomes of cryotherapy versus transpupillary diode laser photocoagulation for threshold retinopathy of prematurity. *J.AAPOS.* 3, 234-240

14. Centers for Disease Control and Prevention (2003) Prevalence of diabetes and impaired fasting glucose in adults--United States, 1999-2000. *MMWR Morb.Mortal.Wkly.Rep.* 52, 833-837

15. American Diabetes Association (1997) *Diabetes Facts and Figures*. American Diabetes Association Alexandria, VA..

16. Macular Photocoagulation Study Group (1991) Subfoveal neovascular lesions in age-related macular degeneration. Guidelines for evaluation and treatment in the macular photocoagulation study. *Arch.Ophthalmol.* 109, 1242-1257

17. Campochiaro, P. A., Soloway, P., Ryan, S. J., Miller, J. W. (1999) The pathogenesis of choroidal neovascularization in patients with age-related macular degeneration. *Mol.Vis.* 5, 34

18. Spraul, C. W., Grossniklaus, H. E. (1997) Characteristics of Drusen and Bruch's membrane in postmortem eyes with age-related macular degeneration. *Arch.Ophthalmol* 115, 267-273

19. Midena, E., Degli, A. C., Blarzino, M. C., Valenti, M., Segato, T. (1997) Macular function impairment in eyes with early age-related macular degeneration. *Invest Ophthalmol Vis.Sci.* 38, 469-477

20. Curcio, C. A., Medeiros, N. E., Millican, C. L. (1996) Photoreceptor loss in age-related macular degeneration. *Invest Ophthalmol Vis.Sci.* 37, 1236-1249

21. Zarbin, M. A. (1998) Morphology of early choroidal neovascularization in age-related macular degeneration: correlation with activity. *Surv.Ophthalmol.* 43, 89-90

22. Chang, T. S., Freund, K. B., de la, C. Z., Yannuzzi, L. A., Green, W. R. (1994) Clinicopathologic correlation of choroidal neovascularization demonstrated by indocyanine green angiography in a patient with retention of good vision for almost four years. *Retina* 14, 114-124

23. Green, W. R., Wilson, D. J. (1986) Choroidal neovascularization. *Ophthalmology* 93, 1169-1176

24. Green, W. R., Enger, C. (1993) Age-related macular degeneration histopathologic studies. The 1992 Lorenz E. Zimmerman Lecture. *Ophthalmology* 100, 1519-1535

25. Macular Photocoagulation Study Group (1991) Laser photocoagulation of subfoveal recurrent neovascular lesions in age-related macular degeneration. Results of a randomized clinical trial. *Arch.Ophthalmol.* 109, 1232-1241

26. Macular Photocoagulation Study Group (1994) Visual outcome after laser photocoagulation for subfoveal choroidal neovascularization secondary to age-related macular degeneration. The influence of initial lesion size and initial visual acuity. *Arch.Ophthalmol.* 112, 480-488

27. Thomas, M. A., Dickinson, J. D., Melberg, N. S., Ibanez, H. E., Dhaliwal, R. S. (1994) Visual results after surgical removal of subfoveal choroidal neovascular membranes. *Ophthalmology* 101, 1384-1396

28. de Juan E Jr, Loewenstein, A., Bressler, N. M., Alexander, J. (1998) Translocation of the retina for management of subfoveal choroidal neovascularization II: a preliminary report in humans. *Am.J.Ophthalmol.* 125, 635-646

29. Husain, D., Miller, J. W., Michaud, N., Connolly, E., Flotte, T. J., Gragoudas, E. S. (1996) Intravenous infusion of liposomal benzoporphyrin derivative for photodynamic therapy of experimental choroidal neovascularization. *Arch.Ophthalmol.* 114, 978-985

30. Husain, D., Kramer, M., Kenny, A. G., Michaud, N., Flotte, T. J., Gragoudas, E. S., Miller, J. W. (1999) Effects of photodynamic therapy using verteporfin on experimental choroidal neovascularization and normal retina and choroid up to 7 weeks after treatment. *Invest Ophthalmol.Vis.Sci.* 40, 2322-2331

31. Dougherty, T. J., Gomer, C. J., Henderson, B. W., Jori, G., Kessel, D., Korbelik, M., Moan, J., Peng, Q. (1998) Photodynamic therapy. *J.Natl.Cancer Inst.* 90, 889-905

32. Gomer, C. J. (1989) Photodynamic therapy in the treatment of malignancies. *Semin.Hematol.* 26, 27-34

33. Ladd, B. S., Solomon, S. D., Bressler, N. M., Bressler, S. B. (2001) Photodynamic therapy with verteporfin for choroidal neovascularization in patients with diabetic retinopathy. *Am.J.Ophthalmol.* 132, 659-667

34. Schmidt-Erfurth, U., Hasan, T. (2000) Mechanisms of action of photodynamic therapy with verteporfin for the treatment of age-related macular degeneration. *Surv.Ophthalmol.* 45, 195-214

35. Michaelson I. (1948) The mode of development of the vascular system of the retina with some observations on its significance for certain retinal diseases. *Trans Ophthalmol Soc U K* 68, 137-180

36. Ashton, N. (1980) Oxygen and the retinal blood vessels. *Trans Ophthalmol Soc U K* 100, 359-362

37. Ashton, N. (1966) Oxygen and the growth and development of retinal vessels. In vivo and in vitro studies. The XX Francis I. Proctor Lecture. *Am.J.Ophthalmol* 62, 412-435

38. Shimizu, K., Kobayashi, Y., Muraoka, K. (1981) Midperipheral fundus involvement in diabetic retinopathy. *Ophthalmology* 88, 601-612

39. Grunwald, J. E., Hariprasad, S. M., DuPont, J., Maguire, M. G., Fine, S. L., Brucker, A. J., Maguire, A. M., Ho, A. C. (1998) Foveolar choroidal blood flow in age-related macular degeneration. *Invest Ophthalmol Vis.Sci.* 39, 385-390

40. Ross, R. D., Barofsky, J. M., Cohen, G., Baber, W. B., Palao, S. W., Gitter, K. A. (1998) Presumed macular choroidal watershed vascular filling, choroidal neovascularization, and systemic vascular disease in patients with age-related macular degeneration. *Am.J.Ophthalmol* 125, 71-80

41. Lambooij, A. C., van Wely, K. H., Lindenbergh-Kortleve, D. J., Kuijpers, R. W., Kliffen, M., Mooy, C. M. (2003) Insulin-like growth factor-I and its receptor in neovascular age-related macular degeneration. *Invest Ophthalmol.Vis.Sci.* 44, 2192-2198

42. Witmer, A. N., Vrensen, G. F., Van Noorden, C. J., Schlingemann, R. O. (2003) Vascular endothelial growth factors and angiogenesis in eye disease. *Prog.Retin.Eye Res.* 22, 1-29

43. Zubilewicz, A., Hecquet, C., Jeanny, J. C., Soubrane, G., Courtois, Y., Mascarelli, F. (2001) Two distinct signalling pathways are involved in FGF2-stimulated proliferation of choriocapillary endothelial cells: a comparative study with VEGF. *Oncogene* 20, 1403-1413

44. Okamoto, N., Tobe, T., Hackett, S. F., Ozaki, H., Vinores, M. A., LaRochelle, W., Zack, D. J., Campochiaro, P. A. (1997) Transgenic mice with increased expression of vascular endothelial growth factor in the retina: a new model of intraretinal and subretinal neovascularization. *Am.J.Pathol.* 151, 281-291

45. Tobe, T., Okamoto, N., Vinores, M. A., Derevjanik, N. L., Vinores, S. A., Zack, D. J., Campochiaro, P. A. (1998) Evolution of neovascularization in mice with

overexpression of vascular endothelial growth factor in photoreceptors. *Invest Ophthalmol Vis.Sci.* 39, 180-188

46. Adamis, A. P., Shima, D. T., Tolentino, M. J., Gragoudas, E. S., Ferrara, N., Folkman, J., D'Amore, P. A., Miller, J. W. (1996) Inhibition of vascular endothelial growth factor prevents retinal ischemia-associated iris neovascularization in a nonhuman primate. *Arch.Ophthalmol.* 114, 66-71

47. Aiello, L. P., Pierce, E. A., Foley, E. D., Takagi, H., Chen, H., Riddle, L., Ferrara, N., King, G. L., Smith, L. E. (1995) Suppression of retinal neovascularization in vivo by inhibition of vascular endothelial growth factor (VEGF) using soluble VEGF-receptor chimeric proteins. *Proc.Natl.Acad.Sci.U.S.A* 92, 10457-10461

48. Robinson, G. S., Pierce, E. A., Rook, S. L., Foley, E., Webb, R., Smith, L. E. (1996) Oligodeoxynucleotides inhibit retinal neovascularization in a murine model of proliferative retinopathy. *Proc.Natl.Acad.Sci.U.S.A* 93, 4851-4856

49. Carrasquillo, K. G., Ricker, J. A., Rigas, I. K., Miller, J. W., Gragoudas, E. S., Adamis, A. P. (2003) Controlled delivery of the anti-VEGF aptamer EYE001 with poly(lactic-co-glycolic)acid microspheres. *Invest Ophthalmol.Vis.Sci.* 44, 290-299

50. Adamis, A. P., Miller, J. W., Bernal, M. T., D'Amico, D. J., Folkman, J., Yeo, T. K., Yeo, K. T. (1994) Increased vascular endothelial growth factor levels in the vitreous of eyes with proliferative diabetic retinopathy. *Am.J.Ophthalmol* 118, 445-450

51. Aiello, L. P., Avery, R. L., Arrigg, P. G., Keyt, B. A., Jampel, H. D., Shah, S. T., Pasquale, L. R., Thieme, H., Iwamoto, M. A., Park, J. E. (1994) Vascular endothelial growth factor in ocular fluid of patients with diabetic retinopathy and other retinal disorders. *N.Engl.J.Med.* 331, 1480-1487

52. Pe'er, J., Shweiki, D., Itin, A., Hemo, I., Gnessin, H., Keshet, E. (1995) Hypoxia-induced expression of vascular endothelial growth factor by retinal cells is a common factor in neovascularizing ocular diseases. *Lab Invest* 72, 638-645

53. Miller, J. W., Adamis, A. P., Shima, D. T., D'Amore, P. A., Moulton, R. S., O'Reilly, M. S., Folkman, J., Dvorak, H. F., Brown, L. F., Berse, B., . (1994) Vascular endothelial growth factor/vascular permeability factor is temporally and spatially correlated with ocular angiogenesis in a primate model. *Am.J.Pathol.* 145, 574-584

54. Pierce, E. A., Avery, R. L., Foley, E. D., Aiello, L. P., Smith, L. E. (1995) Vascular endothelial growth factor/vascular permeability factor expression in a mouse model of retinal neovascularization. *Proc.Natl.Acad.Sci.U.S.A* 92, 905-909

55. Amin, R., Puklin, J. E., Frank, R. N. (1994) Growth factor localization in choroidal neovascular membranes of age-related macular degeneration. *Invest Ophthalmol Vis.Sci.* 35, 3178-3188

56. Frank, R. N., Amin, R. H., Eliott, D., Puklin, J. E., Abrams, G. W. (1996) Basic fibroblast growth factor and vascular endothelial growth factor are present in epiretinal and choroidal neovascular membranes. *Am.J.Ophthalmol* 122, 393-403

57. Lopez, P. F., Sippy, B. D., Lambert, H. M., Thach, A. B., Hinton, D. R. (1996) Transdifferentiated retinal pigment epithelial cells are immunoreactive for vascular endothelial growth factor in surgically excised age-related macular degeneration-related choroidal neovascular membranes. *Invest Ophthalmol Vis.Sci.* 37, 855-868

58. Kvanta, A., Algvere, P. V., Berglin, L., Seregard, S. (1996) Subfoveal fibrovascular membranes in age-related macular degeneration express vascular endothelial growth factor. *Invest Ophthalmol Vis.Sci.* 37, 1929-1934

59. Yi, X., Ogata, N., Komada, M., Yamamoto, C., Takahashi, K., Omori, K., Uyama, M. (1997) Vascular endothelial growth factor expression in choroidal neovascularization in rats. *Graefes Arch.Clin.Exp.Ophthalmol* 235, 313-319

60. Ishibashi, T., Hata, Y., Yoshikawa, H., Nakagawa, K., Sueishi, K., Inomata, H. (1997) Expression of vascular endothelial growth factor in experimental choroidal neovascularization. *Graefes Arch.Clin.Exp.Ophthalmol* 235, 159-167

61. Krzystolik, M. G., Afshari, M. A., Adamis, A. P., Gaudreault, J., Gragoudas, E. S., Michaud, N. A., Li, W., Connolly, E., O'Neill, C. A., Miller, J. W. (2002) Prevention of experimental choroidal neovascularization with intravitreal anti-vascular endothelial growth factor antibody fragment. *Arch.Ophthalmol* 120, 338-346

62. Okamoto, N., Tobe, T., Hackett, S. F., Ozaki, H., Vinores, M. A., LaRochelle, W., Zack, D. J., Campochiaro, P. A. (1997) Transgenic mice with increased expression of vascular endothelial growth factor in the retina: a new model of intraretinal and subretinal neovascularization. *Am.J.Pathol.* 151, 281-291

63. Ohno-Matsui, K., Hirose, A., Yamamoto, S., Saikia, J., Okamoto, N., Gehlbach, P., Duh, E. J., Hackett, S., Chang, M., Bok, D., Zack, D. J., Campochiaro, P. A. (2002) Inducible expression of vascular endothelial growth factor in adult mice causes severe proliferative retinopathy and retinal detachment. *Am.J.Pathol.* 160, 711-719

64. Ryan, S. J. (1982) Subretinal neovascularization. Natural history of an experimental model. *Arch.Ophthalmol* 100, 1804-1809

65. van der, Z. E., Fankhauser, F., Raes, K. (1985) Choroidal reaction and vascular repair after chorioretinal photocoagulation with the free-running neodymium-YAG laser. *Arch.Ophthalmol* 103, 580-589

66. Dobi, E. T., Puliafito, C. A., Destro, M. (1989) A new model of experimental choroidal neovascularization in the rat. *Arch.Ophthalmol* 107, 264-269

67. Frank, R. N., Das, A., Weber, M. L. (1989) A model of subretinal neovascularization in the pigmented rat. *Curr.Eye Res.* 8, 239-247

68. Amin, R., Puklin, J. E., Frank, R. N. (1994) Growth factor localization in choroidal neovascular membranes of age-related macular degeneration. *Invest Ophthalmol Vis.Sci.* 35, 3178-3188

69. Cui, J. Z., Kimura, H., Spee, C., Thumann, G., Hinton, D. R., Ryan, S. J. (2000) Natural history of choroidal neovascularization induced by vascular endothelial growth factor in the primate. *Graefes Arch.Clin.Exp.Ophthalmol* 238, 326-333

70. Okamoto, N., Tobe, T., Hackett, S. F., Ozaki, H., Vinores, M. A., LaRochelle, W., Zack, D. J., Campochiaro, P. A. (1997) Transgenic mice with increased expression of vascular endothelial growth factor in the retina: a new model of intraretinal and subretinal neovascularization. *Am.J.Pathol.* 151, 281-291

71. Nair, P. M., Ganesh, A., Mitra, S., Ganguly, S. S. (2003) Retinopathy of prematurity in VLBW and extreme LBW babies. *Indian J.Pediatr.* 70, 303-306

72. Little, G. A. (1992) Neonatal and infant care and outcomes. *Curr.Opin.Obstet.Gynecol.* 4, 55-60

73. Chow, L. C., Wright, K. W., Sola, A. (2003) Can changes in clinical practice decrease the incidence of severe retinopathy of prematurity in very low birth weight infants? *Pediatrics* 111, 339-345

74. Clemons, T. E., Chew, E. Y., Bressler, S. B., McBee, W. (2003) National Eye Institute Visual Function Questionnaire in the Age-Related Eye Disease Study (AREDS): AREDS Report No. 10. *Arch.Ophthalmol* 121, 211-217

75. Hammond, B. R., Jr., Johnson, M. A. (2002) The age-related eye disease study (AREDS). *Nutr.Rev.* 60, 283-288

76. Taylor, H. R., Tikellis, G., Robman, L. D., McCarty, C. A., McNeil, J. J. (2002) Vitamin E supplementation and macular degeneration: randomised controlled trial. *BMJ* 325, 11

77. Spranger, J., Pfeiffer, A. F. (2001) New concepts in pathogenesis and treatment of diabetic retinopathy. *Exp.Clin.Endocrinol.Diabetes* 109, S438-S450

78. Votruba, M., Gregor, Z. (2001) Neovascular age-related macular degeneration: present and future treatment options. *Eye* 15, 424-429

79. Le, D., Murphy, R. P. (1994) Laser treatment of diabetic macular edema. *Semin.Ophthalmol.* 9, 2-9

80. Boulanger, A., Liu, S., Henningsgaard, A. A., Yu, S., Redmond, T. M. (2000) The upstream region of the Rpe65 gene confers retinal pigment epithelium-specific expression in vivo and in vitro and contains critical octamer and E-box binding sites. *J.Biol.Chem.* 275, 31274-31282

81. Lamkin, J. C., Singerman, L. J. (1994) Laser treatment of choroidal neovascularization. *Semin.Ophthalmol.* 9, 10-22

82. Binder, S., Stolba, U., Krebs, I., Kellner, L., Jahn, C., Feichtinger, H., Povelka, M., Frohner, U., Kruger, A., Hilgers, R. D., Krugluger, W. (2002) Transplantation of autologous retinal pigment epithelium in eyes with foveal neovascularization resulting from age-related macular degeneration: a pilot study. *Am.J.Ophthalmol.* 133, 215-225

83. Margherio, R. R., Margherio, A. R., DeSantis, M. E. (2000) Laser treatments with verteporfin therapy and its potential impact on retinal practices. *Retina* 20, 325-330

84. Smiddy, W. E., Flynn, H. W., Jr. (1999) Vitrectomy in the management of diabetic retinopathy. *Surv.Ophthalmol.* 43, 491-507

85. Dogru, M., Nakamura, M., Inoue, M., Yamamoto, M. (1999) Long-term visual outcome in proliferative diabetic retinopathy patients after panretinal photocoagulation. *Jpn.J.Ophthalmol.* 43, 217-224

86. Luke, C., Aisenbrey, S., Luke, M., Marzella, G., Bartz-Schmidt, K. U., Walter, P. (2001) Electrophysiological changes after 360 degrees retinotomy and macular translocation for subfoveal choroidal neovascularisation in age related macular degeneration. *Br.J.Ophthalmol.* 85, 928-932

87. Votruba, M., Gregor, Z. (2001) Neovascular age-related macular degeneration: present and future treatment options. *Eye* 15, 424-429

88. Bunn, H. F., Poyton, R. O. (1996) Oxygen sensing and molecular adaptation to hypoxia. *Physiol Rev.* 76, 839-885

89. Forsythe, J. A., Jiang, B. H., Iyer, N. V., Agani, F., Leung, S. W., Koos, R. D., Semenza, G. L. (1996) Activation of vascular endothelial growth factor gene transcription by hypoxia-inducible factor 1. *Mol.Cell Biol.* 16, 4604-4613

90. Gerber, H. P., Condorelli, F., Park, J., Ferrara, N. (1997) Differential transcriptional regulation of the two vascular endothelial growth factor receptor genes. Flt-1, but not Flk-1/KDR, is up-regulated by hypoxia. *J.Biol.Chem.* 272, 23659-23667

91. Iyer, N. V., Kotch, L. E., Agani, F., Leung, S. W., Laughner, E., Wenger, R. H., Gassmann, M., Gearhart, J. D., Lawler, A. M., Yu, A. Y., Semenza, G. L. (1998) Cellular and developmental control of O2 homeostasis by hypoxia-inducible factor 1 alpha. *Genes Dev.* 12, 149-162

92. Bold, G., Altmann, K. H., Frei, J., Lang, M., Manley, P. W., Traxler, P., Wietfeld, B., Bruggen, J., Buchdunger, E., Cozens, R., Ferrari, S., Furet, P., Hofmann, F., Martiny-Baron, G., Mestan, J., Rosel, J., Sills, M., Stover, D., Acemoglu, F., Boss, E., Emmenegger, R., Lasser, L., Masso, E., Roth, R., Schlachter, C., Vetterli, W. (2000) New anilinophthalazines as potent and orally well absorbed inhibitors of the VEGF receptor tyrosine kinases useful as antagonists of tumor-driven angiogenesis. *J.Med.Chem.* 43, 2310-2323

93. Aiello, L. P., Bursell, S. E., Clermont, A., Duh, E., Ishii, H., Takagi, C., Mori, F., Ciulla, T. A., Ways, K., Jirousek, M., Smith, L. E., King, G. L. (1997) Vascular endothelial growth factor-induced retinal permeability is mediated by protein kinase C in vivo and suppressed by an orally effective beta-isoform-selective inhibitor. *Diabetes* 46, 1473-1480

94. Ferrara, N., Gerber, H. P. (2001) The role of vascular endothelial growth factor in angiogenesis. *Acta Haematol.* 106, 148-156

95. Tombran-Tink, J., Chader, G. G., Johnson, L. V. (1991) PEDF: a pigment epithelium-derived factor with potent neuronal differentiative activity. *Exp.Eye Res.* 53, 411-414

96. Taraboletti, G., Roberts, D., Liotta, L. A., Giavazzi, R. (1990) Platelet thrombospondin modulates endothelial cell adhesion, motility, and growth: a potential angiogenesis regulatory factor. *J.Cell Biol.* 111, 765-772

97. Cao, Y. (1998) Endogenous angiogenesis inhibitors: angiostatin, endostatin, and other proteolytic fragments. *Prog.Mol.Subcell.Biol.* 20, 161-176

98. Steele, F. R., Chader, G. J., Johnson, L. V., Tombran-Tink, J. (1993) Pigment epithelium-derived factor: neurotrophic activity and identification as a member of the serine protease inhibitor gene family. *Proc.Natl.Acad.Sci.U.S.A* 90, 1526-1530

99. Araki, T., Taniwaki, T., Becerra, S. P., Chader, G. J., Schwartz, J. P. (1998) Pigment epithelium-derived factor (PEDF) differentially protects immature but

not mature cerebellar granule cells against apoptotic cell death. *J.Neurosci.Res.* 53, 7-15

100. Becerra, S. P. (1997) Structure-function studies on PEDF. A noninhibitory serpin with neurotrophic activity. *Adv.Exp.Med.Biol.* 425, 223-237

101. Cayouette, M., Smith, S. B., Becerra, S. P., Gravel, C. (1999) Pigment epithelium-derived factor delays the death of photoreceptors in mouse models of inherited retinal degenerations. *Neurobiol.Dis.* 6, 523-532

102. Simonovic, M., Gettins, P. G., Volz, K. (2001) Crystal structure of human PEDF, a potent anti-angiogenic and neurite growth-promoting factor. *Proc.Natl.Acad.Sci.U.S.A* 98, 11131-11135

103. Alberdi, E., Aymerich, M. S., Becerra, S. P. (1999) Binding of pigment epithelium-derived factor (PEDF) to retinoblastoma cells and cerebellar granule neurons. Evidence for a PEDF receptor. *J.Biol.Chem.* 274, 31605-31612

104. Aymerich, M. S., Alberdi, E. M., Martinez, A., Becerra, S. P. (2001) Evidence for pigment epithelium-derived factor receptors in the neural retina. *Invest Ophthalmol.Vis.Sci.* 42, 3287-3293

105. Volpert, O. V., Zaichuk, T., Zhou, W., Reiher, F., Ferguson, T. A., Stuart, P. M., Amin, M., Bouck, N. P. (2002) Inducer-stimulated Fas targets activated endothelium for destruction by anti-angiogenic thrombospondin-1 and pigment epithelium-derived factor. *Nat.Med.* 8, 349-357

106. Nagata, S., Golstein, P. (1995) The Fas death factor. *Science* 267, 1449-1456

107. Volpert, O. V., Zaichuk, T., Zhou, W., Reiher, F., Ferguson, T. A., Stuart, P. M., Amin, M., Bouck, N. P. (2002) Inducer-stimulated Fas targets activated endothelium for destruction by anti-angiogenic thrombospondin-1 and pigment epithelium-derived factor. *Nat.Med.* 8, 349-357

108. Wong, P., Pfeffer, B. A., Bernstein, S. L., Chambers, M. L., Chader, G. J., Zakeri, Z. F., Wu, Y. Q., Wilson, M. R., Becerra, S. P. (2000) Clusterin protein diversity in the primate eye. *Mol.Vis.* 6, 184-191

109. Tombran-Tink, J., Pawar, H., Swaroop, A., Rodriguez, I., Chader, G. J. (1994) Localization of the gene for pigment epithelium-derived factor (PEDF) to chromosome 17p13.1 and expression in cultured human retinoblastoma cells. *Genomics* 19, 266-272

110. Goliath, R., Tombran-Tink, J., Rodriquez, I. R., Chader, G., Ramesar, R., Greenberg, J. (1996) The gene for PEDF, a retinal growth factor is a prime

candidate for retinitis pigmentosa and is tightly linked to the RP13 locus on chromosome 17p13.3. *Mol.Vis.* 2, 5

111. Kirsch, M., Schackert, G., Black, P. M. (2000) Angiogenesis, metastasis, and endogenous inhibition. *J.Neurooncol.* 50, 173-180

112. Cao, Y. (2001) Endogenous angiogenesis inhibitors and their therapeutic implications. *Int.J.Biochem.Cell Biol.* 33, 357-369

113. Lucas, R., Holmgren, L., Garcia, I., Jimenez, B., Mandriota, S. J., Borlat, F., Sim, B. K., Wu, Z., Grau, G. E., Shing, Y., Soff, G. A., Bouck, N., Pepper, M. S. (1998) Multiple forms of angiostatin induce apoptosis in endothelial cells. *Blood* 92, 4730-4741

114. Griscelli, F., Li, H., Bennaceur-Griscelli, A., Soria, J., Opolon, P., Soria, C., Perricaudet, M., Yeh, P., Lu, H. (1998) Angiostatin gene transfer: inhibition of tumor growth in vivo by blockage of endothelial cell proliferation associated with a mitosis arrest. *Proc.Natl.Acad.Sci.U.S.A* 95, 6367-6372

115. O'Reilly, M. S., Holmgren, L., Chen, C., Folkman, J. (1996) Angiostatin induces and sustains dormancy of human primary tumors in mice. *Nat.Med.* 2, 689-692

116. Wu, Z., O'Reilly, M. S., Folkman, J., Shing, Y. (1997) Suppression of tumor growth with recombinant murine angiostatin. *Biochem.Biophys.Res.Commun.* 236, 651-654

117. O'Reilly, M. S., Holmgren, L., Shing, Y., Chen, C., Rosenthal, R. A., Moses, M., Lane, W. S., Cao, Y., Sage, E. H., Folkman, J. (1994) Angiostatin: a novel angiogenesis inhibitor that mediates the suppression of metastases by a Lewis lung carcinoma. *Cell* 79, 315-328

118. Gao, G., Li, Y., Gee, S., Dudley, A., Fant, J., Crosson, C., Ma, J. X. (2002) Down-regulation of vascular endothelial growth factor and up-regulation of pigment epithelium-derived factor: a possible mechanism for the anti-angiogenic activity of plasminogen kringle 5. *J.Biol.Chem.* 277, 9492-9497

119. Piccaluga, P. P., Visani, G., Isidori, A., Malagola, M., Ascani, S., Pileri, S. A. (2003) Microdose alpha-interferon shows clinical and antiangiogenic effect in extramedullary myeloid tumor: a case report. *Leukemia* 17, 986-987

120. McCarty, M. F., Bielenberg, D., Donawho, C., Bucana, C. D., Fidler, I. J. (2002) Evidence for the causal role of endogenous interferon-alpha/beta in the regulation of angiogenesis, tumorigenicity, and metastasis of cutaneous neoplasms. *Clin.Exp.Metastasis* 19, 609-615

121. Folkman, J., Ingber, D. (1992) Inhibition of angiogenesis. *Semin.Cancer Biol.* 3, 89-96

122. Stout, A. J., Gresser, I., Thompson, W. D. (1993) Inhibition of wound healing in mice by local interferon alpha/beta injection. *Int.J.Exp.Pathol.* 74, 79-85

123. Guyer, D. R., Tiedeman, J., Yannuzzi, L. A., Slakter, J. S., Parke, D., Kelley, J., Tang, R. A., Marmor, M., Abrams, G., Miller, J. W. (1993) Interferon-associated retinopathy. *Arch.Ophthalmol.* 111, 350-356

124. Jaakkola, A., Anttila, P. M., Immonen, I. (1994) Interferon alpha-2a in the treatment of exudative senile macular degeneration. *Acta Ophthalmol.(Copenh)* 72, 545-549

125. Engler, C., Sander, B., Villumsen, J., Lund-Andersen, H. (1994) Interferon alfa-2a modifies the course of subfoveal and juxtafoveal choroidal neovascularisation. *Br.J.Ophthalmol.* 78, 749-753

126. Chan, C. K., Kempin, S. J., Noble, S. K., Palmer, G. A. (1994) The treatment of choroidal neovascular membranes by alpha interferon. An efficacy and toxicity study. *Ophthalmology* 101, 289-300

127. Groeneveld, E., Eliadis, P. (1993) Interferon for subfoveal choroidal neovascularisation. *Aust.N.Z.J.Ophthalmol.* 21, 133-134

128. Stuebiger, N., Koetter, I., Zierhut, M. (2000) Complete regression of retinal neovascularization after therapy with interferon alfa in Behcet's disease. *Br.J.Ophthalmol.* 84, 1437-1438

129. Wakelee-Lynch, J. (1992) Interferon may offer first drug therapy for diabetic retinopathy. New research showing that alpha-interferon blocks new blood vessel formation in the iris of monkeys may point the way to new treatment for diabetes retinopathy. *Diabetes Care* 15, 300-301

130. Nguyen, N., Goldberg, M., Pico, J., Kim, W., Abbott, R. L., Levy, B. (1995) Topical and subcutaneous alpha-interferon fails to suppress corneal neovascularization. *Cornea* 14, 147-151

131. Zatterstrom, U. K., Felbor, U., Fukai, N., Olsen, B. R. (2000) Collagen XVIII/endostatin structure and functional role in angiogenesis. *Cell Struct.Funct.* 25, 97-101

132. Nguyen, J. T. (2000) Adeno-associated virus and other potential vectors for angiostatin and endostatin gene therapy. *Adv.Exp.Med.Biol.* 465, 457-466

133. O'Reilly, M. S., Boehm, T., Shing, Y., Fukai, N., Vasios, G., Lane, W. S., Flynn, E., Birkhead, J. R., Olsen, B. R., Folkman, J. (1997) Endostatin: an endogenous inhibitor of angiogenesis and tumor growth. *Cell* 88, 277-285

134. Takahashi, K., Saishin, Y., Saishin, Y., Silva, R. L., Oshima, Y., Oshima, S., Melia, M., Paszkiet, B., Zerby, D., Kadan, M. J., Liau, G., Kaleko, M., Connelly, S., Luo, T., Campochiaro, P. A. (2003) Intraocular expression of endostatin reduces VEGF-induced retinal vascular permeability, neovascularization, and retinal detachment. *FASEB J.* 17, 896-898

135. Mori, K., Ando, A., Gehlbach, P., Nesbitt, D., Takahashi, K., Goldsteen, D., Penn, M., Chen, C. T., Mori, K., Melia, M., Phipps, S., Moffat, D., Brazzell, K., Liau, G., Dixon, K. H., Campochiaro, P. A. (2001) Inhibition of choroidal neovascularization by intravenous injection of adenoviral vectors expressing secretable endostatin. *Am.J.Pathol.* 159, 313-320

136. Noma, H., Funatsu, H., Yamashita, H., Kitano, S., Mishima, H. K., Hori, S. (2002) Regulation of angiogenesis in diabetic retinopathy: possible balance between vascular endothelial growth factor and endostatin. *Arch.Ophthalmol.* 120, 1075-1080

137. Handa, H., Carter, B. J. (1979) Adeno-associated virus DNA replication complexes in herpes simplex virus or adenovirus-infected cells. *J.Biol.Chem.* 254, 6603-6610

138. Berns, K. I. (1996) *Parvoviridae*: The viruses and their replication. pp. 1017-1041, Lippincott-Raven, Philadelphia.

139. Kotin, R. M., Linden, R. M., Berns, K. I. (1992) Characterization of a preferred site on human chromosome 19q for integration of adeno-associated virus DNA by non-homologous recombination. *EMBO J.* 11, 5071-5078

140. Schnepp, B. C., Clark, K. R., Klemanski, D. L., Pacak, C. A., Johnson, P. R. (2003) Genetic fate of recombinant adeno-associated virus vector genomes in muscle. *J.Virol.* 77, 3495-3504

141. Muzyczka, N. (1992) Use of adeno-associated virus as a general transduction vector for mammalian cells. *Curr.Top.Microbiol.Immunol.* 158, 97-129

142. Flotte, T. R., Carter, B. J. (1995) Adeno-associated virus vectors for gene therapy. *Gene Ther.* 2, 357-362

143. Atchison, R. W., Casto, B. C., Hammon, W. M. (1966) Electron microscopy of adenovirus-associated virus (AAV) in cell cultures. *Virology* 29, 353-357

144. Bantel-Schaal, U., zur, H. H. (1984) Characterization of the DNA of a defective human parvovirus isolated from a genital site. *Virology* 134, 52-63

145. Bantel-Schaal, U., Delius, H., Schmidt, R., zur, H. H. (1999) Human adeno-associated virus type 5 is only distantly related to other known primate helper-dependent parvoviruses. *J.Virol.* 73, 939-947

146. Georg-Fries, B., Biederlack, S., Wolf, J., zur, H. H. (1984) Analysis of proteins, helper dependence, and seroepidemiology of a new human parvovirus. *Virology* 134, 64-71

147. Hoggan, M. D., Blacklow, N. R., Rowe, W. P. (1966) Studies of small DNA viruses found in various adenovirus preparations: physical, biological, and immunological characteristics. *Proc.Natl.Acad.Sci.U.S.A* 55, 1467-1474

148. Rutledge, E. A., Halbert, C. L., Russell, D. W. (1998) Infectious clones and vectors derived from adeno-associated virus (AAV) serotypes other than AAV type 2. *J.Virol.* 72, 309-319

149. Gao, G. P., Alvira, M. R., Wang, L., Calcedo, R., Johnston, J., Wilson, J. M. (2002) Novel adeno-associated viruses from rhesus monkeys as vectors for human gene therapy. *Proc.Natl.Acad.Sci.U.S.A* 99, 11854-11859

150. Summerford, C., Samulski, R. J. (1998) Membrane-associated heparan sulfate proteoglycan is a receptor for adeno-associated virus type 2 virions. *J.Virol.* 72, 1438-1445

151. Rabinowitz, J. E., Rolling, F., Li, C., Conrath, H., Xiao, W., Xiao, X., Samulski, R. J. (2002) Cross-packaging of a single adeno-associated virus (AAV) type 2 vector genome into multiple AAV serotypes enables transduction with broad specificity. *J.Virol.* 76, 791-801

152. Summerford, C., Bartlett, J. S., Samulski, R. J. (1999) AlphaVbeta5 integrin: a co-receptor for adeno-associated virus type 2 infection. *Nat.Med.* 5, 78-82

153. Qing, K., Mah, C., Hansen, J., Zhou, S., Dwarki, V., Srivastava, A. (1999) Human fibroblast growth factor receptor 1 is a co-receptor for infection by adeno-associated virus 2. *Nat.Med.* 5, 71-77

154. Walters, R. W., Pilewski, J. M., Chiorini, J. A., Zabner, J. (2002) Secreted and transmembrane mucins inhibit gene transfer with AAV4 more efficiently than AAV5. *J.Biol.Chem.* 277, 23709-23713

155. Walters, R. W., Yi, S. M., Keshavjee, S., Brown, K. E., Welsh, M. J., Chiorini, J. A., Zabner, J. (2001) Binding of adeno-associated virus type 5 to 2,3-linked sialic acid is required for gene transfer. *J.Biol.Chem.* 276, 20610-20616

156. Fraites, T. J., Jr., Schleissing, M. R., Shanely, R. A., Walter, G. A., Cloutier, D. A., Zolotukhin, I., Pauly, D. F., Raben, N., Plotz, P. H., Powers, S. K., Kessler, P. D., Byrne, B. J. (2002) Correction of the enzymatic and functional deficits in a model of Pompe disease using adeno-associated virus vectors. *Mol.Ther.* 5, 571-578

157. Chiorini, J. A., Afione, S., Kotin, R. M. (1999) Adeno-associated virus (AAV) type 5 Rep protein cleaves a unique terminal resolution site compared with other AAV serotypes. *J.Virol.* 73, 4293-4298

158. Chiorini, J. A., Yang, L., Liu, Y., Safer, B., Kotin, R. M. (1997) Cloning of adeno-associated virus type 4 (AAV4) and generation of recombinant AAV4 particles. *J.Virol.* 71, 6823-6833

159. Xiao, W., Chirmule, N., Berta, S. C., McCullough, B., Gao, G., Wilson, J. M. (1999) Gene therapy vectors based on adeno-associated virus type 1. *J.Virol.* 73, 3994-4003

160. Girod, A., Ried, M., Wobus, C., Lahm, H., Leike, K., Kleinschmidt, J., Deleage, G., Hallek, M. (1999) Genetic capsid modifications allow efficient re-targeting of adeno-associated virus type 2. *Nat.Med.* 5, 1438

161. Shi, W., Bartlett, J. S. (2003) RGD inclusion in VP3 provides adeno-associated virus type 2 (AAV2)-based vectors with a heparan sulfate-independent cell entry mechanism. *Mol.Ther.* 7, 515-525

162. Hauswirth, W. W., Lewin, A. S., Zolotukhin, S., Muzyczka, N., Palczewski, K. (2000) Vertebrate Phototransduction and the Visual Cycle. *Methods Enzymol.* 316,

163. Zolotukhin, S., Byrne, B. J., Mason, E., Zolotukhin, I., Potter, M., Chesnut, K., Summerford, C., Samulski, R. J., Muzyczka, N. (1999) Recombinant adeno-associated virus purification using novel methods improves infectious titer and yield. *Gene Ther.* 6, 973-985

164. Flannery, J. G., Zolotukhin, S., Vaquero, M. I., LaVail, M. M., Muzyczka, N., Hauswirth, W. W. (1997) Efficient photoreceptor-targeted gene expression in vivo by recombinant adeno-associated virus. *Proc.Natl.Acad.Sci.U.S.A* 94, 6916-6921

165. Guy, J., Qi, X., Muzyczka, N., Hauswirth, W. W. (1999) Reporter expression persists 1 year after adeno-associated virus-mediated gene transfer to the optic nerve. *Arch.Ophthalmol.* 117, 929-937

166. Song, S., Morgan, M., Ellis, T., Poirier, A., Chesnut, K., Wang, J., Brantly, M., Muzyczka, N., Byrne, B. J., Atkinson, M., Flotte, T. R. (1998) Sustained secretion

of human alpha-1-antitrypsin from murine muscle transduced with adeno-associated virus vectors. *Proc.Natl.Acad.Sci.U.S.A* 95, 14384-14388

167. Lai, Y. K., Shen, W. Y., Brankov, M., Lai, C. M., Constable, I. J., Rakoczy, P. E. (2002) Potential long-term inhibition of ocular neovascularisation by recombinant adeno-associated virus-mediated secretion gene therapy. *Gene Ther.* 9, 804-813

168. Auricchio, A., Behling, K. C., Maguire, A. M., O'Connor, E. M., Bennett, J., Wilson, J. M., Tolentino, M. J. (2002) Inhibition of retinal neovascularization by intraocular viral-mediated delivery of anti-angiogenic agents. *Mol.Ther.* 6, 490-494

169. Rasmussen, H., Chu, K. W., Campochiaro, P., Gehlbach, P. L., Haller, J. A., Handa, J. T., Nguyen, Q. D., Sung, J. U. (2001) Clinical protocol. An open-label, phase I, single administration, dose-escalation study of ADGVPEDF.11D (ADPEDF) in neovascular age-related macular degeneration (AMD). *Hum.Gene Ther.* 12, 2029-2032

170. Kennedy, B. N., Goldflam, S., Chang, M. A., Campochiaro, P., Davis, A. A., Zack, D. J., Crabb, J. W. (1998) Transcriptional regulation of cellular retinaldehyde-binding protein in the retinal pigment epithelium. A role for the photoreceptor consensus element. *J.Biol.Chem.* 273, 5591-5598

171. Lem, J., Applebury, M. L., Falk, J. D., Flannery, J. G., Simon, M. I. (1991) Tissue-specific and developmental regulation of rod opsin chimeric genes in transgenic mice. *Neuron* 6, 201-210

172. Rao, C. D., Pech, M., Robbins, K. C., Aaronson, S. A. (1988) The 5' untranslated sequence of the c-sis/platelet-derived growth factor 2 transcript is a potent translational inhibitor. *Mol.Cell Biol.* 8, 284-292

173. Bok, D., Yasumura, D., Matthes, M. T., Ruiz, A., Duncan, J. L., Chappelow, A. V., Zolutukhin, S., Hauswirth, W., LaVail, M. M. (2002) Effects of adeno-associated virus-vectored ciliary neurotrophic factor on retinal structure and function in mice with a P216L rds/peripherin mutation. *Exp.Eye Res.* 74, 719-735

174. McGee Sanftner, L. H., Abel, H., Hauswirth, W. W., Flannery, J. G. (2001) Glial cell line derived neurotrophic factor delays photoreceptor degeneration in a transgenic rat model of retinitis pigmentosa. *Mol.Ther.* 4, 622-629

175. Ali, R. R., Reichel, M. B., Thrasher, A. J., Levinsky, R. J., Kinnon, C., Kanuga, N., Hunt, D. M., Bhattacharya, S. S. (1996) Gene transfer into the mouse retina mediated by an adeno-associated viral vector. *Hum.Mol.Genet.* 5, 591-594

176. Mori, K., Gehlbach, P., Ando, A., Wahlin, K., Gunther, V., McVey, D., Wei, L., Campochiaro, P. A. (2002) Intraocular adenoviral vector-mediated gene transfer in proliferative retinopathies. *Invest Ophthalmol.Vis.Sci.* 43, 1610-1615

177. Dawson, D. W., Volpert, O. V., Gillis, P., Crawford, S. E., Xu, H., Benedict, W., Bouck, N. P. (1999) Pigment epithelium-derived factor: a potent inhibitor of angiogenesis. *Science* 285, 245-248

178. Hauswirth, W. W., Lewin, A. S., Zolotukhin, S., Muzyczka, N. (2000) Production and purification of recombinant adeno-associated virus. *Methods Enzymol.* 316, 743-761

179. Bennett, J., Duan, D., Engelhardt, J. F., Maguire, A. M. (1997) Real-time, noninvasive in vivo assessment of adeno-associated virus-mediated retinal transduction. *Invest Ophthalmol.Vis.Sci.* 38, 2857-2863

180. Smith, L. E., Wesolowski, E., McLellan, A., Kostyk, S. K., D'Amato, R., Sullivan, R., D'Amore, P. A. (1994) Oxygen-induced retinopathy in the mouse. *Invest Ophthalmol.Vis.Sci.* 35, 101-111

181. D'Amato, R., Wesolowski, E., Smith, L. E. (1993) Microscopic visualization of the retina by angiography with high-molecular-weight fluorescein-labeled dextrans in the mouse. *Microvasc.Res.* 46, 135-142

182. Mino, R. P., Spoerri, P. E., Caballero, S., Player, D., Belardinelli, L., Biaggioni, I., Grant, M. B. (2001) Adenosine receptor antagonists and retinal neovascularization in vivo. *Invest Ophthalmol.Vis.Sci.* 42, 3320-3324

183. Penn, J. S., Henry, M. M. (1996) Assessing retinal neovascularization in an animal model of proliferative retinopathy. *Microvasc.Res.* 51, 126-130

184. Mokdad, A. H., Ford, E. S., Bowman, B. A., Nelson, D. E., Engelgau, M. M., Vinicor, F., Marks, J. S. (2001) The continuing increase of diabetes in the US. *Diabetes Care* 24, 412

185. Lip, P. L., Blann, A. D., Hope-Ross, M., Gibson, J. M., Lip, G. Y. (2001) Age-related macular degeneration is associated with increased vascular endothelial growth factor, hemorheology and endothelial dysfunction. *Ophthalmology* 108, 705-710

186. Yannuzzi, L. A., Negrao, S., Iida, T., Carvalho, C., Rodriguez-Coleman, H., Slakter, J., Freund, K. B., Sorenson, J., Orlock, D., Borodoker, N. (2001) Retinal angiomatous proliferation in age-related macular degeneration. *Retina* 21, 416-434

187. Connolly, S. E., Hores, T. A., Smith, L. E., D'Amore, P. A. (1988) Characterization of vascular development in the mouse retina. *Microvasc.Res.* 36, 275-290

188. Ito, M., Yoshioka, M. (1999) Regression of the hyaloid vessels and pupillary membrane of the mouse. *Anat.Embryol.(Berl)* 200, 403-411

189. Larrazabal, L. I., Penn, J. S. (1990) Fluorescein angiography of the newborn rat. Implications in oxygen-induced retinopathy. *Invest Ophthalmol.Vis.Sci.* 31, 810-818

190. Meneses, P. I., Hajjar, K. A., Berns, K. I., Duvoisin, R. M. (2001) Recombinant angiostatin prevents retinal neovascularization in a murine proliferative retinopathy model. *Gene Ther.* 8, 646-648

191. Stellmach, V., Crawford, S. E., Zhou, W., Bouck, N. (2001) Prevention of ischemia-induced retinopathy by the natural ocular antiangiogenic agent pigment epithelium-derived factor. *Proc.Natl.Acad.Sci.U.S.A* 98, 2593-2597

192. Alexiades, M. R., Cepko, C. (1996) Quantitative analysis of proliferation and cell cycle length during development of the rat retina. *Dev.Dyn.* 205, 293-307

193. Daly, T. M., Ohlemiller, K. K., Roberts, M. S., Vogler, C. A., Sands, M. S. (2001) Prevention of systemic clinical disease in MPS VII mice following AAV-mediated neonatal gene transfer. *Gene Ther.* 8, 1291-1298

194. Hansen, K. A., Sugino, I. K., Yagi, F., Wang, H., Tsukahara, I., Gullapalli, V., Bennett, J., Zarbin, M. A. (2003) Adeno-associated virus encoding green fluorescent protein as a label for retinal pigment epithelium. *Invest Ophthalmol.Vis.Sci.* 44, 772-780

195. Surace, E. M., Auricchio, A., Reich, S. J., Rex, T., Glover, E., Pineles, S., Tang, W., O'Connor, E., Lyubarsky, A., Savchenko, A., Pugh, E. N., Jr., Maguire, A. M., Wilson, J. M., Bennett, J. (2003) Delivery of adeno-associated virus vectors to the fetal retina: impact of viral capsid proteins on retinal neuronal progenitor transduction. *J.Virol.* 77, 7957-7963

196. Mori, K., Gehlbach, P., Yamamoto, S., Duh, E., Zack, D. J., Li, Q., Berns, K. I., Raisler, B. J., Hauswirth, W. W., Campochiaro, P. A. (2002) AAV-mediated gene transfer of pigment epithelium-derived factor inhibits choroidal neovascularization. *Invest Ophthalmol.Vis.Sci.* 43, 1994-2000

197. Chi, J. T., Chang, H. Y., Haraldsen, G., Jahnsen, F. L., Troyanskaya, O. G., Chang, D. S., Wang, Z., Rockson, S. G., Van De, R. M., Botstein, D., Brown, P. O. (2003) Endothelial cell diversity revealed by global expression profiling. *Proc.Natl.Acad.Sci.U S.A* 100, 10623-10628

198. Liu, C., Shao, Z. M., Zhang, L., Beatty, P., Sartippour, M., Lane, T., Livingston, E., Nguyen, M. (2001) Human endomucin is an endothelial marker. *Biochem.Biophys.Res.Commun.* 288, 129-136

199. Burger, P. E., Coetzee, S., McKeehan, W. L., Kan, M., Cook, P., Fan, Y., Suda, T., Hebbel, R. P., Novitzky, N., Muller, W. A., Wilson, E. L. (2002) Fibroblast growth factor receptor-1 is expressed by endothelial progenitor cells. *Blood* 100, 3527-3535

200. Grant, M. B., May, W. S., Caballero, S., Brown, G. A., Guthrie, S. M., Mames, R. N., Byrne, B. J., Vaught, T., Spoerri, P. E., Peck, A. B., Scott, E. W. (2002) Adult hematopoietic stem cells provide functional hemangioblast activity during retinal neovascularization. *Nat.Med.* 8, 607-612

201. Friedlander, M., Theesfeld, C. L., Sugita, M., Fruttiger, M., Thomas, M. A., Chang, S., Cheresh, D. A. (1996) Involvement of integrins alpha v beta 3 and alpha v beta 5 in ocular neovascular diseases. *Proc.Natl.Acad.Sci.U.S.A* 93, 9764-9769

202. Luna, J., Tobe, T., Mousa, S. A., Reilly, T. M., Campochiaro, P. A. (1996) Antagonists of integrin alpha v beta 3 inhibit retinal neovascularization in a murine model. *Lab Invest* 75, 563-573

203. Muller, O. J., Kaul, F., Weitzman, M. D., Pasqualini, R., Arap, W., Kleinschmidt, J. A., Trepel, M. (2003) Random peptide libraries displayed on adeno-associated virus to select for targeted gene therapy vectors. *Nat.Biotechnol.* 21, 1040-1046

204. Biermann, V., Volpers, C., Hussmann, S., Stock, A., Kewes, H., Schiedner, G., Herrmann, A., Kochanek, S. (2001) Targeting of high-capacity adenoviral vectors. *Hum.Gene Ther.* 12, 1757-1769

205. Nicklin, S. A., Von Seggern, D. J., Work, L. M., Pek, D. C., Dominiczak, A. F., Nemerow, G. R., Baker, A. H. (2001) Ablating adenovirus type 5 fiber-CAR binding and HI loop insertion of the SIGYPLP peptide generate an endothelial cell-selective adenovirus. *Mol.Ther.* 4, 534-542

206. Nettelbeck, D. M., Miller, D. W., Jerome, V., Zuzarte, M., Watkins, S. J., Hawkins, R. E., Muller, R., Kontermann, R. E. (2001) Targeting of adenovirus to endothelial cells by a bispecific single-chain diabody directed against the adenovirus fiber knob domain and human endoglin (CD105). *Mol.Ther.* 3, 882-891

207. Korhonen, J., Lahtinen, I., Halmekyto, M., Alhonen, L., Janne, J., Dumont, D., Alitalo, K. (1995) Endothelial-specific gene expression directed by the tie gene promoter in vivo. *Blood* 86, 1828-1835

208. Tang, Y., Jackson, M., Qian, K., Phillips, M. I. (2002) Hypoxia inducible double plasmid system for myocardial ischemia gene therapy. *Hypertension* 39, 695-698

209. Bainbridge, J. W., Mistry, A., De Alwis, M., Paleolog, E., Baker, A., Thrasher, A. J., Ali, R. R. (2002) Inhibition of retinal neovascularisation by gene transfer of soluble VEGF receptor sFlt-1. *Gene Ther.* 9, 320-326

210. Bora, P. S., Hu, Z., Tezel, T. H., Sohn, J. H., Kang, S. G., Cruz, J. M., Bora, N. S., Garen, A., Kaplan, H. J. (2003) Immunotherapy for choroidal neovascularization in a laser-induced mouse model simulating exudative (wet) macular degeneration. *Proc.Natl.Acad.Sci.U.S.A* 100, 2679-2684

211. Ishibashi, T., Hata, Y., Yoshikawa, H., Nakagawa, K., Sueishi, K., Inomata, H. (1997) Expression of vascular endothelial growth factor in experimental choroidal neovascularization. *Graefes Arch.Clin.Exp.Ophthalmol.* 235, 159-167

212. Frykman, P. K., Brown, M. S., Yamamoto, T., Goldstein, J. L., Herz, J. (1995) Normal plasma lipoproteins and fertility in gene-targeted mice homozygous for a disruption in the gene encoding very low density lipoprotein receptor. *Proc.Natl.Acad.Sci.U.S.A* 92, 8453-8457

213. Trommsdorff, M., Gotthardt, M., Hiesberger, T., Shelton, J., Stockinger, W., Nimpf, J., Hammer, R. E., Richardson, J. A., Herz, J. (1999) Reeler/Disabled-like disruption of neuronal migration in knockout mice lacking the VLDL receptor and ApoE receptor 2. *Cell* 97, 689-701

214. Tacken, P. J., Teusink, B., Jong, M. C., Harats, D., Havekes, L. M., van Dijk, K. W., Hofker, M. H. (2000) LDL receptor deficiency unmasks altered VLDL triglyceride metabolism in VLDL receptor transgenic and knockout mice. *J.Lipid Res.* 41, 2055-2062

215. Chen, S. J., Rader, D. J., Tazelaar, J., Kawashiri, M., Gao, G., Wilson, J. M. (2000) Prolonged correction of hyperlipidemia in mice with familial hypercholesterolemia using an adeno-associated viral vector expressing very-low-density lipoprotein receptor. *Mol.Ther.* 2, 256-261

216. Yoshida, S., Yoshida, A., Matsui, H., Takada, Y., Ishibashi, T. (2003) Involvement of macrophage chemotactic protein-1 and interleukin-1beta during inflammatory but not basic fibroblast growth factor-dependent neovascularization in the mouse cornea. *Lab Invest* 83, 927-938

217. Silvestre, J. S., Mallat, Z., Duriez, M., Tamarat, R., Bureau, M. F., Scherman, D., Duverger, N., Branellec, D., Tedgui, A., Levy, B. I. (2000) Antiangiogenic effect of interleukin-10 in ischemia-induced angiogenesis in mice hindlimb. *Circ.Res.* 87, 448-452

218. Kohno, T., Mizukami, H., Suzuki, M., Saga, Y., Takei, Y., Shimpo, M., Matsushita, T., Okada, T., Hanazono, Y., Kume, A., Sato, I., Ozawa, K. (2003) Interleukin-10-mediated inhibition of angiogenesis and tumor growth in mice bearing VEGF-producing ovarian cancer. *Cancer Res.* 63, 5091-5094

219. Kowluru, R. A. (2002) Retinal metabolic abnormalities in diabetic mouse: comparison with diabetic rat. *Curr.Eye Res.* 24, 123-128

220. Pi-Sunyer, F. X. (1993) Medical hazards of obesity. *Ann.Intern.Med.* 119, 655-660

221. Mokdad, A. H., Ford, E. S., Bowman, B. A., Nelson, D. E., Engelgau, M. M., Vinicor, F., Marks, J. S. (2000) Diabetes trends in the U.S.: 1990-1998. *Diabetes Care* 23, 1278-1283

222. Volpert, O. V., Zaichuk, T., Zhou, W., Reiher, F., Ferguson, T. A., Stuart, P. M., Amin, M., Bouck, N. P. (2002) Inducer-stimulated Fas targets activated endothelium for destruction by anti-angiogenic thrombospondin-1 and pigment epithelium-derived factor. *Nat.Med.* 8, 349-357

223. McCarty, C. A., Mukesh, B. N., Fu, C. L., Mitchell, P., Wang, J. J., Taylor, H. R. (2001) Risk factors for age-related maculopathy: the Visual Impairment Project. *Arch.Ophthalmol.* 119, 1455-1462

224. Delcourt, C., Carriere, I., Ponton-Sanchez, A., Fourrey, S., Lacroux, A., Papoz, L. (2001) Light exposure and the risk of age-related macular degeneration: the Pathologies Oculaires Liees a l'Age (POLA) study. *Arch.Ophthalmol.* 119, 1463-1468

225. West, S. K., Rosenthal, F. S., Bressler, N. M., Bressler, S. B., Munoz, B., Fine, S. L., Taylor, H. R. (1989) Exposure to sunlight and other risk factors for age-related macular degeneration. *Arch.Ophthalmol.* 107, 875-879

226. Klein, M. L., Schultz, D. W., Edwards, A., Matise, T. C., Rust, K., Berselli, C. B., Trzupek, K., Weleber, R. G., Ott, J., Wirtz, M. K., Acott, T. S. (1998) Age-related macular degeneration. Clinical features in a large family and linkage to chromosome 1q. *Arch.Ophthalmol.* 116, 1082-1088

227. Seddon, J. M., Ajani, U. A., Mitchell, B. D. (1997) Familial aggregation of age-related maculopathy. *Am.J.Ophthalmol.* 123, 199-206

228. Silvestri, G., Johnston, P. B., Hughes, A. E. (1994) Is genetic predisposition an important risk factor in age-related macular degeneration? *Eye* 8 (Pt 5), 564-568

229. Silvestri, G. (1997) Age-related macular degeneration: genetics and implications for detection and treatment. *Mol.Med.Today* 3, 84-91

230. Seddon, J. M., Willett, W. C., Speizer, F. E., Hankinson, S. E. (1996) A prospective study of cigarette smoking and age-related macular degeneration in women. *JAMA* 276, 1141-1146

231. Christen, W. G., Glynn, R. J., Manson, J. E., Ajani, U. A., Buring, J. E. (1996) A prospective study of cigarette smoking and risk of age-related macular degeneration in men. *JAMA* 276, 1147-1151

232. Delcourt, C., Diaz, J. L., Ponton-Sanchez, A., Papoz, L. (1998) Smoking and age-related macular degeneration. The POLA Study. Pathologies Oculaires Liees a l'Age. *Arch.Ophthalmol.* 116, 1031-1035

233. Smith, W., Mitchell, P. (1996) Alcohol intake and age-related maculopathy. *Am.J.Ophthalmol.* 122, 743-745

234. Ajani, U. A., Christen, W. G., Manson, J. E., Glynn, R. J., Schaumberg, D., Buring, J. E., Hennekens, C. H. (1999) A prospective study of alcohol consumption and the risk of age-related macular degeneration. *Ann.Epidemiol.* 9, 172-177

235. Husain, D., Ambati, B., Adamis, A. P., Miller, J. W. (2002) Mechanisms of age-related macular degeneration. *Ophthalmol Clin.North Am.* 15, 87-91

236. Acland, G. M., Aguirre, G. D., Ray, J., Zhang, Q., Aleman, T. S., Cideciyan, A. V., Pearce-Kelling, S. E., Anand, V., Zeng, Y., Maguire, A. M., Jacobson, S. G., Hauswirth, W. W., Bennett, J. (2001) Gene therapy restores vision in a canine model of childhood blindness. *Nat.Genet.* 28, 92-95

237. Acland, G. M., Aguirre, G. D., Ray, J., Zhang, Q., Aleman, T. S., Cideciyan, A. V., Pearce-Kelling, S. E., Anand, V., Zeng, Y., Maguire, A. M., Jacobson, S. G., Hauswirth, W. W., Bennett, J. (2001) Gene therapy restores vision in a canine model of childhood blindness. *Nat.Genet.* 28, 92-95

238. Krzystolik, M. G., Afshari, M. A., Adamis, A. P., Gaudreault, J., Gragoudas, E. S., Michaud, N. A., Li, W., Connolly, E., O'Neill, C. A., Miller, J. W. (2002) Prevention of experimental choroidal neovascularization with intravitreal anti-vascular endothelial growth factor antibody fragment. *Arch.Ophthalmol* 120, 338-346

239. Murata, T., Cui, J., Taba, K. E., Oh, J. Y., Spee, C., Hinton, D. R., Ryan, S. J. (2000) The possibility of gene therapy for the treatment of choroidal neovascularization. *Ophthalmology* 107, 1364-1373

240. Zhang, D., Kaufman, P. L., Gao, G., Saunders, R. A., Ma, J. X. (2001) Intravitreal injection of plasminogen kringle 5, an endogenous angiogenic inhibitor, arrests retinal neovascularization in rats. *Diabetologia* 44, 757-765

241. Mori, K., Duh, E., Gehlbach, P., Ando, A., Takahashi, K., Pearlman, J., Mori, K., Yang, H. S., Zack, D. J., Ettyreddy, D., Brough, D. E., Wei, L. L., Campochiaro, P. A. (2001) Pigment epithelium-derived factor inhibits retinal and choroidal neovascularization. *J.Cell Physiol* 188, 253-263

242. Lambert, V., Munaut, C., Noel, A., Frankenne, F., Bajou, K., Gerard, R., Carmeliet, P., Defresne, M. P., Foidart, J. M., Rakic, J. M. (2001) Influence of plasminogen activator inhibitor type 1 on choroidal neovascularization. *FASEB J.* 15, 1021-1027

BIOGRAPHICAL SKETCH

Brian Raisler was born and raised in Florida. After graduating from the University of Florida in 1995 with a Bachelor of Science in microbiology, he worked for three years conducting pharmacology studies for Dr. Raymond Bergeron's group in medicinal chemistry at the University of Florida. Brian returned to school in 1998 to pursue his doctoral training. Guided by his interests in vascular regulation in cancer, Brian sought a research project involving angiogenesis. After his first year in graduate school, he refined his goals and accepted a position in the laboratory of Dr. William Hauswirth working toward the control of pathological ocular angiogenesis. Through his dissertation project he was able to expand his knowledge and gain tools and skills that will serve him well in the science to come. Through hard work and perseverance, Brian saw the research to its successful fulfillment and enjoyed the privilege of presenting his work at several international meetings. His research was awarded first place in Human Physiology and Medicine in the University of Florida 2002 Graduate Student Forum and second place at the 2002 Medical Guild Research Day sponsored by the College of Medicine. Following graduation, Brian will briefly complete post-doctoral training before relocating out of state to pursue further research interests.